SANDIA REPORT

SAND2014-17718
Unlimited Release
September 2014

Scoping Study: Networked Microgrids

Eddy Trinklei	Michigan Technological University
Gordon Parker	Michigan Technological University
Wayne Weaver	Michigan Technological University
Rush Robinett	Michigan Technological University
Lucia Gauchia Babe	Michigan Technological University
Chee-Wooi Ten	Michigan Technological University
Ward Bower	Ward Bower Innovations LLC
Steve Glover	Sandia National Laboratories
Steve Bukowski	Sandia National Laboratories

Prepared by
Michigan Technological University
Houghton, Michigan 49931

Sandia National Laboratories
Albuquerque, New Mexico 87185 and Livermore, California 94550

Sandia National Laboratories is a multi-program laboratory managed and operated by Sandia Corporation, a wholly owned subsidiary of Lockheed Martin Corporation, for the U.S. Department of Energy's National Nuclear Security Administration under contract DE-AC04-94AL85000.

Issued by Sandia National Laboratories, operated for the United States Department of Energy by Sandia Corporation.

Available to DOE and DOE contractors from
U.S. Department of Energy
Office of Scientific and Technical Information
P.O. Box 62
Oak Ridge, TN 37831

Telephone: (865) 576-8401
Facsimile: (865) 576-5728
E-Mail: reports@adonis.osti.gov
Online ordering: http://www.osti.gov/bridge

Available to the public from
U.S. Department of Commerce
National Technical Information Service
5285 Port Royal Rd.
Springfield, VA 22161

Telephone: (800) 553-6847
Facsimile: (703) 605-6900
E-Mail: orders@ntis.fedworld.gov
Online order: http://www.ntis.gov/help/ordermethods.asp?loc=7-4-0#online

SAND2014-17718
Unlimited Release
Printed September 2014

Scoping Study: Networked Microgrids

Eddy Trinklei, Gordon Parker, Wayne Weaver, Rush Robinett
Lucia Gauchia Babe, Chee-Wooi Ten
Michigan Technological University
Houghton, Michigan 49931

Ward Bower
Ward Bower Innovations, LLC

Steven Glover, Steve Bukowski
Electrical Science and Experiments
Sandia National Laboratories
P.O. Box 5800
Albuquerque, New Mexico 87185-MS1152

Abstract

This report presents a scoping study for networked microgrids which are defined as "Interoperable groups of multiple Advanced Microgrids that become an integral part of the electricity grid while providing enhanced resiliency through self-healing, aggregated ancillary services, and real-time communication." They result in optimal electrical system configurations and controls whether grid-connected or in islanded modes and enable high penetrations of distributed and renewable energy resources.

The vision for the purpose of this document is: "Networked microgrids seamlessly integrate with the electricity grid or other Electric Power Sources (EPS) providing cost effective, high quality, reliable, resilient, self-healing power delivery systems."

Scoping Study: Networked Microgrids

September 4, 2014

Eddy Trinklein, Michigan Technological University
Gordon Parker, Michigan Technological University
Wayne Weaver, Michigan Technological University
Rush Robinett, Michigan Technological University
Lucia Gauchia Babe, Michigan Technological University
Chee-Wooi Ten, Michigan Technological University
Ward Bower, Ward Bower Innovations LLC
Steve Glover, Sandia National Laboratories
Steve Bukowski, Sandia National Laboratories

Prepared by
Michigan Technological University
Houghton, Michigan 49931

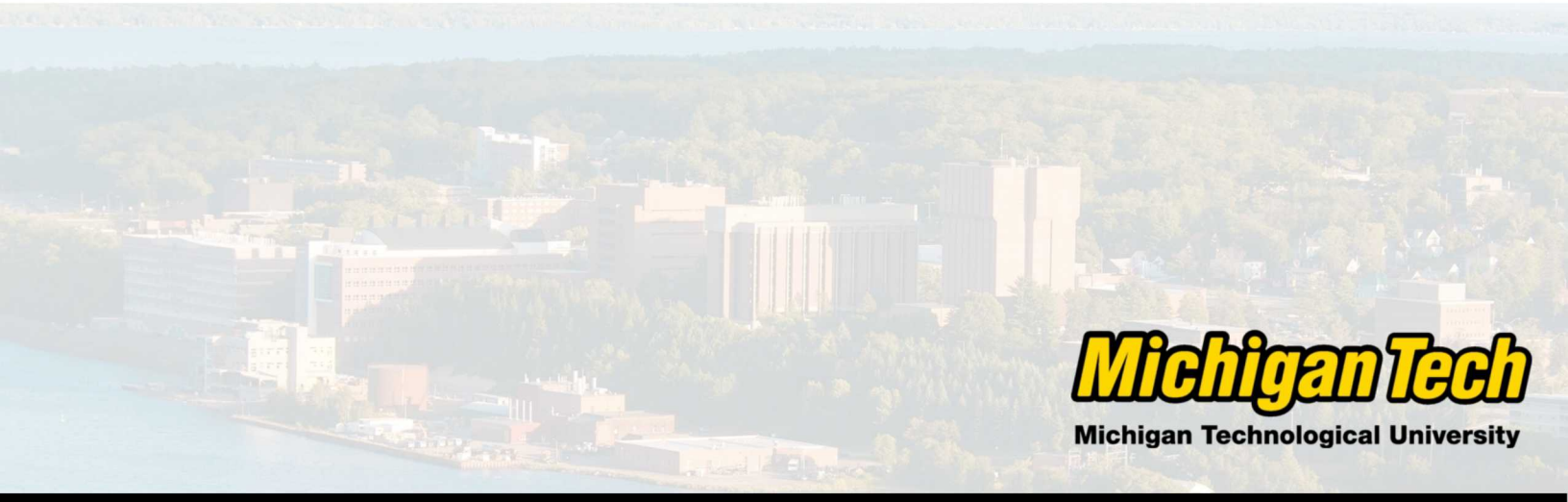

Contents

List of Figures

List of Tables

Acronyms and Abbreviations

CERTS	Consortium of Electric Reliability Solutions
CHP	combined heat and power
DER	distributed energy resource
DER-CAM	Distributed Energy Resources Customer Adoption Model
DG	distributed generation
DOE OE	U.S. DOE Office of Electricity Delivery and Energy Reliability
DR	distributed resource
DRGS	Distributed Renewables, Generators, and Storage
DSO	distribution system operator
EMS	energy-management system
IEEE	Institute of Electrical and Electronic Engineers
MO	market operator
NERC	North American Electric Reliability Corporation
NIST	National Institute of Standards and Technology
NREL	National Renewable Energy Laboratory
PCC	point of common coupling
PG&E	Pacific Gas & Electric
PRM	Performance Reliability Model
PV	photovoltaic(s)
QF	(FERC-jurisdictional) qualifying facility
QOS	quality of service
R&D	research and development
RTO	Regional Transmission Operators
SCADA	supervisory control and data acquisition
SPIDERS	Smart Power Infrastructure Demonstration for Energy Reliability and Security
T&D	transmission and distribution
TMO	Technology Management Optimization
TOU	Time of Use
VAR	Volt-Ampere reactive
PJM	Pennsylvania-New Jersey-Maryland Interconnection
FERC	Federal Energy Regulatory Commission
ERCOT	Electric Reliability Council of Texas
PHEV	Plug-in Hybrid Electric Vehicle
ISO	Independent System Operator

CAISO	California Independent System Operator
PV	Photovoltaics
SEL	Schweitzer Engineering Laboratories
MAS	Multi-Agent Systems
DDC	Distribution Dispatching Center
FRTU-FTU	Feeder Remote Terminal Unit - Feeder Terminal Unit
RTU	Remote Terminal Unit
DMS	Distribution Management System
DTM	Distribution Transformer Monitoring
AMR	Automatic Meter Reading
AMI	Automatic Meter Infrastructure
FDU	
PMU	Phasor Measurement Units
HAN	Home Area Network
NAN	Near-me Area Network
BW/FW	Backward/Forward
MatLab	Matrix Laboratory
WECC	Western Electricity Coordinating Council
DFACTS	Distributed Flexible AC Transmission System
UPS	Uninterrupted Power Supply
EPS	Electric Power System
DA	Day Ahead
LMP	Locational Marginal Price
GHG	Greenhouse Gasses
SNL	Sandia National Laboratories
LBNL	Lawrence Berkeley National Laboratory
PNNL	Pacific Northwest National Laboratory

1 Abstract

This report presents a scoping study for networked microgrids which are defined as "Interoperable groups of multiple Advanced Microgrids that become an integral part of the electricity grid while providing enhanced resiliency through self-healing, aggregated ancillary services, and real-time communication. They result in optimal electrical system configurations and controls whether grid-connected or in islanded modes and enable high penetrations of distributed and renewable energy resources.

The vision for the purpose of this document is: "Networked microgrids seamlessly integrate with the electricity grid or other Electric Power Sources (EPS) providing cost effective, high quality, reliable, resilient, self-healing power delivery systems."

Benefits of networked microgrids are presented as well as additional costs and barriers to their full implementation into the electrical power grid. Their benefits include ancillary service providers, structured aggregators, enhanced resiliency and self-healing capabilities due to their intrinsic distributed decentralized architecture. On the other hand, this new architecture requires a more sophisticated communications system that introduces additional cyber security concerns due to more communication nodes. The single largest barrier to the implementation of networked microgrids is the uncertainty in the grid/utility space, as described by King, "Despite the fact that microgrids might have a legal right to exist in many states, there are still many barriers to microgrid development that stem from regulatory ambiguity. A prospective microgrid faces considerable uncertainty with regard to where and how it can be built and operated under the existing regulatory environment. This uncertainty poses a large financial risk for entrepreneurs; such risks can swamp an investment decision and lead to chronic under-investment for even highly cost-effective applications."[1]

There are several networked microgrids that are being developed at present. One of the most well developed to date is the Tres Amigas SuperStation. The Tres Amigas SuperStation project's goal is connecting the Western Interconnection, Eastern Interconnection and ERCOT (The Electric Reliability Council of Texas) for controlled power sharing across North America. In essence, this is a peer-to-peer, transmission-level connection of three massive, autonomous microgrids for the purpose of increasing renewable penetration and equalizing energy prices.

This scoping study provides preliminary analyses based on DER-CAM that show near term economic benefits while demonstrating the need for more advanced analysis tools to fully account for the interconnected structure of networked microgrids. A top-down and bottoms-up analysis procedure was carried out on two test cases that basically spanned the space of possible networked microgrid configurations. Given the available tools set, it was determined that these test cases could be reduce to a single representative canonical test case of four microgrids networked together. Several value streams associated with interconnected microgrids are identified and categorized into economic and social benefit. Different ownership models are explored with how certain value streams can be monetized.

R&D needs are identified and described in the following chapters. The technical challenges for microgrids and networked microgrids can be summed up as: Control Systems - algorithms, software and communications:

- Hardware and Architecture - Interconnections, energy storage
- Modeling and Simulation - Tools to design, develop and optimize system
- Testing - Hardware testing platforms to validate solutions

2 Executive Summary

This study focuses on the prospects and challenges of networked microgrids for reliable power service delivery. The benefits of single microgrids to their operator/customer in terms of power quality, reliability, and cost have been studied and demonstrated. A network of microgrids can expand upon these features while also providing benefits to its distribution-level utility primarily be reducing load uncertainty. For example, the network can manage its maintenance schedule such that the nominal load to the utility is constant. Another example is its potential for satisfying high frequency load requirements by using its shared excess capacity typically designed into a microgrid to facilitate expected growth. This can offload the utility's need for regulation reserve or possibly the utility could rely on the networked microgrid high frequency capacity for regulation. It's important to note that networked microgrid citing is important. For example, locations where the power delivery system is nearly at its limits and the expected load growth rate is low are favorable conditions. The value-stream examples above will require a level of sensing and control that does not exist in current microgrid designs, but is embodied in the recently developed Advanced Microgrid concept [2]. This leads to several technical challenges including scalable designs, efficient sensing, programmable power electronic "actuation," and control algorithm design.

Deploying and operating a network of Advanced Microgrids within the existing U.S. power delivery system can provide value streams to both the owner/operator and the utility as mentioned above, but there are significant non-technical challenges as well. It's essential that the network not attain utility status. It's unlikely that any state utility service commission would allow a utility designation to a network of microgrids operating within an existing utilities service area. Furthermore, if a microgrid network is perceived to be a threat to the local utility, legal challenges may result adding prohibitive costs. Therefore, the design requirements for a microgrid network should contain not only those of the customers but also the host utility. Single microgrid design and analysis tools are needed that consider all of the effected constituents. Eventually, a successful demonstration is needed. A member-operated, cooperative utility whose business model balances the needs of both the customer and the utility is a likely candidate.

It's worth noting that this study is by no means the first investigation into the networked microgrid concept. Many articles that focus on single microgrids often mention the expanded capability of networked microgrids. This is usually motivated by resiliency and power quality benefits. The Tres Amigas project, whose objective is the interconnection of the Eastern and Western Interconnections with ERCOT, can be considered a network of extremely large, autonomous microgrids. The projected cost of this project is substantial, but the expected financial benefits make it viable along with its facilitation of increased renewable penetration.

3 Introduction and Background

The rising demand of energy coupled with increasing government regulation on fossil fuel usage has left the traditional macro electric grid near full capacity during peak demand times. Inflexibility of base load generation limits the penetration of renewable energy sources to $10 - 20\%$ [3]. This limitation is caused by the variable nature of wind and PV coupled with non-coincident load profiles, resulting in over or under generation leading to frequency deviation. In some cases regionally dependent transmission constrains of the macro grid impose a congestion limit when excess generation cannot be provided to neighboring grids [4]. These congestion limits increase local electric prices and decrease transmission efficiency. Furthermore, long distance transmission is inherently inefficient even at the high voltages that are used. Many of these challenges could be address by interconnected microgrids. In this document, the interconnection between microgrids is provided by the utility based macro grid.

Microgrids are a collection of distributed loads and generation sources within well-defined electrical boundaries that can be connected or disconnected (island) from the macro electric grid. Microgrids could be further defined by peak output which ranges up to 10 MW, although in most cases larger grids have been built. Due to smaller output, a microgrid's primary generators, typically natural gas or diesel, can respond to load changes and cold starting in less time than large coal fire plants. This ability lends itself to match the variability of renewable generation where cycling of fossil generation is required for stability. On-site energy storage at the microgrid scale is far more manageable financially and physically as compared to at the macro scale. Energy storage provides generation smoothing for intermittent renewables which could reduce fuel costs. Furthermore, since microgrids will require advanced controls and metering, a load hierarchy should be implemented to allow for shedding of non-essential loads during peak demand. The macro to microgrid point of common coupling (PCC) allows for bi-directional connection energy flow and islanding (disconnecting) during macro grid outages. These features allow for untapped values streams that are not found with simple backup generation mated with an uninterrupted power supply (UPS). Additionally, these new value streams must be utilized to offset the additional capital cost of implementing a microgrid.

When considering converting existing feeder lines from utility distribution into microgrids, a size limit is reached at the substation level. This is because the PCC is located on the low voltage side of the substation. Additional infrastructure could be added which would allow combining several feeders into a larger microgrid. However, it is logical that some benefits of microgrids begin to diminish beyond a certain geographical size due to efficiency losses. Therefore, multiple local microgrids could be conceived that are commonly connected to the macro grid via substations and high voltage transmission lines. During emergency situations the macro grid may experience an outage, leaving the transmission network inoperable and each microgrid islanded. In these situations, it would be impossible to transmit energy between microgrids without additional switchgear since the macro grid would appear to the microgrid as an infinite load.

4 The Benefits of Microgrids

Hyams et al. provides a basis of microgrid value streams stating "Microgrid value streams are derived principally from two sources: (1) the benefits provided by the specific DER applications that are deployed within a given microgrid (e.g., clean generation and controls systems) and (2) the additional benefits created by the unique configuration of DERs into the microgrid architecture (e.g., reduction of line losses and improved efficiency associated with cogeneration). As small networks that use distributed generation, energy storage and system control technologies, microgrids will provide benefits associated with the particular DER applications and energy distribution design and control schemes deployed. For example, benefits might include the greater energy efficiency achieved through the use of CHP, reduced air pollution from the incorporation of renewable technologies, or enhanced power quality and reliability from the application of advanced storage and power conditioning technologies. The scale and type of benefits created from microgrids will also vary depending on customer and location-specific circumstances, including the thermal and electric demands of interconnected loads, the configuration of the local distribution system, the ability of existing macro-grid infrastructure to meet local or regional load growth, the local utility's mix of resources, and the retail cost of energy, among others." [5]

Hyams et al. also describes additional benefits that can be attained through networking. "A substantial body of research has established the benefits associated with distributed generation and DERs. While many of these benefits flow directly to system owners or hosts energy cost savings and improved reliability, for example other benefits are more diffuse and frequently may not be captured by system owners (e.g., the value of reduced CO_2 emissions or electric distribution system deferrals). Unlike single-site applications of DG, a microgrid may create additional value through the exchange of power or heat across multiple sites. By using appropriate electronic controls and aggregating multiple end-user loads a microgrid can combine some of the benefits of the macro-grid (e.g., load diversity and economies of scale associated with aggregated demand) with the benefits of DERs." [5]

A taxonomy of microgrid value streams are also described by Hyams et al. "The potential benefits provided by microgrids can be bundled into four principal categories: economic, environmental, reliability and security. Figure 1 provides a basic schematic of these categories and the benefits typically associated with each. These categories are fluid in the sense that certain benefits commonly spill over into multiple categories. For example, reduced line losses simultaneously deliver both economic and environmental benefits and reduced power interruptions can provide both economic (e.g., uninterrupted productivity) and security/safety benefits." [5]

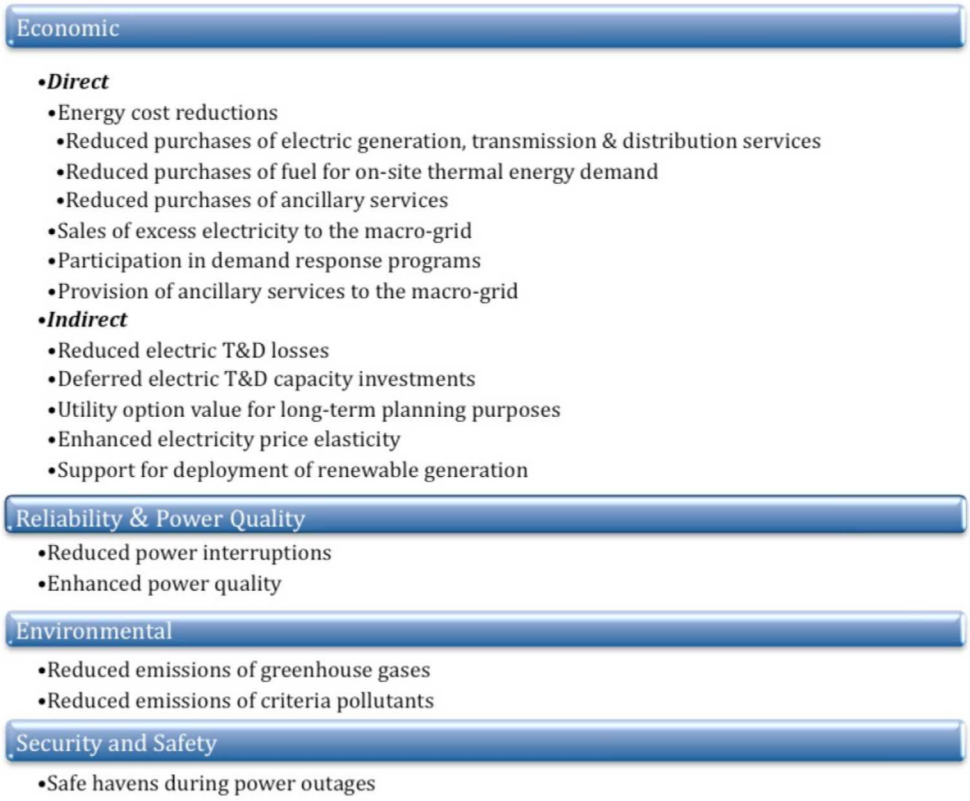

Figure 1: Taxonomy of Microgrid Value Streams [5].

5 Motivation and Potential Advantages of Networked Microgrids

Microgrids have four attributes: generation, storage, loads, and the ability to connect/disconnect from a primary distribution system. This means that a wide range of devices and systems are in fact microgrids. Hybrid electric vehicles, CHP enabled buildings/industrial parks are two examples. Connecting several HEVs to a conventional building's power supply creates a networked microgrid scenario and creates the potential for optimally satisfying the needs of all the microgrids in the collective through a process of service arbitration. It should be noted that microgrids will likely have a nominal draw from their host power distribution system and may operate in islanded mode only occasionally.

There are companies moving towards networked microgrids at the building scale, such as Emerge Alliance [6]. Their vision of a proposed system is one that, "Forms a family of application/area-specific DC microgrids that, when interconnected, create a resilient and versatile building or campus energy network. Each semi-autonomous microgrid can operate with or without the need for connectivity to a higher-order supervising microgrid" [6]. This suggests that industry has identified the benefits of Networked Microgrids and actively solving the implementation issues.

The examples of networked microgrids above are at the distribution level. However, this type of peer-to-peer connection could be done at all levels of power delivery - distribution, sub-transmission, and transmission. At the transmission level, peer-to-peer is standard and governed by Independent System Operators, such as MISO, PJM, or CAISO. These governing bodies provide optimal generator set points in 5 min intervals to best utilize the transmission system. A similar approach could be used at lower voltage levels.

Excess capacity, likely built into a microgrid design to accommodate future growth, can be used to reduce uncertainty in the load serviced by the utility. Since observability is limited in much of the distribution system, microgrids with advanced metering and controls could improve this. Reduction in uncertainty could stem from microgrid load profiles that are flat or that can track a prescribed profile through on site generation. Flat load profiles are desired by utilities and has lead to demand and TOU tariffs aimed at this goal.

Distributed sensing and actuation are needed to fully enable a self-healing structure. Since a network of microgrids, by definition, has these attributes, they have the necessary components to implement self-healing properties. Single microgrids are subject to their own failures. The redundancy due to the increased DG of multiple microgrids allows sharing of the resources. Redundant pathways and generation are requirements for self-healing and resiliency. These resources need to be optimized to reduce costs while satisfying both the individual microgrid requirements and those of the network.

Devices that were designed for a single function (e.g. a PHEV) can be instilled with additional functions, simply by their connection with other microgrids. For example, aftermarket products are available for PHEVs (Converdant, http://www.converdant.biz) that

allow export of power for general use or interconnection.

6 Status of Networked Microgrids Today

The Tres Amigas SuperStation project's goal is connecting the Western Interconnection, Eastern Interconnection and ERCOT for controlled power sharing across North America, Figure 2. In essence, this is a peer-to-peer, transmission-level connection of three massive, autonomous microgrids for the purpose of increasing renewable penetration and equalizing energy prices.

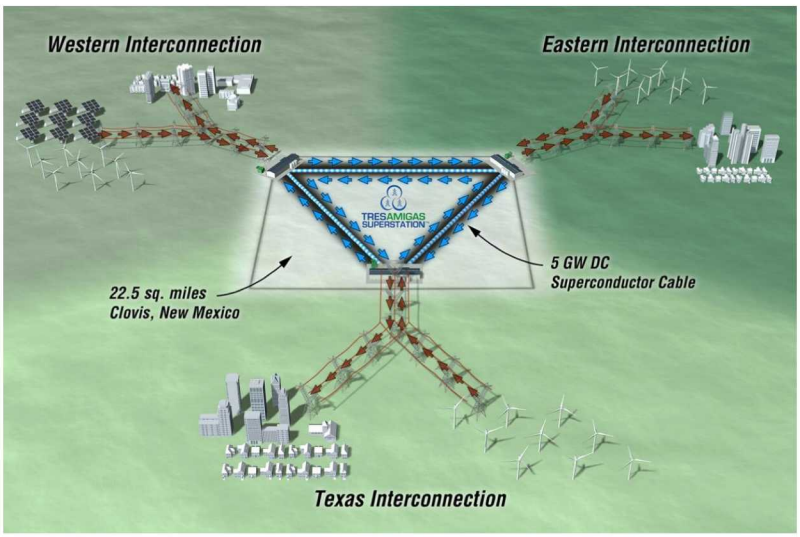

Figure 2: The Tres-Amigas SuperStation Concept.

Large buildings (e.g. Willis Tower) have multiple substations located on multiple floors and could be configured as a network of microgrids to provide resiliency within.

Sandia National Labs recently completed a three year, Grand Challenge LDRD to investigate high penetration of renewables within a networked microgrid configuration. One of the outcomes was an analysis methodology for maximizing performance and minimizing storage requirements for power systems consisting of networked microgrids.

Researchers have postulated the benefits of networked microgrids (Lasseter, 2011 [7]) to ensure power quality requirements. Others have suggested a top-down, utility-controlled interconnection of microgrids at the distribution level to provide self-healing functions (Vadari and Stokes 2013 [8] and Shahnia et al. 2014 [9]). Market motivations for interconnected microgrids were explored by Kasbekar and Sarker [10] where they showed an efficiency gain by reducing transmission losses. Load management and leveling was considered by Fathi and Bevrani. Mahmoudi [11] developed a power electronics control strategy for interconnecting two DC microgrids.

Below are three quotes that illustrate networked microgrid potential in various parts of the U.S. as described by energy researchers and publicists.

"Remote microgrids will see growth largely in developing economies that don't have a her-

itage of power infrastructure, Asmus said. Although, in the U.S., Alaska has what amounts to a large number of sometimes interconnected microgrids. And in certain jurisdictions' say, the vast, often isolated rural service territory of BC Hydro in British Columbia, Canada the 'obligation to serve' includes assisting remote communities to develop 'remote' microgrids." [12]

"Many smart grid observers think we'll be living in a world of federated microgrids sometime in the next decade. Universities, hospitals, office parks, military bases and 'ecodistrict' will generate much of their own power and distribute it locally via a microgrid. The main grid will interconnect all of those microgrids and provide a 'market' to receive and deliver power back and forth as needed." [13]

There are companies forming where their business model is based on constructing and selling networked microgrids such as Pareto Energy. "Pareto Energy takes a similar approach, by designing, building and operating peer-to-peer microgrid networks. Panelist Matthew Fairy, Pareto's director of sales, described a vision in which the national grid is gradually replaced over time by clusters of interconnected microgrids. This is the only way, he said, that we will be able to move to a smarter grid system. 'The move to the smart grid is impossible to achieve in one big operational mass', he explained, 'Breaking it into bite-sized pieces this is the future of the microgrid market.' Fairy described the shift to microgrids as analogous to the move from land lines to cellular phones a shift that will 'make the end product much more versatile and user friendly.' " [14] [15]

7 Vision for the Networked Microgrid

As microgrids become more common place and show value to the interconnected utility they will become an integrated "value added" element in the utility electrical distribution system. When called upon to provide economic or utility support services the microgrid must have communications links with the utility network operator or dispatch center. There will be some isolated instances when dedicated power lines are used for peer to peer operations then communication will also be needed for peer to peer operations. A vision for "Networked Microgrids" must contain the full extent of operational scenarios.

The vision for the purpose of this document is: Networked microgrids seamlessly integrate with the electricity grid or other Electric Power Sources (EPS) providing cost effective, high quality, reliable, resilient, self-healing power delivery systems.

7.1 Networked Microgrid Definition

Networked microgrids can be defined as:

Interoperable groups of multiple Advanced Microgrids that become an integral part of the electricity grid while providing enhanced resiliency through self-healing, aggregated ancillary services, and real-time communication. They result in optimal electrical system configurations and controls whether grid-connected or in islanded modes and enable high penetrations of distributed and renewable energy resources.

8 Networked Microgrid Objectives

Networked microgrids provide an enhancement for microgrids with additional value added through redundancy and distributed generation. Enabling grid modernization and interoperability of multiple smart-grid interconnections and technologies is one objective for developing and deploying networked microgrids. Supporting the existing grid infrastructure by adding resilience to the grid infrastructure, locally compensating for the variable supply of renewable energy, and supplying ancillary services such as Volt-Ampere reactive (VAR) support and voltage regulation to sections of the bulk power system is a second very important objective. Meeting end-user needs by ensuring power for critical loads, controlling power quality and reliability at the local level, and promoting customer participation through demand-side management and community involvement in electricity supply is another.

A list of common stakeholder needs for the owner of networked microgrids includes the following:

1. 100 % uptime for Critical Loads
2. Maintain critical loads while avoiding demand charges AND during times of crisis

3. Apportion available resources during times of crisis
4. Inter-operational agreements for all grid-connected conditions
5. Operations must remain profitable during times of normal operations
6. Low maintenance
7. Automatic and understandable operations

Identify R&D gaps, market barriers, conduct research and demonstrate system feasibility

9 Networked Microgrid Program Scope

Networked microgrids up to 10 MW individual rated capacity will seamlessly integrate with the electric grid and provide cost effective, reliable, resilient, self-healing power delivery systems. The Interoperable groups of multiple networked microgrids can become an integral part of the electricity grid with aggregated ancillary services, and real-time communication. They result in optimal electrical system configurations and controls whether grid-connected or islanded and enable high penetrations of distributed and renewable energy resources

10 Networked Microgrid Operational Modes

10.1 Basic Operational Modes

The basic operational modes of operation for networked microgrids are Interconnected and Islanded. The islanded modes of operation when the microgrid is not connected to either the utility or another networked microgrid include the basic requirements placed on utilities for supplying power its customers. They include frequency stability and voltage regulation, but with caveats related to the limitations of the energy resources. When loads exceed the energy resource capabilities at any point in time, the networked microgrid controller must shed non-critical loads. Load shedding should take place before the loads become excessive. This requires enough intelligence to forecast the ratio of loads to resources. The forecasting can be a preferred complex set of algorithms built into the controller or be a conservative operational mode based on previous operation. The IEEE1547.4 standard provides the guidelines for islanded microgrids [16].

When two networked microgrids are connected together and the utility is not connected, the mode of operation must become one of master-slave where one networked microgrid provides the voltage and frequency reference and the other follows. The slave micro grid can become a current source. Alternately, if frequency droop control is implemented, both microgrids can share the load at the expense of frequency regulation. If both become an islanded system then there must be an energy robbing interconnection impedance between the two to insure stability of the interconnected networked system. Interconnected networked microgrids then become a master utility with an interconnected secondary system. A provision to exchange roles will likely be required to insure optimum performance or resiliency. Integrated support for devices requiring VARs, surge capabilities, and protection-device coordination are a challenging requirement.

An interconnected and networked microgrid system that is connected to a distribution grid must provide all of the operational and interconnection requirements to loads that utility electric grids must provide. The integrated and networked microgrid systems will provide high-quality power to their loads with safety protections, synchronization, harmonic distortion limits, voltage limits, and frequency stabilization especially when load surges

occur.

The Point of Common Coupling (PCC) is typically where the standards and codes for interconnection and interoperability take effect. The same will apply to integrated networked microgrids except there are now two PCCs. New rules to cover the anti-islanding that have been in place for over a decade are now changed. The revisions to IEEE1547 Recommended Practice are being drafted. There is a new recommended practice on the way (IEEE1547a) and the revised IEEE1547.4 has provisions for allowing islanding. Results of the evolution of the microgrid concept have been captured in the latest version of IEEE1547.4. Seamless transfers from grid-interactive to islanded modes will be necessary. Networked microgrids will be required to meet the new IEEE1547a as the interconnection standard once it is published in the U.S. Other standards are also likely to provide requirements for microgrid components and systems as harmonization of international and domestic standards evolves. Regardless, R&D for advanced microgrid systems must be broad-base in order to meet today's interconnect standards, but also to support utility value propositions, such as the supply of fault current, that may yet to be reflected in current standards.

10.2 Dispatched, Scheduled, and Autonomous Microgrid Operation

Whether future networked microgrid support to utility distribution lines will be prioritized, dispatched, scheduled, or automatic will depend on many factors such as but not limited to:

- power throughput capabilities of the microgrids' resident controllers or inverter-controllers,
- speed of detection and speed of response of all equipment,
- communications and the need for dispatch,
- number and locations of microgrids on the same feeder,
- energy storage capacity and peak power delivery, and
- codes and standards requirements for interconnection and interoperability.

Networked microgrid development will provide opportunities for deploying, monitoring, and exercising new advanced capabilities, advanced control algorithms, utility interconnectivity, and resulting distribution system impacts as well as the impacts on local loads that will be supplied by the microgrid in an islanded state. Automatic or dynamic utility support by networked microgrids will need extensive testing and analysis with a majority of the interconnected systems. A networked microgrid system connected to a utility grid where the majority of the power supplied by the primary energy system should present a benign addition to the distribution system while providing reliable backup power to the microgrid system loads.

10.3 Commanded Shutdown, Ramp-Up and Ramp-Down While Grid-Interconnected

Networked microgrids, connected to a primary energy source such as a utility electricity distribution system, will have built-in algorithms and communications for shutdown, start-up, and curtailment. Each of these functionalities may also be commanded when the stability or voltage regulation of a section of distribution line is in danger of drifting out of specification due to a load/distribution mismatch. Adequate communications methods between utilities and networked microgrids will be necessary for these conditions.

Commanded shutdown that overrides normal shutdown processes will not be as likely, but if intermittent renewable energy sources such as PV are linked into the system there may be a need for curtailment, commanded startup slew rates, and energy-storage interactions.

10.4 Low Voltage and out of spec Frequency Ride Through While Grid-Interconnected

As new and revised interconnect standards emerge the advanced and networked microgrid will be required to support new functionalities that will be commonplace for DG on the grid of the future. One of the most common events on a distribution grid is voltage sag due to temporary low impedance loads or short caused by tree limbs or accidents involving the line.

The networked microgrid will be required to support the distribution system under these temporary adverse conditions. Low voltage ride through is already being demonstrated with PV systems even without energy storage in the PV system.

The LVRT capabilities of networked microgrids will likely be required as part of an inter connection agreement. Conversely, when the smart-grid capabilities on newly developed PV inverters and the new controls were first demonstrated during the DOE Solar Energy Grid Integration Systems (SEGIS) program conservative approaches were the first steps taken by Pacific Gas & Electric (PG&E) and other utilities to allow for scheduled VAR support as a smart-grid function. This was generally only where the needs for distributed VAR support were predictable. Recently, however, demonstrations of dispatched and automatic support are taking place. PG&E, for instance, reported that on March 17, 2012, a total of four LVRT events took place. The low-voltage condition was caused by momentary phase-to-phase faults on an adjacent 12 kV circuit that was fed from the same substation where a PV system was connected. The inverter provided power during that low-voltage event instead of dropping off line per the current IEEE1547 requirements when the support was needed.

According to the same report, a similar event occurred at the same location when an adjacent feeder experienced a short-circuit condition causing both A and B phases at the connected substation to experience a voltage sag to 50% of normal, which activated the inverter's LVRT capabilities. The protective relays on the faulted 12 kV circuit detected the short circuit and cleared the fault in 7 cycles. The inverters successfully rode through

the event and returned to normal operation upon clearance of the short-circuit condition. Schweitzer Engineering Laboratories (SEL) graphs were collected and reviewed by PG&E's Renewable Resource Development department. Figure 3 shows the voltage and current waveforms taken from the SEL relay on the substation.

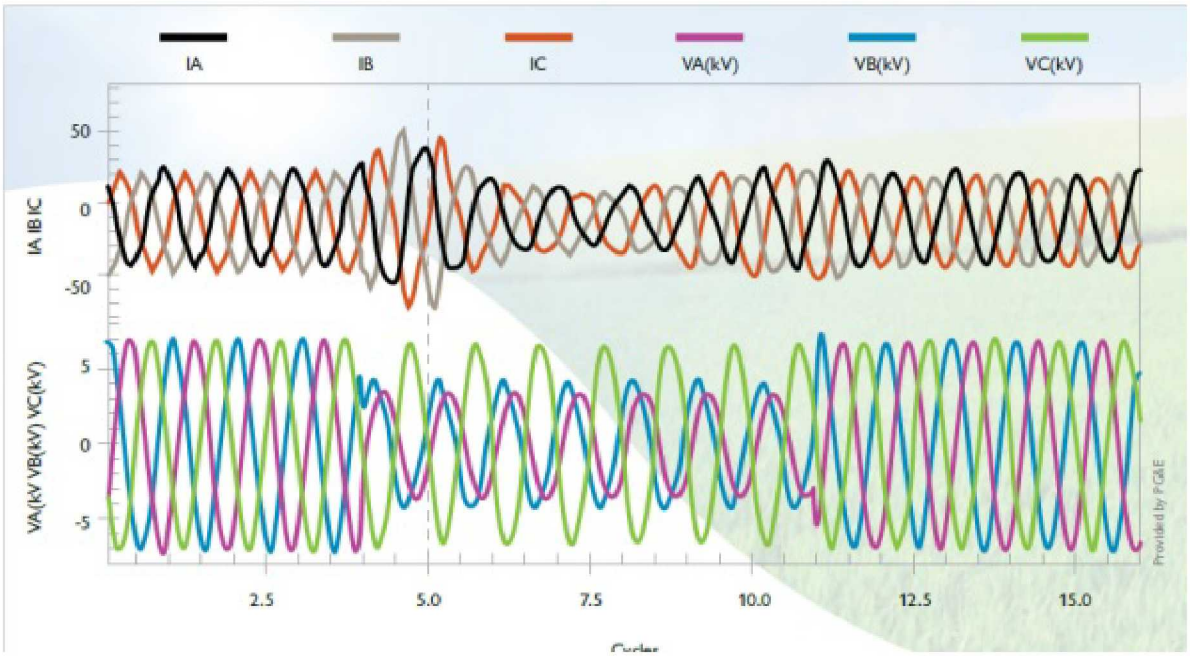

Figure 3: Voltage and current plot from the SEL relay for the voltage-sag event.

These real-time events have demonstrated the LVRT capabilities for inverters without energy storage. Extended periods of other smart-grid functionalities are probable with advanced and networked microgrid systems. Networked microgrids will require energy storage as well as advanced controls to autonomously transition further into an islanded state or to provide more extended periods of grid support.

LVRT standards for low power applications have been around since the 1970's. A commonly used standard was developed by Information Technology Industry Council (ITI) revised in 2000. The standard for allowed voltage deviation is shown in Figure 4 [17]. The purpose was to provide manufactures with acceptable boundaries to design computer power supplies.

The curve provides guidance on the following operating regions:

- Steady-State Tolerances
- Voltage Swell
- Low-Frequency Decaying Ringwave
- High-Frequency Impulse and Ringwave
- Voltage Sags
- Dropout
- No Damage Region
- Prohibited Region

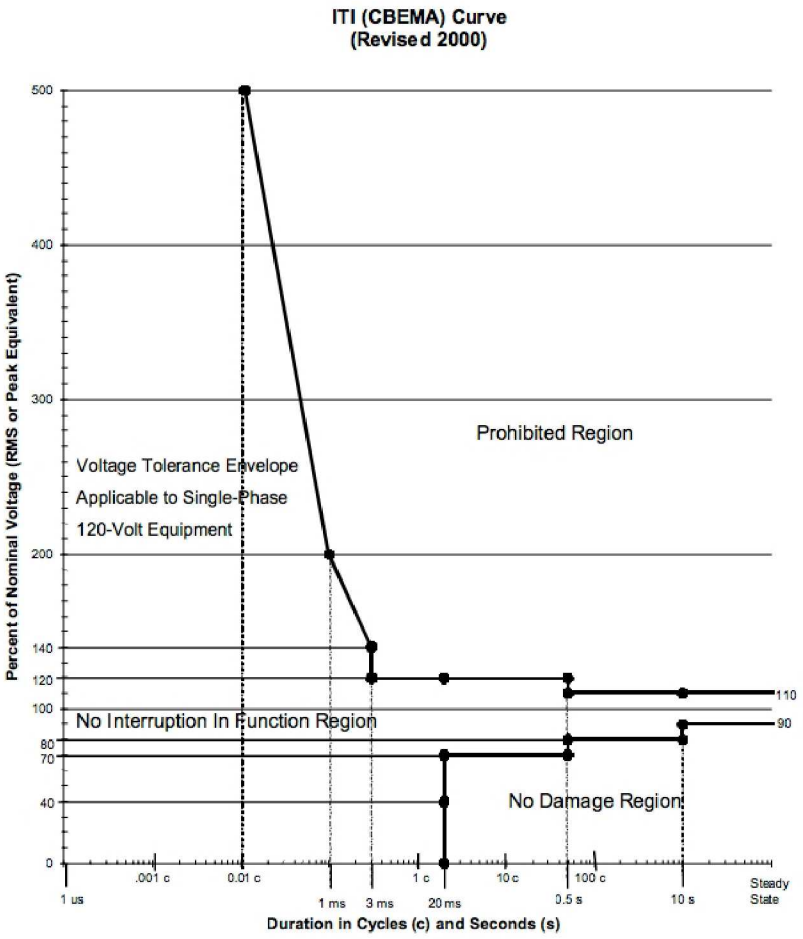

Figure 4: Voltage-Time ITI Curve for 120V AC Electronics.

10.5 Black Start While Islanded

Black start while islanded should be considered as a separate mode of operation. It is a critical requirement when reconnection to loads occurs in the islanded state especially after the microgrid has been inoperable but loads are still connected. This connection of the microgrid to the loads in the islanded state when motor loads and other loads require surges of power is called black start. Where conditions on the main grid result in the microgrid being disconnected from the main utility, the microgrid should transition either seamlessly or as quickly as possible and continue to operate as connected DG. During the reconnection state, the operating states of reconnecting to the load reclosing must be considered as must the capability of the advanced microgrid to provide startup surges and voltage regulation.

Local controllers in close co-ordination with a distributed microgrid central controller must be evaluated from the dynamic-operation point of view. The black-start functionality will help assure local power system operation, power supply reliability, and protection to critical loads. Black-start functionalities within advanced microgrids will need minor changes in

available standards such as IEEE 519 [18] for harmonics and voltage, with time-dependent or load-dependent specifications called out for microgrids. Load shedding may be an alternative method to assure the microgrid power supply that meets today's interconnection standards requirements.

11 Networked Microgrid Technical Challenges

The model of centralized generation is gradually being replaced by a distributed generation model [19]. The emerging technologies in renewable and distributed generation can have lower emissions and cost. The microgrid concept gives a solution for integration of a large number of distributed generations without causing disruption in the utility network. Microgrids also allow for local control of the distributed generation units and attests to the flexibility to operate autonomously during disturbances in the main network. However, one of the main challenges for microgrid design and control is that generation capacity is very close to load demand. In addition, with the stochastic nature of most renewable energy sources there is a large need for energy storage[20], [21], [22]. Energy storage can also be used mitigate both long-term and short-term system transients. For example, a long term transient would be the generation variations over hours and days from a wind turbine or photo-voltaic array due to weather patterns. Short-term transients could include step changes A proper energy storage strategy will include devices that can respond with the proper bandwidth of the system transients of the sources and loads.

The technical challenges for microgrids and networked microgrids can be summed up as:

- Control Systems - algorithms, software and communications
- Hardware and Architecture - interconnections, energy storage
- Modeling and Simulation - tools to design, develop and optimize system
- Testing - hardware testing platforms to validate solutions

11.1 Control Systems

Within microgrids, there are many approaches to the control and optimization of each element. A centralized approach is able to reach higher levels of performance at the cost of single points of failure and lack of flexibility. A distributed and de-centralized approach allows a very flexible system that can adapt to changing system structures and situations. A typical approach to distributed control is droop control [23], [24]. In DC microgrids, droop control is equivalent to creating a virtual impedance between the source and the bus, such that the total load current is distributed to the sources based on the weighed sum of the droop settings. The standard way to implement droop control is through the duty cycle control of the DC to DC converter interface to the bus.

A global optimization of efficiency and flexibility is possible given perfect system-wide information. However, more information implies an increasingly complex communication infrastructure and with it an increase in failure modes. A method that distributes the control to the individual components and minimizes the need for communication could provide stability and robustness, but may limit performance to local optima [25], [26]. For instance, if the power system has a dedicated communication network, then more information can be shared and integrated into each local physical layer control. Total load power, losses, transients, and general system health could be factored into the optimal design. Nevertheless, the lag time in a communication system would be much longer than the reaction time required to correct a high frequency transient problem [27]. This means that local information should be the foremost basis of the control, but there may be a trade off with long term performance.

In the last decade, concepts and technology from the field of multi-agent systems (MAS) have been applied to the problem of managing autonomous microgrids [28]. Several researchers have addressed the application of MAS technology to DC microgrids and distributed power electronics. A relatively recent survey of MAS application to microgrids is given by2011 Kulasekera2011. Much of the early MAS research focused on the economic aspects of notional microgrid electricity markets, but more recent work is addressing the challenging real-time coordination and control problems that arise in microgrid operations, including managing multiple microgrids.

11.1.1 Hardware Development

Centralized control framework empowered by computer systems and applications has advanced system observability and controllability. The control center sends commands either to open or closed on the pole-mounted and substation devices for reconfiguration during fault occurrence. The operations have undergone major improvements with state-of-the-art technologies. The communication technologies include the pole-mounted devices that are located around the distribution network, transmitting the analog and digital measurements to the distribution dispatching center (DDC). The pathways are between communication devices and DDC. As these metering devices are also connected with the switching devices, the dispatchers at DDC would be able to send the control commands to the devices either in open or closed state through SCADA functions. Remote control capability includes the switching devices in distribution substation or the any part of the distribution network with FRTU/FTU. This is recommended by DMS applications to identify the most economic paths during emergency conditions that help restoring power from other feeders with sequential switching procedures. The hardware deployment is depicted in Figure 5. Major categories of IP-based metering infrastructure in both primary and secondary distribution networks are summarized as follows:

1. Remote terminal units (RTU) instrumenting circuit breakers at the feeder head of distribution substations in primary network.

2. Feeder remote terminal units (FRTU/FTU) connecting to load break switches or re-

closers in primary network. The combined elements of switches and sensors are referred as "feeder automated switches."

3. Distribution transformer monitoring (DTM) units in secondary network.

4. "Smart" meters at the customer level of secondary network. This is referred to AMR or AMI. Energy meters (EM) is used throughout the chapter.

5. Frequency disturbance recorder (FDR) in secondary network. This is sometimes named as "single-phase phasor measurement units (PMU)."

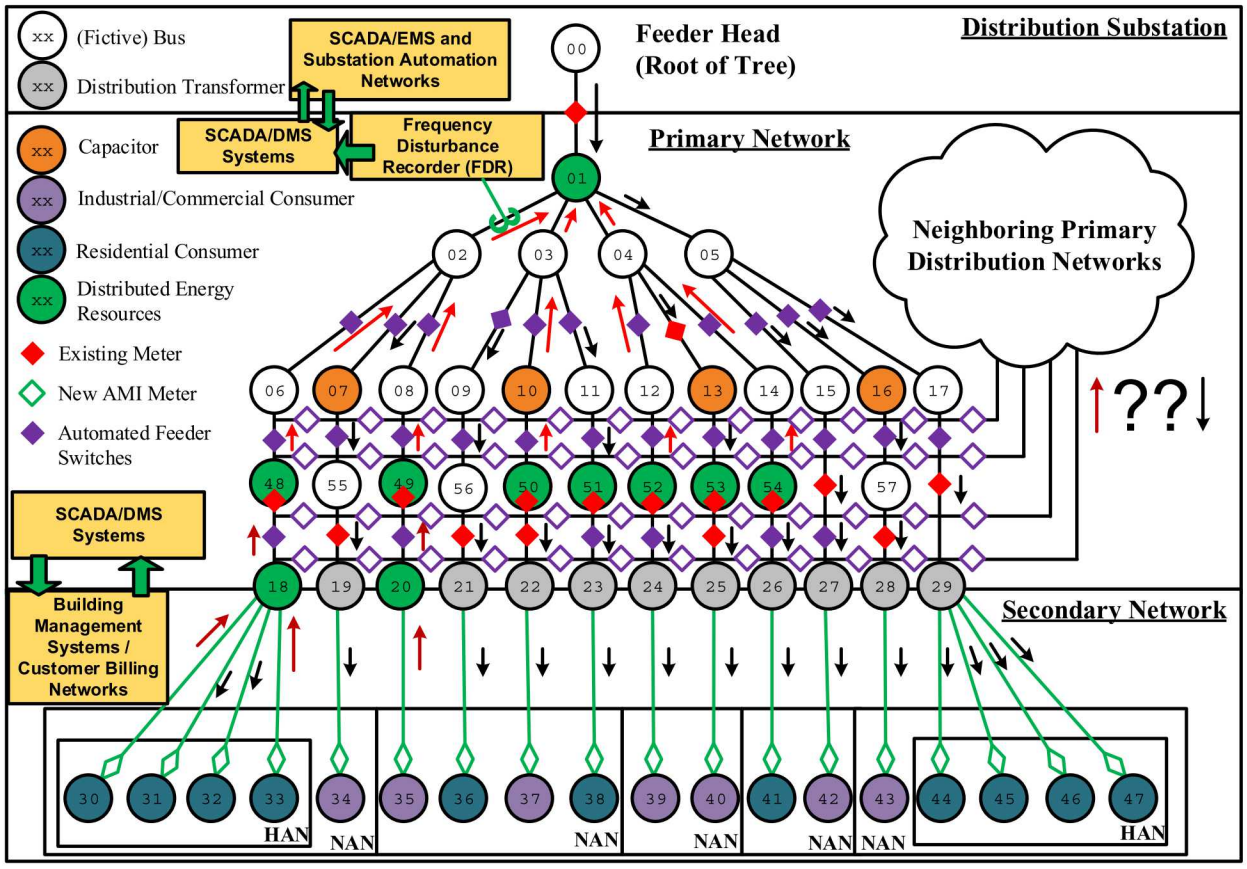

Figure 5: Hardware Deployment.

11.1.2 DC Microgrids

Since many renewable sources, such as photovoltaics, are DC sources they require power conversion to connect to an AC system. In addition, most electronic loads require a DC power conversion step and many energy storage technologies, such as batteries or super-capacitors are also DC. Therefore a DC system is a viable option for a power distribution within a microgrids [29], [30]. However, a DC microgrid with a high penetration of renewable sources

can require large energy storage capacity to maintain the system and to mitigate variations in the sources. Therefore hardware for DC power distribution within individual microgrids within the network will need further study. DC microgrid architectures are already a focal point of research and are common within applications such as telecom and data centers[31], [32]. However, the application of DC microgrids networked through a AC distribution system has not been studied.

11.2 Connectivity

Loop/radial configuration of the network is part of the overall algorithm to detect "what-if" scenarios and ensure optimal solutions [33], [34]. Figure 6 illustrates the possibilities of enhanced bidirectional power flow by including new metering points and distributed generation within the primary and secondary networks. The figure also shows the complexity of the new infrastructure and the combinations of bidirectional power flows from neighboring distribution networks through additional tie-switches. As the setup of the distribution network topology differs from transmission network, i.e., radial/mesh and unbalanced/balanced in nature, a BW/FW sweeping technique has been developed to adopt the properties of network configuration.

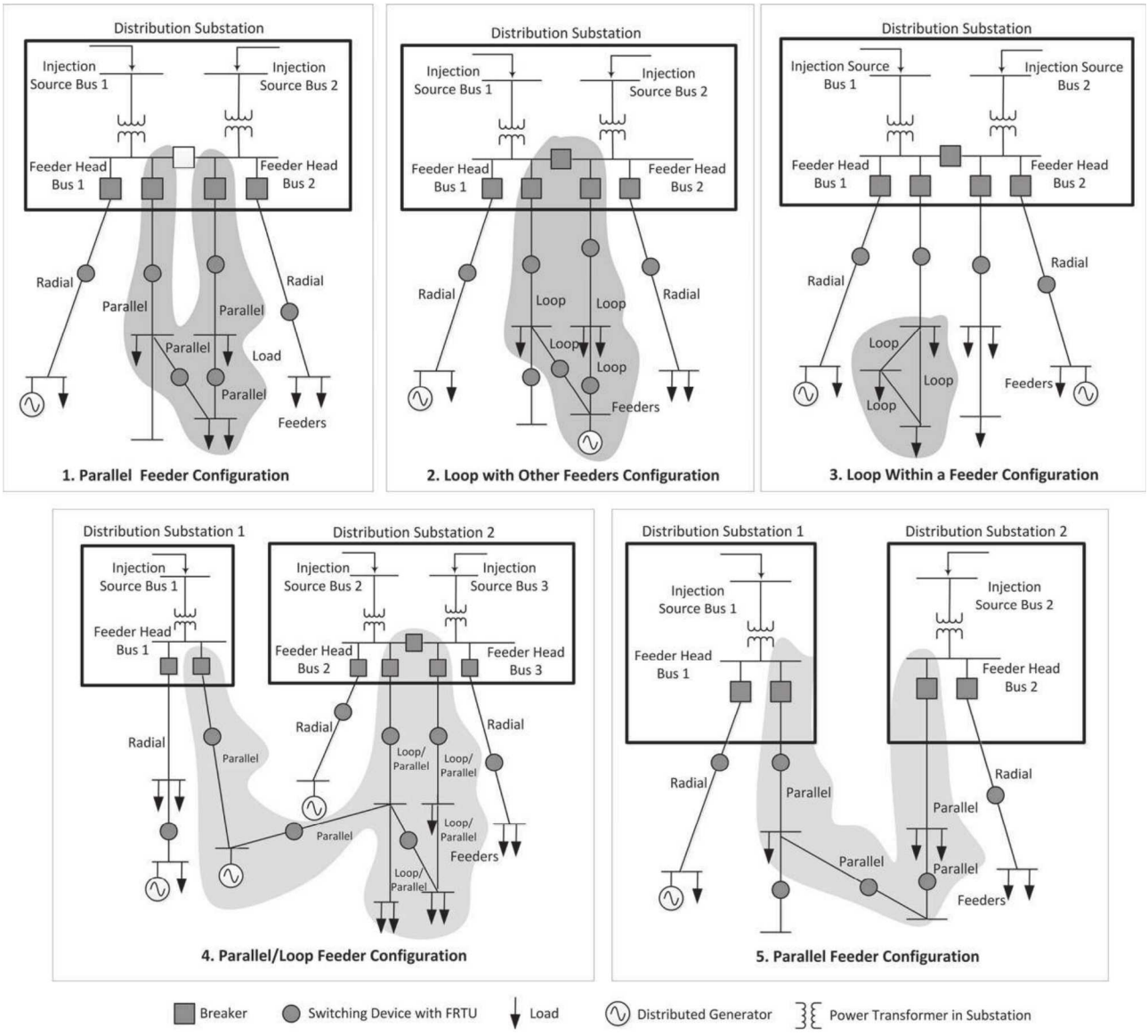

Figure 6: Connectivity.

Improved algorithms have been exhaustively addressed to exploit the radial structure of the unidirectional power flow for fast and flexible unbalanced networks [35], [36], [37]. Also, an algorithm to challenge the existing BW/FW technique has been improved in [37]. A robust method for multiphase power flow and generalization of radialized distribution network is proposed in [36]. An important factor of all these techniques is to employ the fast and higher accuracy of computational results to evaluate overall power losses. A systematic loss analysis by a Taiwan power utility has been reported in [38].

11.3 Measurement Systems

Over the past decade, advanced metering infrastructure (AMI) devices have been deployed to improve the infrastructure of electrical distribution grids. These devices not only include the highly publicized "smart" meters replacing the older mechanical meters for consumers, but also additional remote metering and instrumentation across electrical distribution grids. The key feature of deploying this technology is to increase the number of additional IP-based data collection points across the electrical grid so that a closer to real-time measurement status of the electrical distribution grid can be available to utilities. These data points are networked over an existing communication infrastructure connecting to a distribution dispatching center (DDC) with distribution management system (DMS) with supervisory control and data acquisition (SCADA) functionality. The functionalities include accumulating the data, performing network analysis and outage management, and then recommending engineering solutions to improve system reliability.

Cyber infrastructure of distribution control networks has been the central hub of system operations where DMS is the key component of the SCADA system. Typically, it is a multi-computer system networked with redundant servers and workstations with online software packages. The basic applications provided by DMS generally include network outage management, unbalanced power flow, short circuit analysis, fault location, isolation and service restoration, load modeling and forecast. The system enables operators to reconfigure the system under emergency conditions for improving overall system reliability.

With increased reliance on cyber infrastructure to maintain and control microgrids, cyber security will become a challenge. When considering AMI a recent paper by Guo explores security strategies against Distributed Denial of Service (DDoS) attacks [39]. While this only focuses on one specific attack, much more research in this area is needed.

In an effort to retrofit existing analog meters with additional observability, Tang explored outfitting meters with smart phones [40]. An application on the phone captures pictures of the meter, through image processing estimates energy use, then transmits the results back to a central location. While a proof of concept, this could reduce the cost of obtaining high quality energy information for an existing system.

11.4 Scalability

Another challenge in testing technologies for networked microgrids is the scalability of the solution. For example, an optimization algorithm for a ten node microgrid may not scale to a hundred node microgrid. Furthermore, technologies developed for single microgrids may not scale to networked microgrids. To test scalability, a testbed needs to be scalable. A highly modular system could be developed that has the potential to be a single microgrid with 10's of nodes, up to several networked microgrids each with 100's of nodes. The key to this testbed would be custom designed power electronics hardware that will be building blocks of the scalable microgrid. Each power electronic block could be programmed to emulate various energy technologies (sources, loads, storage) and could also emulate DC, single phase AC or three phase AC systems. A testbed of this kind would be highly valuable in testing and validating the scalability of controls and algorithms over several orders of magnitude. It could also be capable of testing a wide range of technical challenges from short-term transient stability issues to long term economic optimization.

11.4.1 Optimal Control of Scalable Microgrids

Recent research has focused on scalable networked microgrid optimization and controls architectures. These techniques scale linearly or polynomially with increasing number of states and control inputs. Sandia National Laboratories Secure Scalable Microgrid Grand Challenge LDRD project is one example [41].

Nonlinear control principles have recently been applied to single DC microgrids in work by Robinett et al. [42] and expanded to networked DC microgrids by Wilson et al. [22]. In both papers, the Hamiltonian Surface Shaping and Power Flow Control (HSSPFC) is applied which ensures stability and performance. This work was then coupled with an optimization scheme in [43], where the target was networked microgrids with 1) wind turbines and 2) on a naval ship with three microgrids. Future work in this area would be to apply nonlinear control to problems that are much larger, 100's or 1000's of nodes to ensure these algorithms are scalable.

It would be advantageous it these algorithms applied to AC, DC, and Hybrid AC/DC networked microgrids because existing power systems will be interconnected with new advanced microgrids.

Formulating a closed form optimal control solution of networked microgrids would allow for vast numbers of microgrids to be controlled instantaneously. If a closed form solution cannot be found, numerical optimization must be employed. This adds computation time since many methods are iterative and require solving n power flow equations plus m constraints. To explore closed form solutions, the DC networked microgrid equations developed by [43] were selected. In this related work by Sandia National Laboratoies LDRD the closed form solution was found for single microgrids [41]. Therefore this solution was expanded to the networked microgrid case. The DC power flow equations are given as Eq 1-4, with

index limits given as Eq 5. In these power flow equations, Eq 1 represents a reduced order model for a DC boost converter circuit, working between low source and a microgrid bus. A similar boost converter model is used in Eq 3 which converts between the microgrid and transmission line buses. Eq 2 and Eq 4 are the individual microgrid buses and transmission or connection buses respectively. These equations are subject to indexing functions given as Eq. 5.

$$L_{ij}\dot{i_{ij}} = -R_{ij}i_{ij} - \lambda_{ij}v_{Bj} + v_{ij} + u_{ij} \tag{1}$$

$$C_{Bj}\dot{v_{Bj}} = \left(\sum_{i=1}^{m_j} \lambda_{ij}i_{ij}\right) - \frac{v_{Bj}}{R_{Bj}} - \left(\sum_{i=1}^{m_{Lj}} \frac{v_{Bj}}{R_{Li}}\right) + u_{Bj} + \left(\sum_{l=1}^{\Sigma_{k=1}^{q} E_{jk}} \bar{s}_{j\kappa_j(l)}\big(\lambda_{Cj\kappa_j(l)}\big) i_{Cj\kappa_j(l)}\right) \tag{2}$$

$$L_{Cj\kappa_j(l)}\dot{i_{Cj\kappa_j(l)}} = -R_{Cj\kappa_j(l)}i_{Cj\kappa_j(l)} - s_{j\kappa_j(l)}\big(\lambda_{Cj\kappa_j(l)}\big)v_{T\kappa_j(l)} - \bar{s}_{j\kappa_j(l)}\big(\lambda_{Cj\kappa_j(l)}\big)v_{Bj} + u_{Cj\kappa_j(l)} \tag{3}$$

$$C_{Tk}\dot{v_{Tk}} = \left(\sum_{l=1}^{\Sigma_{j=1}^{p} E_{jk}} s_{\iota_k(l)k}\lambda_{C\iota_k(l)k}\dot{i}_{C\iota_k(l)k}\right) - \frac{v_{Tk}}{R_{Tk}} + u_{Tk} \tag{4}$$

$$1 \le i \le m_j, \quad 1 \le j \le p, \quad 1 \le l \le \sum_{k=1}^{q} E_{jk}, \quad 1 \le k \le q \tag{5}$$

To explore the steady state closed form solution space, a radial networked microgrid topology was chosen since it represents the simplest form of networking. The connection topology is defined using matrix E, Eq 6 and the number of boost converters per microgrid defined using m, Eq 7

$$E = \begin{bmatrix} 1 \\ 1 \end{bmatrix} \tag{6}$$

$$m = \begin{bmatrix} 2 \\ 2 \end{bmatrix}, \tag{7}$$

In Figure 7, the test case is shown in graphical form. Note that in the figure, the microgrid boost converter energy sources, the microgrid loads, and the transmission line loads were omitted for clarity. Furthermore, the power flow switches at the connections were set to $s = \lambda$ and $\bar{s} = -1$, meaning the transmission line bus is at a higher voltage then the microgrid busses.

The dynamic power flow equations for the example shown in Figure 7 are given as Eq 8-16.

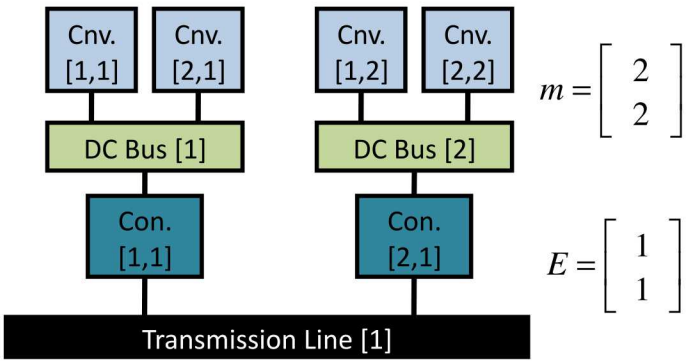

Figure 7: Example 1: Networked Microgrid Example.

$$L_{11}\frac{di_{11}}{dt} = -R_{11}i_{11} - \lambda_{11}v_{B1} + v_{11} + u_{11} \tag{8}$$

$$L_{21}\frac{di_{21}}{dt} = -R_{21}i_{21} - \lambda_{21}v_{B1} + v_{21} + u_{21} \tag{9}$$

$$L_{12}\frac{di_{12}}{dt} = -R_{12}i_{12} - \lambda_{12}v_{B2} + v_{12} + u_{12} \tag{10}$$

$$L_{22}\frac{di_{22}}{dt} = -R_{22}i_{22} - \lambda_{22}v_{B2} + v_{22} + u_{22} \tag{11}$$

$$C_{B1}\frac{dv_{B1}}{dt} = (\lambda_{11}i_{11} + \lambda_{21}i_{21}) - \frac{v_{B1}}{R_{B1}} + u_{B1} - (i_{C11}) \tag{12}$$

$$C_{B2}\frac{dv_{B2}}{dt} = (\lambda_{12}i_{12} + \lambda_{22}i_{22}) - \frac{v_{B2}}{R_{B2}} + u_{B2} - (i_{C21}) \tag{13}$$

$$L_{C11}\frac{di_{C11}}{dt} = -R_{C11}i_{C11} - \lambda_{C11}v_{T1} + v_{B1} + u_{C11} \tag{14}$$

$$L_{C21}\frac{di_{C21}}{dt} = -R_{C21}i_{C21} - \lambda_{C21}v_{T1} + v_{B2} + u_{C21} \tag{15}$$

$$C_{T1}\frac{dv_{T1}}{dt} = (\lambda_{C11}i_{C11} + \lambda_{C21}i_{C21}) - \frac{v_{T1}}{R_{T1}} + u_{T1} \tag{16}$$

$$\tag{17}$$

To formulate the steady state optimization problem a general cost function is defined, which is made from the lost power in each of the converters, Eq 18. In general, the cost function is integrated over some define interval (e.g. t_i to t_f). However in steady state, all terms inside the cost function are stationary. Therefore, the cost function can be simplified and the integral and its limits removed. This has the effect of producing a different but proportional cost. This simplified approach is applied to the example case (Figure 7) and given as Eq 19, where the indices are applied appropriately.

$$f = \int_{t_i}^{t_f} \sum \frac{1}{2}(R_{ij} {i_{ij}}^2) + \sum \frac{1}{2}(R_{Cij} {i_{Cij}}^2)\, \mathrm{d}t \tag{18}$$

$$f = \frac{1}{2}(R_{11}i_{11}^2 + R_{21}i_{21}^2 + R_{12}i_{12}^2 + R_{22}i_{22}^2 + R_{C11}i_{C11}^2 + R_{C21}i_{C21}^2) \tag{19}$$

The original set of Equations (8 - 16) are solved for steady state by zeroing the dynamic terms and become the nine constraint equations of the optimization problem, Eq 20 - 28.

$$g_1 = -R_{11}i_{11}^2 - \lambda_{11}v_{B1}i_{11} + v_{11}i_{11} = 0 \tag{20}$$
$$g_2 = -R_{21}i_{21}^2 - \lambda_{21}v_{B1}i_{21} + v_{21}i_{21} = 0 \tag{21}$$
$$g_3 = -R_{12}i_{12}^2 - \lambda_{12}v_{B2}i_{12} + v_{12}i_{12} = 0 \tag{22}$$
$$g_4 = -R_{22}i_{22}^2 - \lambda_{22}v_{B2}i_{22} + v_{22}i_{22} = 0 \tag{23}$$
$$g_5 = (\lambda_{11}i_{11} + \lambda_{21}i_{21})\, v_{B1} - \frac{v_{B1}^2}{R_{B1}} - (i_{C11}v_{B1}) = 0 \tag{24}$$
$$g_6 = (\lambda_{12}i_{12} + \lambda_{22}i_{22})\, v_{B2} - \frac{v_{B2}^2}{R_{B2}} - (i_{C21}v_{B2}) = 0 \tag{25}$$
$$g_7 = -R_{C11}i_{C11}^2 - \lambda_{C11}v_{T1}i_{C11} + v_{B1}i_{C11} = 0 \tag{26}$$
$$g_8 = -R_{C21}i_{C21}^2 - \lambda_{C21}v_{T1}i_{C21} + v_{B2}i_{C21} = 0 \tag{27}$$
$$g_9 = (\lambda_{C11}i_{C11} + \lambda_{C21}i_{C21})\, v_{T1} - \frac{v_{T1}^2}{R_{T1}} = 0 \tag{28}$$
$$\tag{29}$$

The equations are further simplified by substituting boost converter power terms given as Eq 30 - 38 into Eq 20 - 28, yeilding Eq 40 - 48.

$$P_{11} = \lambda_{11} v_{B1} i_{11} \tag{30}$$
$$P_{21} = \lambda_{21} v_{B1} i_{21} \tag{31}$$
$$P_{12} = \lambda_{12} v_{B2} i_{12} \tag{32}$$
$$P_{22} = \lambda_{22} v_{B2} i_{22} \tag{33}$$
$$P_{B1} = \frac{v_{B1}^2}{R_{B1}} \tag{34}$$
$$P_{B2} = \frac{v_{B2}^2}{R_{B2}} \tag{35}$$
$$P_{C11} = \lambda_{C11} v_{T1} i_{C11} \tag{36}$$
$$P_{C21} = \lambda_{C21} v_{T1} i_{C21} \tag{37}$$
$$P_T = \frac{v_{T1}^2}{R_{T1}} \tag{38}$$
$$\tag{39}$$

$$g_1 = - R_{11} i_{11}^2 - P_{11} + v_{11} i_{11} = 0 \tag{40}$$
$$g_2 = - R_{21} i_{21}^2 - P_{21} + v_{21} i_{21} = 0 \tag{41}$$
$$g_3 = - R_{12} i_{12}^2 - P_{12} + v_{12} i_{12} = 0 \tag{42}$$
$$g_4 = - R_{22} i_{22}^2 - P_{22} + v_{22} i_{22} = 0 \tag{43}$$
$$g_5 = P_{11} + P_{21} - P_{B1} - i_{C11} v_{B1} = 0 \tag{44}$$
$$g_6 = P_{12} + P_{22} - P_{B2} - i_{C21} v_{B2} = 0 \tag{45}$$
$$g_7 = - R_{C11} i_{C11}^2 - P_{C11} + v_{B1} i_{C11} = 0 \tag{46}$$
$$g_8 = - R_{C21} i_{C21}^2 - P_{C21} + v_{B2} i_{C21} = 0 \tag{47}$$
$$g_9 = P_{C11} + P_{C21} - P_T = 0 \tag{48}$$

The number of constraints can be reduced by solving constraints g_1 - g_4, g_7 and g_8 for the quadratic currents ($i_i j$). The negative solution is selected because this solution produces minimized power, given as Eq 49 - 54

$$i_{11} = \frac{V_{11} - \sqrt{V_{11}^2 - 4P_{11}R_{11}}}{2R_{11}} \tag{49}$$

$$i_{21} = \frac{V_{21} - \sqrt{V_{21}^2 - 4P_{21}R_{21}}}{2R_{21}} \tag{50}$$

$$i_{12} = \frac{V_{12} - \sqrt{V_{12}^2 - 4P_{12}R_{12}}}{2R_{12}} \tag{51}$$

$$i_{22} = \frac{V_{22} - \sqrt{V_{22}^2 - 4P_{22}R_{22}}}{2R_{22}} \tag{52}$$

$$i_{C11} = \frac{V_{B1} - \sqrt{V_{B1}^2 - 4P_{C11}R_{C11}}}{2R_{C11}} \tag{53}$$

$$i_{C21} = \frac{V_{B2} - \sqrt{V_{B2}^2 - 4P_{C21}R_{C21}}}{2R_{C21}} \tag{54}$$

These currents are then substituted into the cost function, f (Eq 55) and constraint equations g_5, g_6, reducing the number of constraints down to three. The remaining constraints are g_5, g_6, and g_9 (Eq 56, 57, & 58). Now only power terms and known quantities remain in the cost function and constraint equations.

$$\begin{aligned} f = &\frac{\left(v_{11} - \sqrt{{v_{11}}^2 - 4\,P_{11}\,R_{11}}\right)^2}{8\,R_{11}} + \frac{\left(v_{12} - \sqrt{{v_{12}}^2 - 4\,P_{12}\,R_{12}}\right)^2}{8\,R_{12}} + \\ &\frac{\left(v_{21} - \sqrt{{v_{21}}^2 - 4\,P_{21}\,R_{21}}\right)^2}{8\,R_{21}} + \frac{\left(v_{22} - \sqrt{{v_{22}}^2 - 4\,P_{22}\,R_{22}}\right)^2}{8\,R_{22}} + \\ &\frac{\left(v_{B1} - \sqrt{{v_{B1}}^2 - 4\,P_{C11}\,R_{C11}}\right)^2}{8\,R_{C11}} + \frac{\left(v_{B2} - \sqrt{{v_{B2}}^2 - 4\,P_{C21}\,R_{C21}}\right)^2}{8\,R_{C21}} = 0 \end{aligned} \tag{55}$$

$$g_5 = P_{11} + P_{21} - P_{B1} - \frac{v_{B1}\,\left(v_{B1} - \sqrt{{v_{B1}}^2 - 4\,P_{C11}\,R_{C11}}\right)}{2\,R_{C11}} = 0 \tag{56}$$

$$g_6 = P_{12} + P_{22} - P_{B2} - \frac{v_{B2}\,\left(v_{B2} - \sqrt{{v_{B2}}^2 - 4\,P_{C21}\,R_{C21}}\right)}{2\,R_{C21}} = 0 \tag{57}$$

$$g_9 = P_{C11} + P_{C21} - P_T = 0 \tag{58}$$

At this point, the independent variables to solve for are $P_{11}, P_{21}, P_{12}, P_{22}, P_{C11}$, and P_{C21}. The partial derivatives are taken with respect to the cost function and constraint functions

to form a transposed Jacobian matrix, J. This allows Lagrange's equations to be formed as shown in Eq 59.

$$L(i) = J(i,1) - \Lambda_1 J(i,2) - \Lambda_2 J(i,3) - \Lambda_3 J(i,4), \quad 1 <= i <= 6 \tag{59}$$

where Λ_1 - Λ_3 are Lagrange multipliers. A result that is clear at this point is the number of Lagrange multipliers match the total number of buses in the system; one for each microgrid and one for the connection bus between them.

Next the Lagrange equations are solved in terms of the independent variables giving Eq 60 - 65.

$$P_{11} = \frac{\Lambda_1 {v_{11}}^2 (\Lambda_1 + 1)}{R_{11}(2\Lambda_1 + 1)^2} \tag{60}$$

$$P_{21} = \frac{\Lambda_1 {v_{21}}^2 (\Lambda_1 + 1)}{R_{21}(2\Lambda_1 + 1)^2} \tag{61}$$

$$P_{12} = \frac{\Lambda_2 {v_{12}}^2 (\Lambda_2 + 1)}{R_{12}(2\Lambda_2 + 1)^2} \tag{62}$$

$$P_{22} = \frac{\Lambda_2 {v_{22}}^2 (\Lambda_2 + 1)}{R_{22}(2\Lambda_2 + 1)^2} \tag{63}$$

$$P_{C11} = \frac{{v_{B1}}^2 - \frac{(v_{B1} + 2\,\Lambda_1\, v_{B1})^2}{(2\,\Lambda_3 + 1)^2}}{4\,R_{C11}} \tag{64}$$

$$P_{C21} = \frac{{v_{B2}}^2 - \frac{(v_{B2} + 2\,\Lambda_2\, v_{B2})^2}{(2\,\Lambda_3 + 1)^2}}{4\,R_{C21}} \tag{65}$$

The solved boost converter powers are then back substituted into the constraint equations, Eq 66 - 68

$$g_5 = \frac{\Lambda_1\, {v_{11}}^2\, (\Lambda_1 + 1)}{R_{11}\,(2\,\Lambda_1 + 1)^2} + \frac{\Lambda_1\, {v_{21}}^2\, (\Lambda_1 + 1)}{R_{21}\,(2\,\Lambda_1 + 1)^2} - \frac{v_{B1}\left(v_{B1} - \sqrt{\frac{{v_{B1}}^2\,(2\,\Lambda_1 + 1)^2}{(2\,\Lambda_3 + 1)^2}}\right)}{2\,R_{C11}} - P_{B1} = 0 \tag{66}$$

$$g_6 = \frac{\Lambda_2\, {v_{12}}^2\, (\Lambda_2 + 1)}{R_{12}\,(2\,\Lambda_2 + 1)^2} + \frac{\Lambda_2\, {v_{22}}^2\, (\Lambda_2 + 1)}{R_{22}\,(2\,\Lambda_2 + 1)^2} - \frac{v_{B2}\left(v_{B2} - \sqrt{\frac{{v_{B2}}^2\,(2\,\Lambda_2 + 1)^2}{(2\,\Lambda_3 + 1)^2}}\right)}{2\,R_{C21}} - P_{B2} = 0 \tag{67}$$

$$g_9 = \frac{{v_{B1}}^2 - \frac{(v_{B1} + 2\,\Lambda_1\, v_{B1})^2}{(2\,\Lambda_3 + 1)^2}}{4\,R_{C11}} + \frac{{v_{B2}}^2 - \frac{(v_{B2} + 2\,\Lambda_2\, v_{B2})^2}{(2\,\Lambda_3 + 1)^2}}{4\,R_{C21}} - P_T = 0 \tag{68}$$

The next step is to solve the constraint equations for the Lagrange multipliers, Λ_1 - Λ_3, and substitute into the power equations (Eq 60 - 65) to find the individual optimal boost converter powers required. Once required power is known, the individual duty cycles can be determined from Eq 30 - 38 after solving for required currents given in Eq 49 - 54.

However, coupling in the Lagrange multipliers between the constrain equations prevents the determination of a closed form solution. If the power into and out of each bus was given, then the closed form solution method holds. This optimization problem could alternatively be solved using one of many iterative optimization methods, such as SQP (sequential quadratic programming).

11.5 Modeling and Simulation

Modeling and simulation is a key component of complex, engineered systems including networked microgrids. Giacomoni et al. describes a simulation effort for autonomous microgrids which closely resemble the attributes of the Advanced Microgrid concept described earlier [44]. At least three levels of model fidelity are required for networked microgrid development whose objectives are (1) global design and optimization, (2) distributed control system design, and (3) detailed power grid performance.

At the global design and optimization level the focus is on quasi steady-state power flow, ignoring high frequency transients. This serves two purposes. First, it is aid to sizing microgrid components to meet networked microgrid and utility performance goals. A good example is the DER-CAM application [45] that helps developers size CHP, storage, and renewables. This type of code would need to be expanded to include the benefits of sharing power via the networked microgrid concept and to include a utility perspective either in terms of benefits or requirements. A subset of this model could also be used for developing optimal networked microgrid energy management strategies, possibly executing in real-time as part of the distributed control system.

Control system design often relies on simplified models of a dynamic system that retain the dominant transient response characteristics. Since the effectiveness of a networked microgrid will be heavily dependent on the performance of control strategies that negotiate power sharing it will be critical that the key transient features are identified and included. The trade-off between execution time and predictive capability must be managed so that reliable information on closed-loop stability can be assessed while providing a reasonably short analysis cycle. Ideally, this model would also be suitable for refinements to optimal energy management analysis.

The highest fidelity model is needed for final evaluation of closed loop stability and to explore any complex emergent behavior associated with the distributed control architecture. By their nature, reduced order models used for preliminary control system design will often under-predict instability scenarios. This model, while likely slow to execute, is necessary for final evaluation of the entire closed loop, networked microgrid.

11.5.1 Networked Microgrid Modeling Tools

A scalable networked microgrid simulation tool was developed in MATLAB/Simulink; a screen capture is given in Figure 8. This simulation implements the networked microgrid model described in [43] using the Euler integration method. The unique characteristic of this simulation is setup is very efficient and requires the user to modify an external setup script defining the network topology and number of sources per microgrid. The model loads this setup file and automatically sizes and links the dynamic equations to match. This alleviates cumbersome and tedious model construction. The purpose for this type of simulation is to test scalable control and optimization algorithms.

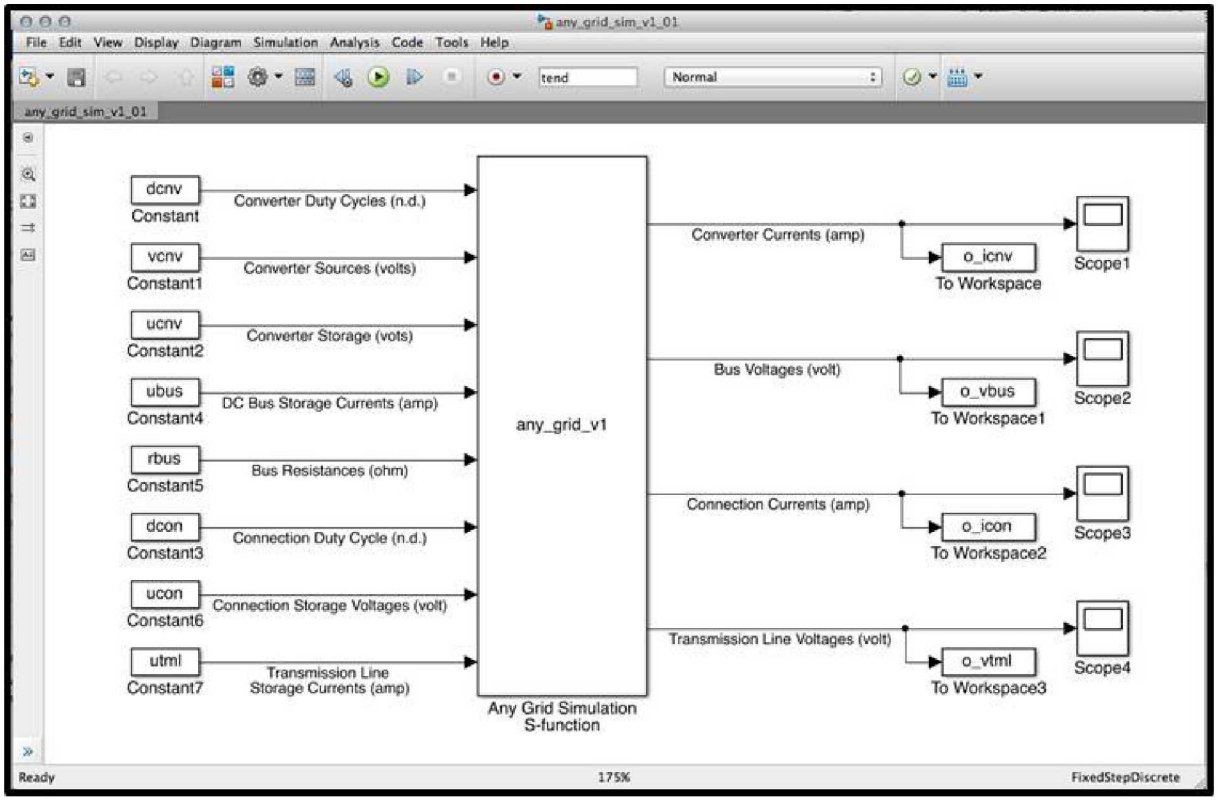

Figure 8: Scalable DC Networked Microgrid Model

11.5.2 Networked Microgrid Canonical Example

In order to study the effects of networked microgrids, a minimum example must be formulated. When considering fully coupled networks, the number of connections, C, is governed by Eq. 69, where N is the number of nodes or microgrids. What is immediately apparent is the quadratic growth of fully connected networks. In a practical sense, networked microgrids will never be fully connected. However, this problem choosing the correct number of connections needs to be investigated. Therefore to understand this redundancy, the mini-

mum number of connections needs to be greater than the number of nodes. With this in mind, Figure 9 shows that four microgrids is the minimum example to study as the canonical example.

$$C = \frac{N(N-1)}{2} \tag{69}$$

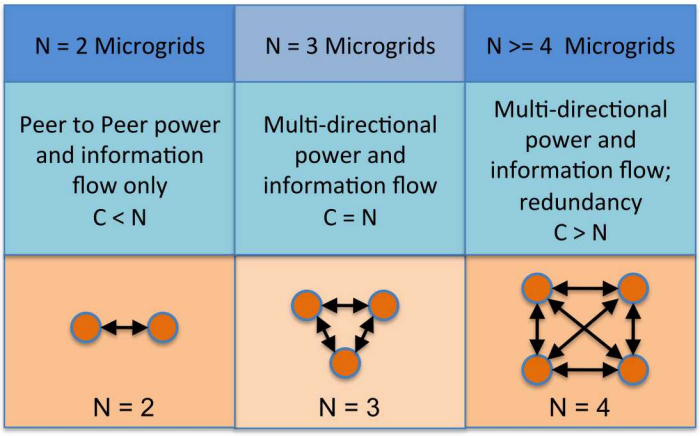

Figure 9: Microgrid Connection Scaling.

11.5.3 DER-CAM Modeling of Canonical Example

As suggested in Section 11.5.2, a four microgrid/building example was formulated and optimized using DER-CAM to understand economic benefits from networking. Monthly energy use data was collected from four different businesses located at the Houghton County Industrial Park, additional details of this park are given in Appendix B. DER-CAM requires electrical and heating curves representing 24 hour averaged data for each month and in each month it needs a peak day, a week day and a weekend day. Since this granularity of data was unavailable, load curves were selected from DER-CAM's internal database and scaled to match the monthly energy usage from the industrial park. The curves were selected to represent an industrial plant, a campus, an airport, and a retail store. Since this analysis was intended to be general, the location and solar irradiance was arbitrarily selected as northern CA. The energy tariffs were also chosen from this region provided by PG&E and were TOU based on the size of the customer. Technologies to select from were limited to NG DG, PV, and battery storage. Three test cases were executed as listed below:

1. Base Case, purchase from utility
2. Four individually optimized microgrid solutions
3. One aggregate microgrid

To provide a basis for comparison, the base case calculates the utility purchased energy costs without installing generation and storage, listed in Table 1.

Table 1: Base Case Estimated Annual Energy Costs

Test Case	Energy Costs
Campus	$229,963.17
Airport	$122,327.90
Industrial	$104,217.15
Retail	$39,620.51
Total	$516,822.94

The second case was to optimize the individual businesses against their respective tariff levels and install generation to minimize the utility purchased energy and provide a payback period of ten years or less. The third case is to sum the load profiles into a single aggregated customer and optimize against a different tariff structure that was appropriate for the customer size. Test case results for two and three are shown in Table 2. The optimized energy costs are given along with the difference from the base case, representing savings. The installed generation/storage mix is also shown for each case along with base annual energy purchase and after installing the microgrid. To compare the three cases, the individual cases were summed to form a total energy cost. This allows direct comparison to the base and aggregated cases shown in Table 3. After installing the individual microgrids, annual energy costs are reduced 35% with a ten year payback period. If these four businesses were to aggregate an additional costs savings an additional 14% could be achieved, although the installed system is smaller comparing the generation between the total individual and aggregate test cases. This analysis shows potential economic benefits of networking microgrids. A more detailed version of this analysis is given in Appendix C.

Table 2: Individual and Aggregate DER-CAM Results

	Test Case	Energy Costs	Electrical Cost Difference	DG & DG_HX (kW)	PV (kW)	Battery (kWh)	Utility Energy Base (kWh)	Utility Energy MG (kWh)
1	Campus	$157,325.59	$156,475.07	250	295	415	1,020,151	378
2	Airport	$71,706.19	$86,174.45	150	125	40	559,074	80,949
3	Industrial	$83,408.03	$55,271.19	60	146	358	504,701	73,316
4	Retail	$21,115.00	$27,912.34	40	37	26	150,441	24,385
	Total	$333,554.81	$325,833.05	500	603	839	2,234,367	179,028
	Aggregate	$287,023.42	$371,887.77	300	697	545	2,234,281	47,083

Table 3: DER-CAM Cost Comparison of Three Test Cases

Test Case	Energy Costs
Base total	$516,822.94
Individual total	$333,554.81
Aggregate	$287,023.42

11.6 Experimental Verification Testbeds

Validating proposed technologies, such as control and optimization approaches, architectures and hardware are a vital step and challenge. Many testbed systems have been built by researchers and industry around the US and the world. However, it is important to pair the proper testbed to the technology being tested. For example, for testing long term economic optimizations a large scale operational testbed, like the Santa Rita Jail project [46], or the White Oak Microgrid [47] are appropriate. However, to test transient response and stabilization methods these testbeds would not be proper to use since they are working power delivery systems that have active customers. Therefore, pairing the technology under test with the proper testbed is a challenge.

Sandia National Laboratories recently completed a three year, Grand Challenge Laboratory Directed Research and Development (LDRD) to investigate high penetration of renewables within a networked microgrid configuration [43]. One of the outcomes was an analysis methodology for maximizing performance and minimizing storage requirements for power systems consisting of networked microgrids. Sandia's experimental networked microgrid equipment is shown in Figure 10

11.7 Self-healing Distribution

Hyams et al. describes the self-healing aspects of a microgrid as "circuits that incorporate feeder/circuit redundancy and smart switches to allow the flow of electricity to be reconfigured on the network. Substation feeder redundancy refers to when there are two or more feeders or distribution circuits that can supply power to end users' locations. For example, if one circuit feeding a customer location is compromised by a tree fall or other outage-inducing event, a section on the circuit can open and the customer can be supplied by the alternate feed. Smart switches allow these sections to be opened or closed remotely and automatically in cases where faults have been detected and communicated through SCADA." [5] The authors illustrated the approach using the Borrego Spring microgrid example shown in Figure 11 where SCADA controlled switches facilitate isolation on particular fault scenarios.

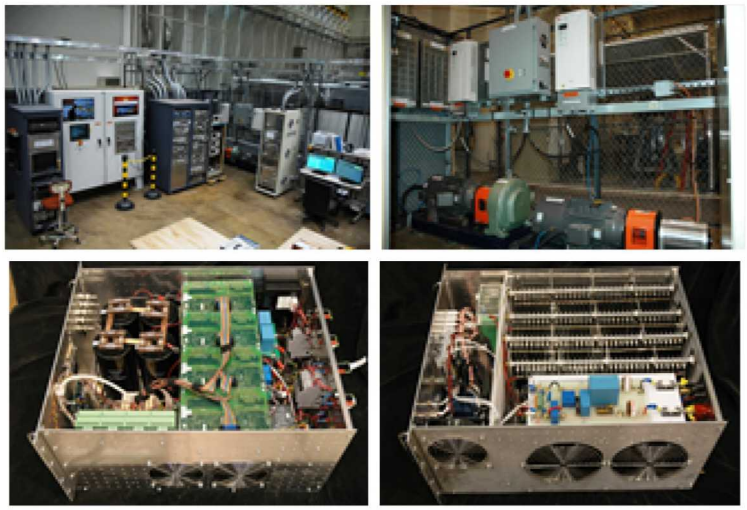

Figure 10: Microgrid testbed (upper left) mechanical source emulators (upper right), energy storage emulator (lower left), and high power digital resistor (lower right), respectively [43].

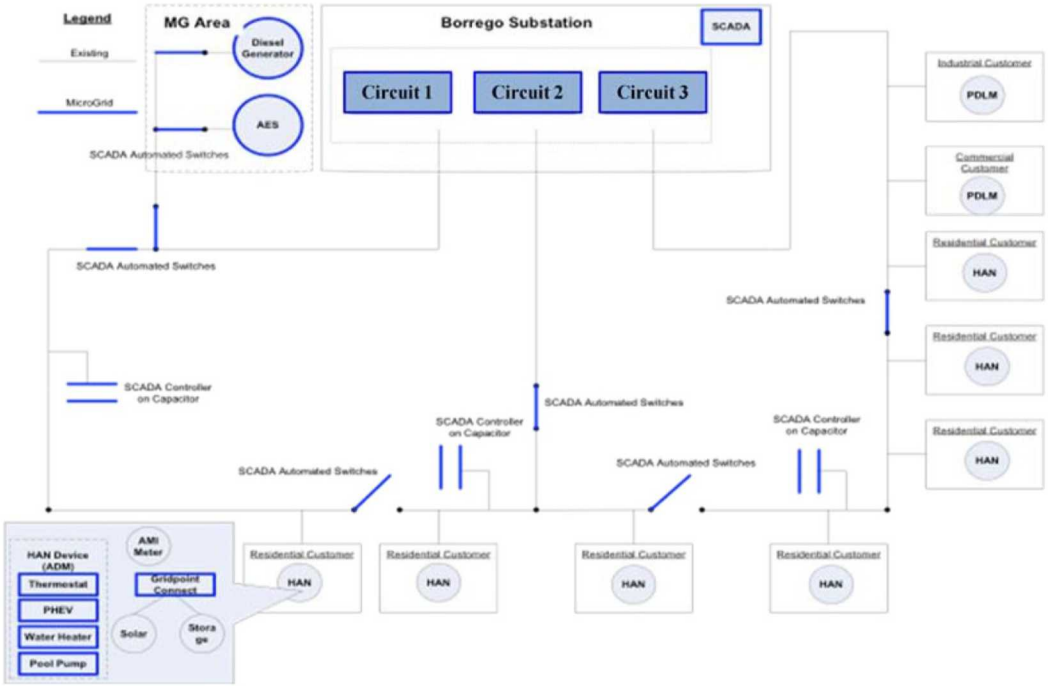

Figure 11: Circuit Diagram Showing use of SCADA on SDG&E Borrego Springs Microgrid [5].

Self-healing is one of the key features of smart grid concept [48]. The essential goal of the self-healing is to reduce the impact of power outage caused by system fault. The self-healing function can automatically respond to the power supply interruption problems based on the real-time information reported by sensors deployed at the power grid. The self-healing has been long studied for transmission system [49]. Efforts are being devoted to introducing self-healing into distribution system and microgrid. The typical technologies utilized by distribution system self-healing include automatic fault isolation and restoration technology, fault self-healing of single phase to ground fault, uninterruptible power supply (UPS) based on DFACTS, and micro grid [50]. Using microgrid for self-healing in distribution system requires performing a sequence of actions, such as sectionalizing the microgrid, building the LV network, small islands synchronization, connecting of controllable loads to the LV network, connecting non-controllable DG or DG without black start capability, increasing load, changing the control mode of DG inverters and synchronizing microgrid with the MV network [51]. Each component in the microgrid can be modeled as an agent [52], [53].

11.8 Energy Management Systems

A microgrid EMS is control software that operates and coordinates a variety of DGs, DESs, and loads to optimize the quality, reliability and sustainability of the power supply and allocation under both interconnected and islanded conditions[54], [55]. Various control strategies are developed to accommodate different microgrids. The strategies can be categorized into three major types: real-time optimization, expert system control, and decentralized control [56]. Generator control is one vital function of the EMS of microgrid. For example, the control variables for microturbines include voltage control, power factor, turbine speed and frequency [57]. With high penetration of renewable energy resources in the microgrid, both robustness and efficiency for system operation must be considered [58], [59].

12 Standards and Codes for Interconnection and Islanding

Standards and codes that spell out the requirements for networked microgrid designs, operations, functionalities, communication protocols, default modes, certifications and even commissioning are basically absent. Today's installations of microgrids are installed using parts of existing standards for DER interconnection, customized agreements between the DSO or utility, certifications of components such as inverters based upon UL1741 the Standard for Inverters, Converters and Controllers for Use In Independent Power Systems. Relevant IEEE are listed in Table 4. *Note: Italics indicates the standard is under development or revision.*

Table 4: Table of IEEE Standards that apply to Microgrids.

Standard	**Title and Description**
IEEE Std 1547™ and Amendment 1	Standard for Interconnecting Distributed Resources with Electric Power Systems [BODY STANDARD FOR THE SERIES]
IEEE P1547™ Original 2003 Amendment#1 2014	*Full revision Draft Standard for Interconnection and Interoperability of Distributed Energy Resources with Associated Power Systems Interfaces*
IEEE Std 1547™ 2011	Guide for Design, Operation, and Integration of Distributed Resource Islanded Systems with Electric Power Systems
IEEE 1547.1™ 2005	Standard for Conformance Test Procedures for Equipment Interconnecting Distributed Resources with Electric Power Systems
IEEE Std P 1547.1a 2014	*Draft amendment 1*
IEEE Std 1547.2 2008	Application Guide for IEEE 1547 Standard for Interconnecting Distributed Resources with Electric Power Systems
IEEE Std 1547.3 2007	Guide for Monitoring, Information Exchange, and Control of Distributed Resources with Electric Power Systems
IEEE Std 1547.4 2011	Guide for Design, Operation, and Integration of Distributed Resource Islanded Systems with Electric Power Systems
IEEE Std 1547.6 2011	*Draft Recommended Practice for Interconnecting Distributed Resources with Electric Power Systems Distribution Secondary Networks*
IEEE Std 1547.7 Sep 2013	*Draft Guide to Conducting Distribution Impact Studies for Distributed Resource Interconnection*
IEEE P1547.8/D5.0 2014	*Draft Recommended Practice for Establishing Methods and Procedures that Provide Supplemental Support for Implementation Strategies for Expanded Use of IEEE 1547 (Clause 8 - Recommended Practice for DR Islanded Systems)*

The Federal Energy Policy Act of 2005 calls for state commissions to consider certain standards for electric utilities. Under Section 1254 of the act: "Interconnection services shall be offered based upon the standards developed by the Institute of Electrical and Electronics Engineers: IEEE Standard 1547 for Interconnecting Distributed Resources with Electric Power Systems, as they may be amended from time to time."

Another IEEE series of standards that apply to networked microgrids especially when connected with smart grid capabilities are the IEEE 2030 Series as listed below.

IEEE Std 2030 - Guide for Smart Grid Interoperability of Energy Technology and Information Technology Operation with the Electric Power System (EPS), End-Use Applications, and Loads

This document provides guidelines for smart grid interoperability. It also provides a knowledge base addressing terminology, characteristics, functional performance and evaluation criteria, and the application of engineering principles for smart grid interoperability of the electric power system (EPS) with end-use applications and loads. The guide discusses alternate approaches to good practices for the Smart Grid.

IEEE P2030.2 Draft Guide for the Interoperability of Energy Storage Systems Integrated with the Electric Power Infrastructure

This document provides guidelines for discrete and hybrid energy storage systems that are integrated with the electric power infrastructure, including end-use applications and loads. This guide builds upon IEEE Std 2030 Guide for Smart Grid Interoperability of Energy Technology and Information Technology Operation With the Electric Power System (EPS), and End-Use Applications and Loads.

Networked microgrids that are designed for international applications are likely required to comply with a number of International Electrotechnical Commission (IEC) standards, Table 5. Some the most used interconnect standards are part of the IEC61850 series. The following table lists some of the IEC standards that will be commonly used with networked microgrids both domestically and internationally.

Table 5: Table of IEC standards that apply to Microgrids.

Standard	**Title and Description**
IEC 61850-1	Introduction and Overview
IEC 61850-7	Basic communication structure for substation & feeder equipment
IEC 61850-7-10	Communication networks & systems in power utility automation
IEC 62351	Security and more
IEC 62109-1	Safety of power converters for use in PV power systems
IEC etc of power systems	DNP3 Protocol

Code Requirements

Besides the standards for design, interconnection and interoperability there are standards that are intended to assure installation practices and requirements that pertain to installation practices, design parameters and both fire and personnel safety. The following list includes codes and installation standards that are in effect today. Codes that will apply to networked microgrids include:

- *National Electrical Code*, NFPA 70 (with the applicable edition determined by local adoption or legislation) [60]
- *National Electrical Code*, American National Standards Institute (ANSI) Standard C2 [61]
- State and local electrical codes that apply in the networked microgrid jurisdiction
- International Building Code

13 Uncertainty as a Barrier to Microgrid Development

King investigated several legal and regulatory issues in his comprehensive, survey-based study of microgrids [1]. Many of his findings are also relevant to networked microgrids. One of his findings was that a microgrid is likely to be legally viable as long as it does not attain utility status. Although potentially legal, he also describes numerous regulatory barriers that could lead to excessive risk to the investors and operators making microgrids and networked microgrids an unattractive solution. King describes the regulatory space as being "murky" and cites "the existence and relevance of utility service territories; utility services and tariffs; and interconnection procedures and technical requirements" as being the primary sources of uncertainty.

13.1 Utility Service Territories

A primary motivation for exclusive service territories is to reduce the financial risk to the utility to make long-term infrastructure investments [1]. King's state survey indicated that the need for this exclusivity would drive the illegal status of microgrids should they attain utility status. That is, creating a competitive market within a service territory. It's important to note that even if a networked microgrid did not attain utility status, its existence would likely be challenged by the utility if it operates within the utility's service territory while attempting to compete with the utility. In summary, any action that a networked microgrid takes that creates a competitive environment with the utility may lead to investment uncertainty due to legal challenges.

13.2 Utility Services and Tariffs

Many states have approved tariff structures for utilities to accommodate distributed generation [1]. Since the state boards must assure that power delivery is provided in the face of uncertain loads, the utilities are typically allowed flexibility regarding tariff structure. The financial objectives of the distributed generator owners are not the primary concern and thus the tariffs likely do not incentivize distributed generation. King also points out that tariffs developed for distributed generation may not be applicable to microgrids. If that determination is made, then utilities may provide unfavorable terms for a microgrid to participate within its service territory.

13.3 Interconnection Procedures

Fair procedures have been developed in many states for providing interconnects for distributed generator owners with a focus on maintaining stability and safety [1]. King's survey of regulatory officials indicates a mixed message for the interconnection of microgrids. They

could be classified as something other than distributed generation and thus existing DG interconnection rules would not apply. This would likely give more authority to the utility to set the rules for networked microgrid interconnection leading to the burden of proof to lie more heavily on the networked microgrid operator.

Hyams provides detailed case studies not only for interconnection but also public access for deploying physical connections separate from the utility in New York State. These are important possible barriers if non-utility connections are made across public spaces [5].

13.4 Uncertainty Reduction through Collaborative Design

Unlike single microgrids, networked microgrids can provide value streams to both the owner and the utility. To maximize the probability of success, they should be designed in conjunction with their interconnection utility. This will further enhance mutually beneficial functions and provide a shared plan for state and regulatory negotiations.

14 Value Streams Associated with Microgrids

There are various value streams associated with Microgrids that fall into two broad categories, economic and social. Furthermore, the particular value stream maybe different depending on the ownership model employed. Both types of values streams will be explored below and how these values streams are mapped to different ownership models.

It must be noted that the effectiveness of any single value stream is interdependent on many factors including, fuel prices, geographic location, local electric costs, electricity tariffs, regulations on generator emissions, real time electric pricing, zoning regulations, maintenance costs, additional personnel etc. Since the application of microgrid technology must be weighed between its potential benefits and installation costs, specific analysis must be done case-by-case.

14.1 Economic Value Streams

1. Reduced energy usage through to higher efficiency.
2. Ability to sell excess generation to macro grid.
3. Peak demand reduction.
4. Increased reliability.
5. Potentially increased power quality.
6. Provide ancillary services to macro grid.
7. Alternative to future macro grid expansion.

14.1.1 Reduced energy usage through higher efficiency

By collocating generation with load, transmission losses could be reduced by 3-4% [7]. Additional efficiency could be extracted using Combined Heating and Power (CHP) generators. The increased efficiency would allow for paying off the capital investment of upgrading to CHP systems. This investment can then be amortized with energy savings over several years. Beyond the payback period, savings are directly realized as profit.

14.1.2 Ability to sell excess generation to macro grid

During peak demand times, it may prove economical to exercise on-site generation and sell excess power to the macro electric grid. Similar to reduced energy use, selling energy would provide the means for offsetting capital investment costs. However, to take advantage of energy exports, the on site generation would likely need to be sized larger than the maximum electric consumption of the microgrid to ensure proper overhead on peak demand days.

There are several requirements under the present regulations to export power to the macro

grid. First, a microgrid would need to have access to high voltage transmission lines though a local substation. If direct access is not available, then fees would be charged from the local utility for transmission onto the bulk power grid. Next, the microgrid would need to register with the Federal Energy Regulatory Commission (FERC) as a qualified generator. After qualification, another registration process is required through the governing interconnection, which for the upper midwest is the Mid-continent Independent System Operator (MISO). The microgrid would also need to adhere to local guidelines for maintaining voltage level, power output, reactive power, and frequency. Additional considerations would be proper grounding, installation of protection equipment, coordination of maintenance, emergency and normal operation requirements.

MISO provides the day-ahead energy market from which the microgrid could bid generation on a per hour basis [62]. The non-discriminatory open access provided by MISO utilizing the day ahead bid system allows for efficient usage of the transmission line system while maintaining low costs for consumers. This is done by allowing each power generation center to bid its hour by hour generation capabilities and costs. Alternately, the demand side is also forecasts its power requirements and price it is willing to pay. MISO then matches the most cost effective generation capabilities with the demand curve, leaving the most costly generation sources for peak demand, called Market Clearing. The clearing cost is based on the most expensive generation required to meet demand while considering transmission constraints. While this hour ahead forecasting provides a planning mechanism, real-time estimates of local demand are calculated and sent to generation in 5 minute intervals. This ensures demand is consistently met while balancing transmission utilization and generation costs.

Due to effective management of resources via MISO or like markets, the power sales to the grid value stream may prove difficult to realize. In open markets, it would very seldom make economic sense to compete with Natural Gas Combine Cycle (NGCC) plants which can achieve efficiencies of 60% [63]. While losses to occur during transmission, small scale diesel generators can only achieve efficiencies of 36% to 43% [64]. This means that at best, a microgrid would be able to sell energy back to the grid a small fraction of the time which correlates with peak demand or grid disturbances.

At a markedly smaller scale, such as single home residential, net metering can provide the means for deep integration of PV or wind systems. For example roof mounted PV can be used to offset energy costs by selling to the local utility grid while the sun is shining and then purchasing electricity during off hours. While many of these systems might not quality as a microgrid since they must remain grid tied to maintain energy storage, it provides a model for microgrid expansion.

14.1.3 Peak demand reduction

High energy demand during hot summer months can push the macro grid to near breaking point. This can drive up the cost of electricity 10 - 20 times the average rates. The ability

for a microgrid to either shed nonessential loads known as Demand Response (DR) or switch to island mode could alleviate the peak loads on the macro grid. Some electric utilities provide incentives to islandable microgrids by lowering overall rates at the possibility of interrupted service when requested by the utility. "Obviously, a customer with a microgrid designed to completely carry their normal daytoday loads can easily participate in a demand response program by switching to an islanded mode of operation when market conditions are favorable."[65] The demand response incentive was exercised by the Michigan Tech campus from Nov. 2007 until Sept. 2013, when electric providers were switched and a better non-interruptible rate was obtained as described in Appendix A.

Alcoa Inc., an aluminum producing company has recently taken advantage of demand response to generate additional revenue and reducing stress to the macro grid [66]. Since producing aluminum is extremely power intensive and highly competitive in the global market, alternate ways of reducing costs must be implemented. The viability of applying DR to the smelting process as addressed using careful analysis of both the physics and economics. It was determined that significant economic value could be provided to the utility while not detrimentally impacting the process. However, it was noted that risks include lowered productivity, reduced efficiency, and potentially increased maintenance costs. Alcoa's Warrick plant has successfully proven that it is possible to dynamically regulate its smelter load up to 70 MW from the baseline of 470 MW using real-time commands from MISO [67]. The Warrick plant also participates in the MISO Ancillary services market.

14.1.4 Increased reliability

The ability to island from the macro grid during times of emergency is critical for improving reliability. Nationally, electric outages account for approximately $119 billion in lost profits and damaged goods [68]. For specific industries, such as financial, data centers, electronics manufactures, and hospitals uninterrupted power is a requirement for operation. For these industries reliability constitutes a primary value stream.

It should be noted that simply having a microgrid will not solve all reliability problems. A holistic design must be considered for reliability, this is suggested by Makhijani as, "Of course, microgrids cannot protect specific locations from flooding or damage. That is a different kind of problem. But with a system of interconnected microgrids, much of the essential equipment in Lower Manhattan out of the reach of flooding would have kept operating." [69]

14.1.5 Potentially increased power quality

Microgrids outfitted with advanced controls have the potential to improve the power quality in terms of voltage tolerance, reactive power, and harmonics. When integrating wind power, switching electronics convert time varying AC voltage and current into DC and then active power filtering converts back to well define AC [70], [71], [72]. While these steps are required for integration they also provide a platform for improving the power quality.

When considering PV integration, chemical storage, and other DC based energy sources, switching electronics are utilized to invert into DC to AC [73], [74], [75]. The active controls embedded into the switching electronics can correct for macro grid disturbances such as voltage sags and unbalanced loading of three phase systems.

The monitory benefit of improved power quality is reduced equipment failure and enhanced up-time for power quality critical process, such as data centers and electronic manufactures. This limits the number of potential participants that would need high quality power and it also requires specialized equipment to measure.

14.1.6 Supply ancillary services to grid

Ancillary Services are closely related to generation and only recently has become a new marketing opportunity due to deregulation and the creation of the energy market. Prior to deregulation, these services were vertically integrated and tightly controlled by individual utility companies. It was determine that while each utility would optimize its individual resources, it left the transmission system either under or over utilized. This lead to the founding of Independent System Operators (ISO's), such as MISO described in Section 14.1.2. The relinquishment of tight control thus has opened the AS markets which are required for delivery of bulk electricity.

The following Ancillary Service products are defined by MISO and are listed in Table 6, along with average and maximum Market Clearing Prices for winter 2013. AS are broken into two categories, Day Ahead (DA) which are forecasts of expected conditions, and real-time (RT) required to maintain grid stability. Regulation reserve is provided by online generation assets that are automatically controlled and can respond to minute-by-minute fluctuations in system loads, therefore maintaining frequency within tight tolerances [76], [77]. Spinning reserve is online generation that remains synchronized to the grid. It provides immediate response to lost grid generation or transmission capability and can reach full output capacity within 10 mins. Supplemental reserve is similar to Spinning reserve but on a longer time frame (30-60 mins to full output).

The monetary benefits to multiple microgrids for providing AS will most likely come from either DA or RT regulation reserves. Regulation reserves account for around 25% of the Locational Marginal Price (LMP), suggesting there is a significant need for these services 7. LMP accounts for macro grid transmission congestion, generation costs, and losses [78].

In recent work by [80], [81], participation in the AS market will require networking of several microgrids to achieve the minimum generation threshold. While the threshold may differ among ISO's, 1MW is a reasonable estimate for minimum capacity, which could represent 10 or more microgrids.

One area that networked microgrids could have a significant impact is reducing the amount regulation reserve required to stabilize the grid. Regulation reserve is purchased commensurate with the amount of imbalance between load and generation. It's estimated

Table 6: MISO Wide hourly MCP summary statistics for winter 2013 [79].

MCP $/MWh	Maximum	Average
Day Ahead Regulation Reserve	$47.32	$7.05
Day Ahead Spinning Reserve	$15.35	$1.41
Day Ahead Supplemental Reserve	$5.00	$0.64
Real Time Regulation Reserve	$316.00	$7.65
Real Time Regulation Mileage Reserve ($/MW)	$3.21	$0.32
Real Time Spinning Reserve	$269.61	$1.53
Real Time Supplemental Reserve	$232.72	$0.48

Table 7: MISO Hourly three month average of real time and Day ahead LMP winter 2013 (Dec. Jan. Feb.) [79]

Day Ahead	Real Time
$28.38	$27.97

that regulation accounts for 1% of the wholesale costs of electricity although it only accounts for 0.1% of the load. Regulation capacity is about 1-2% of peak load.

The relative costs of generation are shown in Figure 12. The uncertainty in the load profile, caused by load peaks, drives the need for regulation reserve. Base generation is the least expensive and provided by long timescale power plants such as nuclear or coal. Intermediate regulation is more expensive and provided by faster timescale power plants. To maintain grid stability during times of high demand, peaker generators are brought online to balance load, which can cost ten times the base production cost. Another use of peaker generators is to provide regulation reserve which is the most expensive form of energy (note in Figure 12, the regulation band is shown exaggerated for emphasis). Annually, $55 B is spent per year to provide regulation [82]. For example, PJM, an RTO servicing 20% of the US population, has 1600 generation suppliers and contracts between 400 MWh and 1100 MWh of regulation reserve at all times.

If networked microgrids could achieve just 1% penetration in regulation, it represents a very significant and mutually beneficial asset for both suppliers and customers. For example, elimination of peak demand charges alone would save customers about $53Billion per year. To show this graphically, Figure 13 shows the concept of eliminating regulation and peaker operation. This can be achieved through on-site generation provided by networked microgrids resulting in a flat consumer load profile. However, achieving a flat load profile is not trivial

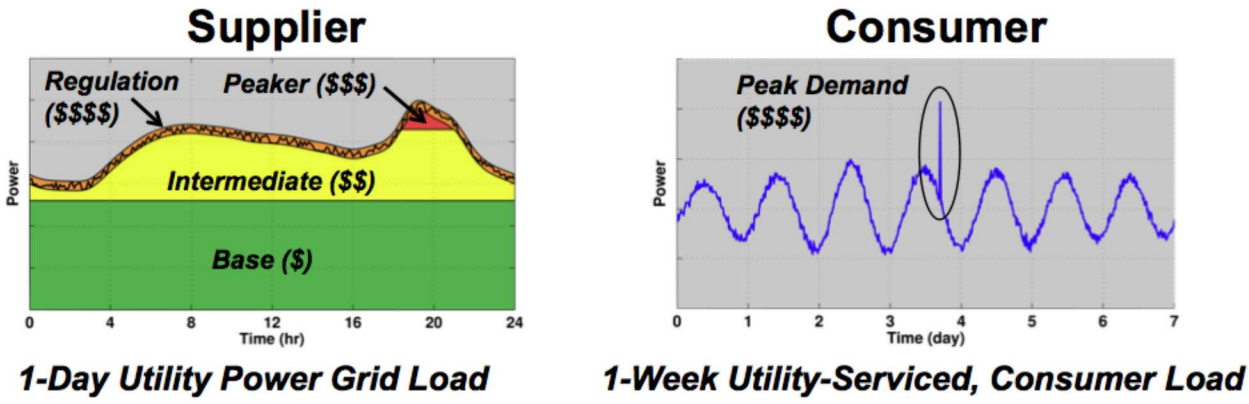

Figure 12: Depiction of relative cost of generation and customer load.

and requires optimization, an aggregation of different load profiles, and real-time actuation.

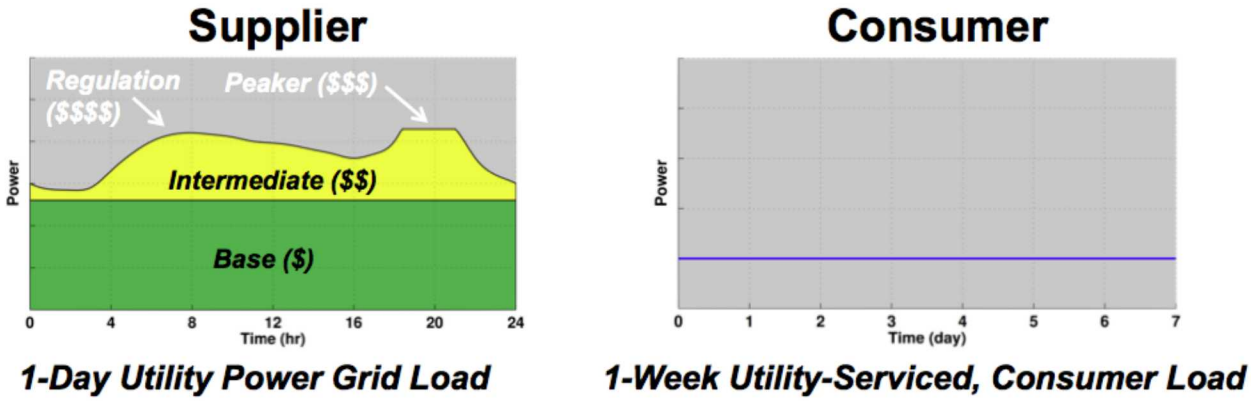

Figure 13: Regulation provided by networked microgrids resulting in flat consumer load profile.

An optimization example was formulated to understand the efficacy of the regulation reduction strategy. Four networked microgrids with individual load profiles were modeled, as shown in Figure 14. It was assumed that CHP was the generation source and it was sized to 2/3 the peak of each electrical load. In this example, an aggregator manages the networked by prescribing a microgrid to microgrid resource exchange resulting in a flat load profile to the utility. For each individual load, the generation cannot provide adequate supply at all times, which under standard tariffs may cause peak demand charges. However, when operated as aggregate, these charges are eliminated. Another observation is excess capacity which exists due to load variation throughout the day could be used in the ancillary services market.

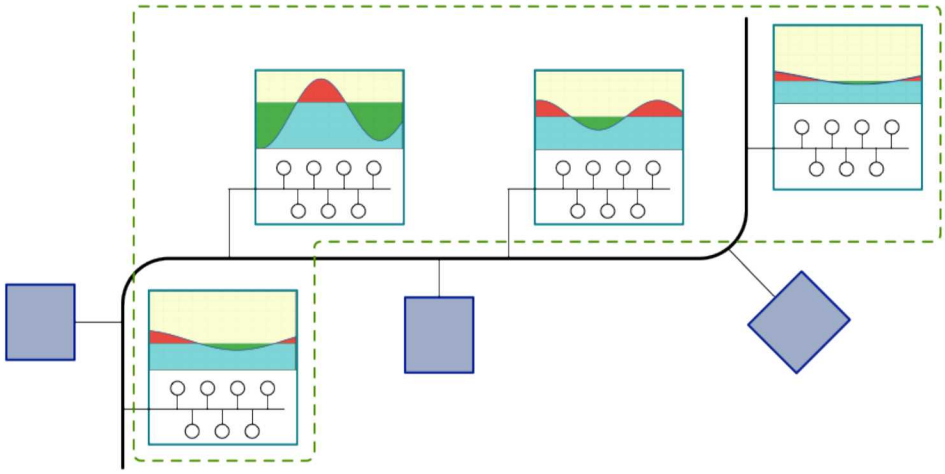

Figure 14: Four Networked Microgrid Load Example

14.1.7 Alternative to future macro grid expansion

Rising electric demand is straining the existing macro grid assets, which will require infrastructure upgrades to alleviate. Construction of new coal, nuclear, or natural gas plants is costly, time consuming, and riddled with numerous regulations. Furthermore, construction of high voltage transmission lines falls under the same difficulties. Microgrids could help reduce the need for major infrastructure upgrades by co-locating generation near its intended use.

14.2 Social Value Streams

Value streams that currently do not have direct monetary benefits are classified based on societal value. In the future, some of these value streams may become far more valuable if government regulations change or specific needs are defined.

1. Reduced emissions of greenhouse gases.
2. Increased security.
3. Human Life Support.

14.2.1 Reduced emissions of greenhouse gases

Increased penetration of renewable clean energy sources, such as wind, solar, and geo-thermal will lead to a direct reduction in green house gasses (GHG). More efficient usage of non-renewable or cleaner burning fuels would reduce GHGs. A large increase in efficiency is gained by installing CHP on new constructions or replacing older boiler systems. Furthermore, by switching from coal or oil to natural gas or bio mass, emissions are further reduced. If cap

and trade regulations are enforced, than this value stream would move from a pure social to a monetary benefit.

14.2.2 Increased security

Microgrids offer substantially higher security during emergency situations in which the macro grid is down. Strategic locations, such as the Santa Rita Jail microgrid, if left without electric service, would pose a threat to the public. Other critical government and military facilities, such as the Naval Air Warfare Center in China Lake CA and Wheeler Air base in Hawaii have implemented microgrids for electric backup. While it is understood that key locations must have backup for national security, it is difficult to monetize since actual threats are seldom.

A recent attack on PG&E's Metcalf Substation which occurred on 16 April 2013 brings serious security questions to the table. While this may have been an isolated event, it highlights the need for an alternative backup system, such as microgrids. System operators were able to divert power and prevent this attack from causing large scale blackout. The method to monetize security is to weigh the costs of improving infrastructure, such as hardening substations or installing microgrids at key facilities vs. the potential downtime costs. It becomes difficult to argue with potential economic and social impacts of multi-day/week outages.

14.2.3 Human Life Support

By increasing reliability and enabling areas to remain powered during adverse conditions and macro grid outages, human lives will be saved. Institutions that promote human life such as hospitals, nursing homes, police stations, fire stations and military installations are always required, especially during outage events. These life preserving entities are prime candidates for networked microgrids.

15 Microgrid Ownership Models

"Most of the findings in this paper have been simplified to focus attention on the issues that have been identified as most relevant to policy-makers. For this reason, microgrids are treated as a single concept. However, many regulators observed either explicitly or implicitly that all microgrid applications are not the same in the eyes of the law. Moreover, the differences among microgrids that matter most to regulators are not (as is often assumed) in the technical details of the microgrid installation and operation, but rather in the microgrid ownership and business practices, that is, in how they make money." [1]

"When asking questions about the regulatory environment for microgrids, regulators generally have a single, predominant conceptual ownership or business model in mind as they answer. When this model is challenged and new models are explored, nuances appear and the regulatory environment becomes even more muddled but possibly more open. I propose the existence of five different models that can be used to categorize microgrids by their ownership and business practices. The use of such models should help reduce confusion and facilitate policy discussion and development. The five models are: 1) Utility model the distribution utility owns and manages the microgrid to reduce customer costs and provide high reliability power to specific customers on the system. 2) Landlord model a single landlord installs a microgrid on-site and provides power and/or heat to tenants under a contractual lease agreement. 3) Co-op model multiple individuals or firms cooperatively own and manage a microgrid to serve their own electric and/or heating needs. Customers voluntarily join the microgrid and are served under contract. 4) Customer-generator model a single individual or firm owns and manages the system, serving the electric and/or heating needs of itself and its neighbors. Neighbors voluntarily join the microgrid and are served under contract. 5) District heating model an independent firm owns and manages the microgrid and sells power and heat to multiple customers. Customers voluntarily join the microgrid and are served under contract." [1]

The potential value streams with networked microgrids map differently when considering varying ownership models. Several ownership models are considered including privately owned, Utility owned, Virtual, and the combination of private and utility ownership. The ownership models must also include other stakeholders and the effects of ownership that are listed in Table 8.

15.1 Privately Owned

The growth of private microgrids will be thrust forward by decreased renewable costs and EV and emerging markets. This trend is described by Mohn, "Consumer ownership of renewable energy, electric vehicle storage and Internet-controlled building automation will force the utility to consider its role in the future. As microgrid development matures to address the energy poverty problems for developing countries, the domestic market will be seen as fertile soil for new opportunities. Microgrids will be owned by the consumer, completely invisible

Table 8: Stakeholders When Considering Networked Microgrids

Participant	Description
Independent System Operator (ISO)	Responsible for managing the macro grid, market operations and dispatching of loads and generation
Utility	Provides generation and maintenance of macro grid
Independent Power Producer (IPP)	Private owner of microgrid(s)
Grid Consumer (GC)	Purchases electric service from macro grid
Microgrid Consumer (UGC)	Purchases electric service from a microgrid
Society	All persons, corporations, and other entities effect by the electric system

to the utility." [83]

A major selling point from the perspective of microgrid consumer is improved reliability. This was the main premise of the Santa Rita Jail microgrid project where electrical outages could threaten the safety of the guards and inmates [46]. Hospitals are vital for health and safety and expected to remain open during outage events; making them prime candidates for microgrids. One example of this is the Shands Cancer Hospital at the University of Florida[65].

For private investors, the main goal is to reduce operating costs in order to maximize return on investment (ROI). Tools like DER-CAM can provide the financial basis for investing in generation and storage. Many successful projects have be centered around CHP, which typically has a payback period of seven years or less [84].

An example showing the potential benefits of networking with microgrids was carried out by the MTU campus several times during the time frame of 2007 to 2013. At that time, MTU was on an interruptible power rate from the utility (UPPCO). Interruptible power rates require either exercising onsite generation during times of economic curtailment or buying through the event which can be expensive. MTU's campus is also split by portage lake where the Mont Ripley ski hill is located across from the main portion which contains the generation. Therefore, separate feeders are required to service all of campus. To reduce overall electric costs during economic curtailment, the MTU generators were set to offset power requirements for both campus and the ski hill. Otherwise, the ski hill would be required to buy through the event at extremely high prices. This was possible though remote metering of the ski hill which was available to the on-site generators.

15.2 Utility Owned

In the article by j. St. John, it states that in some electric failure prone areas Utilities are building and operating microgrids. "Some of the first working examples of a microgrid have been installed by American Electric Power, which wants to own and operate them to help communities prone to loss of grid power and avoid building new transmission lines. And most of the microgrid projects currently underway are being led by utilities." [85] One such project is the CERTS microgrid project [86].

From the utilities prospective, microgrids can pose a threat to their revenue streams. This is pointed out in article by J. St. John "To date, electric utilities' approaches to integrating distributed energy resources using microgrids have varied widely from viewing utility distribution microgrids as an existential threat to the companies' traditional business models to active utilization of microgrid projects in order to integrate renewable energy, improve grid reliability, and reduce peak load." [87] To combat this, utilities may preemptively begin investing in microgrids in specific markets where significant profit margins may exist. For example, if a new data center is constructed and will require premium quality and uninterruptible power, the utility may contract an agreement to install and manage a microgrid. This reduces the capital cost to the data center because backup generation and UPS systems would not need to be purchased. The utility then takes on the capital investment and can charge a slightly higher electric rate for these enhanced services. The utility can then exercise peak demand reduction to the macro grid assuming available capacity of the microgrid or using DR if possible.

Utility companies have federal and state mandates for expanding their Renewable Portfolio Standard (RPS) or penetration of alternate energy [88], [89]. Microgrids provide a platform for this integration since local storage can be utilized to absorb energy fluctuations. At small scale, energy storage remains relatively economically and geographically feasible. Once energy storage increases above 1 MW, the available technologies diminish beyond the realm of microgrids [90]. Furthermore, storage at the macro scale has been significantly more expensive than generation and transmission expansion, leaving the US grid with approximately 2.5% of total power production with storage [91]. The paradigm must shift to account for the variability of renewables,

In the press release by R. Martin, utilities are investing in microgrids for multiple reasons. "Seeking to integrate renewable energy sources, improve grid reliability, and reduce peak loads, a handful of innovative utilities are moving forward with microgrid projects despite significant institutional bias and regulatory obstacles. These early initiatives herald a future in which microgrids will become a more prevalent part of the distribution utility landscape. According to a recent report from Pike Research, a part of Navigant's Energy Practice, annual vendor revenues from utility microgrids including investor-owned utility, public power grid-tied, and remote microgrids will reach nearly $1.4 billion in 2012. That number will grow to just under $3.3 billion in 2018, the study concludes." [92]

15.3 Virtual

Third party or virtual ownership will likely become a popular model. In the article by Hales, the MaaS model is suggested which combines third party investors with customers in need of high quality power. "Though customer-owned microgrids will be the dominant ownership model in the near-term, a recent study by Lux Research Associate Dean Frankel shows that Microgrid-as-a-Service (MaaS) offers flexible ownership structure that attracts third party investors and is the best opportunity for power service providers and financiers to capitalize on this growing market." [93] The microgrid becomes a service that can be purchased rather than equipment that must be installed and managed by a perspective company.

At similar microgrid service concept is expanded by Schneider, "Commercial microgrids can be funded via long-term financial agreements and project financing. Third-party developers can create a bundled power purchase agreement (PPA) and thermal purchase agreement (TPA), in which capital costs for the microgrid are converted to an ongoing operations and maintenance (O&M) cost basis. In an economically viable microgrid, PPAs and TPAs are structured so that the new overall electrical, thermal, and waste prices are lower than the existing purchased costs. The PPAs and TPAs not only yield lower energy prices, but fund capital expenses required to gain improved energy assurance and sustainability." [94]

15.4 Private and Utility Co-ownership

Deciding who owns the electricity generating equipment and wires for linking the loads can have a huge impact on how a microgrid functions. Mechanisms to allow sharing among one or more customers, as an electric cooperative, as a corporation, or as a nonprofit association will be needed. Questions such as "how much input will the end-users have on their microgrid operation?" and "what are the consequences if a customer wants to leave the microgrid entirely?" will need solutions.

How will a microgrid be regulated? Depending on the size, structure, and ownership model, the microgrid can be exempt from most federal and state regulation if it meets the standards as a FERC-jurisdictional qualifying facility (QF). The benefits of QF status include avoiding burdensome regulations regarding rate setting, finances, construction, and operation.

16 Summary

A networked microgrid concept is envisioned to be an important component of next-generation power system for improving efficiency of local power generation, reducing technical losses during power delivery, providing environment-friendly, high quality power supply as well as enhancing the reliability of power system. From the utilities perspective, existing microgrid enables the possibility of providing heterogeneous levels of reliability to various end uses. In the conventional distribution system, the utility has to provide "universal service," that is, the quality and reliability of power delivered to all customers must meet the standards. The networked microgrid concept moves control of power reliability and quality closer to the point of use so that these properties can be optimized for the specific loads served. Ongoing research topics of networked microgrids include reliability enhancement, self-healing functions, market motivations, load management and power electronics control strategy. It is envisioned that the framework will greatly impact the operation and business modal of future power systems.

Despite various potential advantages of network microgrids, there are challenges on implementation and integration with existing power grid. This includes control systems, hardware and architecture, modeling and simulation, and testing. For instance, the high penetration of DERs from microgrids could cause stability issues in transmission system. The basic operation of the microgrid requires the DER controller to have the following functions: (1) regulating power flow on a feeder as loads on that feeder change their operating points, (2) regulating the voltage of each DER as loads on the system change, (3) function that each DER can rapidly accommodate the load when the system is islanded and (4) ability of seamlessly automatic switching between islanding mode and connected mode.

Appendix A Michigan Technological University Microgrid Case Study

A.1 Summary

The microgrid installed at Michigan Technological University was studied to understand the economic basis for justifying the installation costs. A description of the microgrid is given which describes the ownership model, objectives, progression, the installed system, and economics.

A.2 Ownership model

Michigan Technological University's microgrid is privately owned and operated and is intended for self-servicing various buildings located on campus. The distribution of steam and electricity does cross underneath a public road but does not service any non-affiliated customers.

A.3 Background/Project Objectives

Michigan Tech is a public university of higher education located in Houghton Michigan. The University has 6976 total students, 497 facility, 1038 staff members and covers 925 acres. Michigan Tech is one of largest employers in Houghton County.

The thermal and electrical distribution for the campus consists of an underground tunnel system servicing a majority of the buildings. A central heating and generation system is located near the waterfront of Portage Lake. Dedicated natural gas lines are installed for specific buildings. It is used for cooking, laboratory, and other small uses.

The main impetus for investing in a microgrid system consisting of four diesel generators and automatic switchgear was to purely economic and to receive a lower electric rate from the utility. By installing generator sets, MTU moved from firm power to interruptible power, which resulted in saving $500,000 annually. A tertiary benefit of the microgrid was increased reliability during a macro grid outage. However, there could be a downtime of up to 10 minutes before the backup generation is brought online.

A.4 Progression

The addition of backup generation stemmed from determining the most cost effective electricity. In 2003 a proposal to purchase the generators was originally considered but not acted

upon. Later in 2006 the concept was revisited and drafted as part of larger campus wide maintenance program. In March 2007 the generators were available for usage. The program consisted of a $7.5 million grant from the state of Michigan and $2.5 million contributed from MTU. Prior to installation of the generators, MTU purchased power from the Upper Peninsula Power Company (UPPCO) at a firm power rate. After the generators were installed and commissioned March 2007, a new rate was achieved by switching to interruptible power, leading to a savings of $500,000/yr. In September of 2013, electric providers were switched to Wolverine Power COOP, leading to an additional savings of $100,000/yr.

Timeline of utility providers and service type:

- Prior to 2007 March: Firm power from UPPCO.
- 2007 February: UPPCO interruptible power.
- 2013 September: Provider switched to Wolverine Power Cooperative firm power.

A.5 Detailed Microgrid Description

The MTU microgrid is comprised of four diesel backup generators, a central steam system, and a one million gallon diesel storage system. During the 2007-2013 time period, the generators were used very seldom and only during a major grid outage or during an economic curtailment event. The cost of running the generators is around $200/MWh plus maintenance, which is three to four times higher than the bulk electric price. Because of this price differential, it has not proven economically sound to run the generators in non-emergency situations. As of 2013, the electric rate including distribution is around $55/MWh. Total electricity purchases for MTU FY 2013 were $2,300,000 and natural gas purchases were $2,256,000.

A CHP add-on was investigated for the generators, but would not be compatible with the existing steam system. The generators could provide only 15 psi of steam when 80 psi is required. Additionally, if waste heat capturing was added, the generators would need to run continuously. Any savings achieved though this higher efficiency would need to be saved for future equipment replacement and routine maintenance. A final consideration is the Michigan Department of Environmental Quality (DEQ) regulation which limits diesel consumption to 350,000 gallons/yr.

The one million gallon diesel storage is rarely filled since the generators remain offline most of the time. It also doesn't make economic sense to fill this tank, since the fuel must be burned or transferred to a different holding tank every 5 years to allow for inspection of tank integrity.

The overall campus electric reliability has dramatically increased after the generators were installed. Although the macro grid has an outage approximately once a year and ranges from a few minutes to hours, the down-time per event is limited to 10 minutes which allows the diesel generators to come online. The financial benefit of having near continuous

power has not been researched.

The concept of demand response has been considered, but there is little that can be applied at a large scale. Some ideas of incentive based reduced energy usage per room or building are being considered. To facilitate this, additional metering my be installed at the subsystem transformers which provide usable voltages of 120, 208, 277, 480 stepped down from the 12.4 kV grid supply.

Each of the generators at full output (2.25 MW) burn 159 gallons of #2 diesel fuel per hour. Given that diesel fuel contains around 37.95 kWh/gallon, the effective efficiency of the generators is 37.3% at full capacity.

The MTU microgrid topology is given in Table 9, where connection types, resource descriptions, and users are highlighted.

Table 9: Microgrid Topology

Project originator	Private Sector
Energy Usage	Self-service
Crosses Public Street	Yes
Form of Energy Distribution	Electric and Thermal
Interconnection	Low voltage 12.4kV
Operate Independent of Macro Grid	Yes
Multiple Resources	Natural Gas, Diesel, Electric, Oil Backup for Heating
Certified Electric Generator	No
Number of Distinct Customers	One (MTU)
Types of End Users	Administrative Offices, Classrooms, Residential Dormitories, Research Laboratories, and Food Services Operations
Installation cost	$3.6 M

A.6 Technologies Employed

Technologies are broken into two categories, existing and new. Existing technologies are considered on site assets that serviced MTU prior to the installation of the microgrid system. The new technologies are those installed to create a microgrid. The energy annual statistics for MTU are given in Table 10.

Existing Facilities

- Electric: Life preserving backup generation installed inside 21 buildings around campus.
- Thermal: Four Natural Gas Boilers, 230,000 lbs/hr Steam Total Capacity, centrally located. Boilers #2 & #3 have stack condensers which convert 280° steam into 120° water used for heating the GLRC building.

New Facilities

- Electric: Four 2.25MW Caterpillar generators, diesel only.

Table 10: Energy statistics (YF 2013)

Description	Quantity
Peak Electric capacity	9 MW
Peak Electric Demand	6 MW
Annual Electric Usage	36,900 MWh
Peak Thermal Demand	90,000 lbs/h steam
Cooling Capacity	15% of buildings
Annual Thermal usage	324854 MMBtu
Diesel Storage Capacity	1 million gallons
Peak electric Demand	6 MW
Estimated Annual CO2 Reductions	N/A
Estimated Annual NO_x, SO_2, and CO Reductions	N/A
Estimated Annual Particulate Mass Reductions	N/A

Appendix B Houghton County Industrial Park Case Study

B.1 Summary

A case study of the Houghton county industrial park was conducted to understand how ownership models could affect the adoption of networked microgrids. Through this process, implementation issues, regulatory barriers, and economic benefits became apparent. This case study was selected since a majority of the stakeholders at the park are suffering from inadequate power service which must be addressed and high electric costs.

B.2 Introduction and Background

The Houghton county industrial park is located 5 mi northwest of Houghton MI and is comprised of several businesses and a regional airport. A sky view of the park is given in Figure 15, where red lines show present electrical feeder routing. Seven businesses are fed from a single 2 MW substation located 2.4 mi away near Boston Lake. This substation is undersized for the current loads and is inadequate for future expansion at the industrial park. This inadequacy has lead local businesses to explore local generation and microgrid technology a potential solution to the observed power issues.

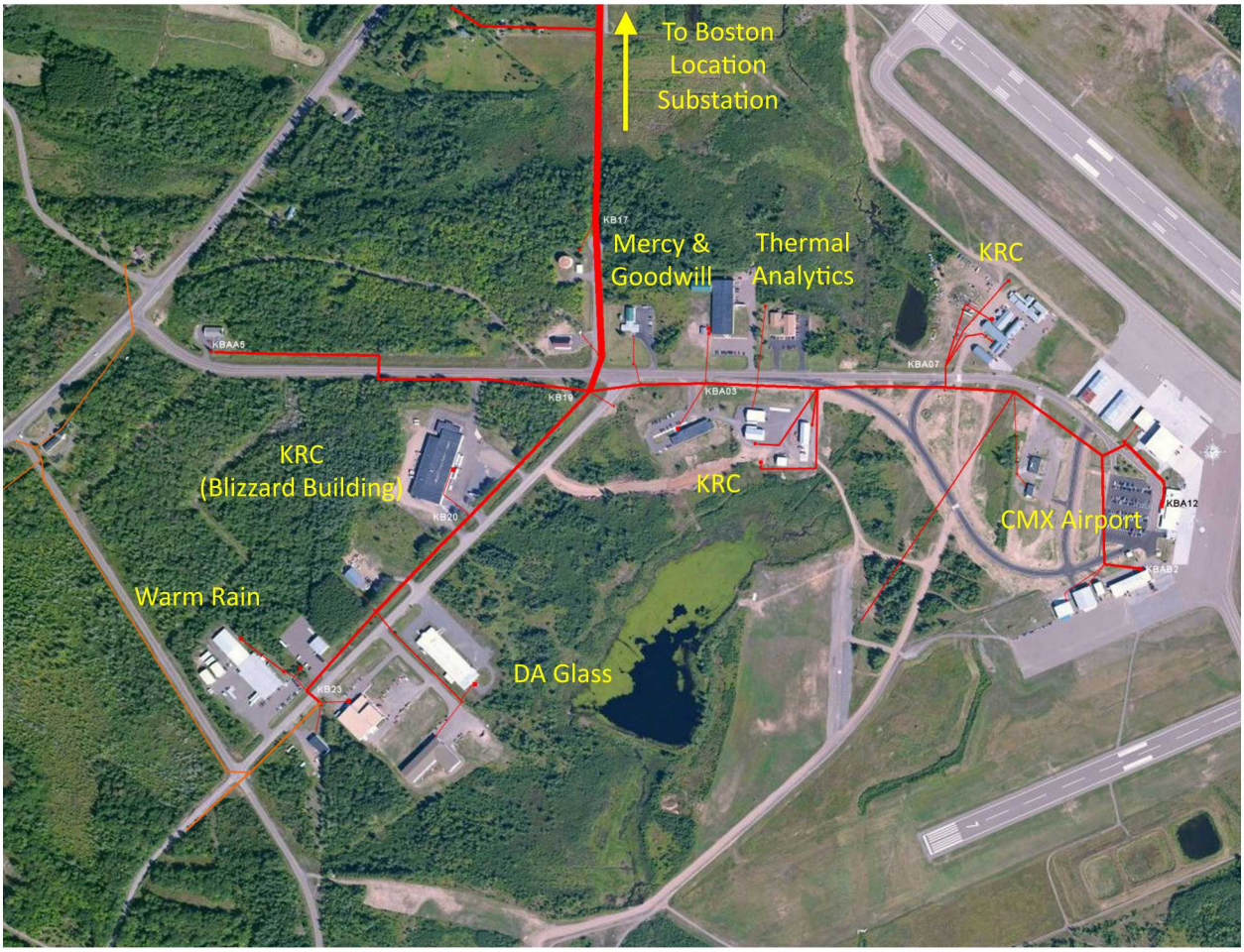

Figure 15: Houghton County Industrial Park.

B.3 Stakeholders

The stakeholders include the seven major electric consumers at the park along with the incumbent utility.

B.3.1 Ontonagon County Rural Electric Association (OCREA)

Electric distribution system at the industrial park is owned and managed by OCREA. OCREA serves a large rural area in the Keweenaw Peninsula in upper Michigan and doesn't own any generation assets. All electric power is purchased from the Upper Peninsula Power Company (UPPCO) which owns and operates high voltage transmission lines (69 kV) which feed from Wisconsin up to the tip of the Keweenaw Peninsula.

The industrial park is connected to OCREA's Boston location substation which is rated for 2 MW at 12.47 kV with a usable capacity of 1.8 MW. The Boston substation also provides electrical service for Lake Linden, Boston Area, and Gay MI. The industrial park consumes a majority of the available energy and will require substation upgrades or other measures to meet the expected demand.

B.3.2 Keweenaw Research Center (KRC)

The Keweenaw Research Center (KRC) is a research institute of Michigan Technological University (MTU). KRC is involved in research for Military and automotive industries specializing in computer modeling, vehicle testing, engine testing, snow and ice research and noise, vibration and harshness testing. While KRC consists of over 10 buildings, the main campus and a large research facility, the Blizzard building account for the majority of the energy consumption. KRC is currently the main OCREA client at the Industrial Park, consuming a 43% of the total 1.6MWh, as depicted in Figure 16.

The Blizzard Building is the largest energy consumer at KRC. This building includes research laboratories for professors at MTU, specifically from the ME-EM department and space for KRC. This building has upgraded its transformer from a 1MVA to a 2MVA, as well as put in place new switchgear, its own recloser and protection coordination with CTs and relays. This will allow the building to be islanded should OCREA consider it necessary. The transformer cannot be used to maximum capacity for the time being due to limitations of the distribution system. The maximum allowable power is 1 MVA.

This building also has power quality issues due to high frequency harmonics caused by switching electronics inside the testing equipment. This problem is not yet solved, but several studies by external companies have been carried out.

There are three types of research that require significant electric power located inside the blizzard building, consisting of IC engines, torque converters, and a torrefaction plant.

Research on internal combustion engines utilizes a 460 hp AC dyno. This laboratory is capable of regenerating power to the grid up to the 360kWh allowed by the State of Michigan. The current regeneration has been below 12kW. There is an expansion plan on place to increase its capabilities to a 750 hp engine, which would increase its consumption to 1.5MW.

Torque converter testing includes a 300hp DC dyno and a 465hp AC dyno, connected through the torque converter. The consumption is around 82kW and is used an average of 2 hours per month, which impact the demand charge on the electric bill, which can be equal to the months energy use costs.

A torrefaction plant is also installed which produces bio-coal. The torrefaction plant is connected to 160kW power bus and incorporates 17 motors. The installation has no regeneration capabilities. In the future it may need to increase four times its bio-coal production.

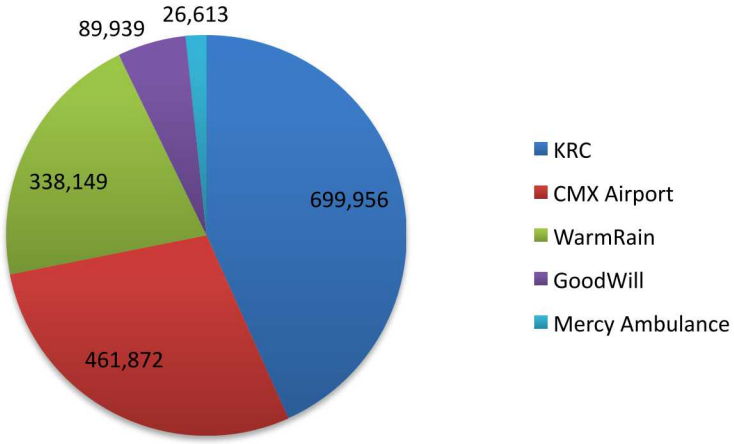

Figure 16: Annual Energy Usage 2013.

B.3.3 Houghton County Regional Airport (CMX)

The airport consumes around 145kW and has a 240kVA diesel generator as a backup in case of a power outage. The airport is working towards a higher efficiency, both by substituting incandescent bulbs for CFL or LED bulbs and by increasing their self-generation. The future plans include building a new terminal and putting in place a combination of renewable energies, gas generator and energy storage. The cost of this upgrade would be around $12M, which could be covered up to 95% by the Federal Aviation Authority.

The airport is also responsible for distributing water in the Industrial Airport Park and has a small diesel generator in place as a backup.

B.3.4 Warm Rain

This company manufactures bathtubs and can consume 150kW for periods of three hours each day, which affects its demand part of the electric bill. For this reason they are considering putting in place their own generation.

B.3.5 Thermal Analytics

This business was a spin-off from thermal modeling research done at MTU. Their consumption is assumed to be below 10kW. Backup generators are installed for their servers.

B.3.6 Mercy Ambulance Service

It is an ambulance service which consume only 2% of the Industrial Airport Park energy.

B.3.7 Goodwill Calumet Work Center

It is a wood workshop located near Mercy. Their energy consumption is a 5% of the total.

B.3.8 DA Glass America

This company is opening a new location at the Industrial Airport Park with a business of glass treatment. The business at the time of this writing was not operational yet. Their expected power consumption is of 300kW. Due to inadequate electric service DA Glass has purchased and is planning to operate a 300kW generator off-grid.

B.4 Do-nothing or Utility Proposed Solution

The least effort solution for the industrial park businesses is to allow the utility to solve the power quality and adequacy issues. OCREA has proposed two solutions; 1) upgrade the existing substation, 2) construct a new substation form the industrial park. With either solution, OCREA has stated that these costs would be passed onto the customers at the industrial park in the form of bulk costs, increased electric tariffs, or some combination. At the writing of this document, these solutions were not finalized or agreed upon and should be considered conceptual only.

The first solution is to upgrade the Boston Location substation to a larger capacity from a rating of 2MW to 5MW or 10MW. This allows OCREA's operational agreements with UPPCO to remain the same. OCREA buys electricity from UPPCO at $0.095/kWh and

a fixed wheeling fee of $160,000 per year, since UPPCO owns the connection to the high voltage transmission system. The estimated costs of this option are $3-$5 million.

The second option is for OCREA to build a dedicated substation for the industrial park that would directly connect to the 69kV high voltage transmission system. Since the new substation would be directly to the transmission, the wheeling fees would be eliminated from UPPCO. The costs of this solution are $5 million.

With either of these solutions, the businesses are at the mercy of the utility. There are concerns that electric rates will continue to climb since rates increased twice in the last year. This is coupled with some of the highest electric costs in the US resulting in an effective industrial electric rate of $0.18/kWh. Furthermore, since OCREA is not state regulated, electric rates are not capped.

From OCREA's point of view, the substation upgrade presents a significant financial risk if the proposed load doesn't fully develop. Since DA Glass has not started production and KRC has not yet centralized all testing dynamometers, the load forecast is still somewhat speculative. This presents a chicken and egg problem where the utility will not improve the electric infrastructure until the load has developed and companies cannot start production without adequate electric supply.

In the above discussion, the utility proposed solutions excludes the addition of local generation or resiliency, only improved access to the transmission system. This represents a business as usual solution which is common for distribution only companies.

B.5 Single Microgrid Solution

Pure economics are driving the stakeholders at the industrial park to consider alternate solutions to the incumbent utility. On possible solution would be to run the entire industrial park as its own microgrid. Considering a private ownership model, one company would purchase the distribution network from OCREA. Then this company would need to register as a power provider. A summary of the FY 2012 and 2013 electric costs that are given in Table 11.

Table 11: Houghton Industrial Park Energy Statistics (YF 2012 & 2013)

	Total Meters	Demand Meters	Total Annual Energy (kWh)	Maximum Monthly Demand (kW)	Average Monthly Demand (kW)	Total Cost
KRC '12	12	6	702,099	353	257	$121,769
KRC '13	10	6	699,956	385	250	$123,449
Airport '12	11	6	462,950	173	125	$75,963
Airport '13	11	6	461,872	169	128	$81,303
WarmRain '12	3	2	334,482	253	204	$80,393
WarmRain '13	3	2	338,149	237	200	$80,394
Goodwill '12	3	1	94,440	66	57	$21,707
Goodwill '13	3	1	89,939	55	52	$21,797
Mercy '12	1	0	24,717	N/A	N/A	$4,312
Mercy '13	1	0	26,613	N/A	N/A	$4,832
Total '12	30	15	1,618,688	845	643	$304,146
Total '13	28	15	1,616,529	846	630	$311,775

Appendix C DER-CAM Four Microgrid Canonical Analysis

C.1 Summary

The overall goal of this analysis was to utilize DER-CAM, an LBNL developed microgrid optimization tool, to demonstrate a potential value stream or financial benefit of interconnecting microgrids on the same distribution feeder[95]. This provides a first step in addressing the question,"Is there value in researching the interconnection of microgrids" Ranade and Mitra raise the perspective of developing the Customer-Driven Microgrid (CDMG) as a metamorphosis of today's distribution systems into tomorrow's microgrids [96], which is the foundation of the initial question of interconnecting microgrids investigated in this document. Fundamentally we present a definition of a microgrid as:

Microgrid*: a collection of cyber-physical device electrically connected that produce and/or consume electrical energy possibly based upon a global objective and where each entity may have time-varying individual objectives and the collection can be viewed as a single equivalent system with potential to interconnect to other systems.*

Extending the definition of a microgrid to a Customer Driven Microgrid as described by Ranade and Mitra [96].

Customer Driven Microgrid (CDMG)*: a distribution feeder where utility-compatible generation sources, primarily renewable, are installed by the customers and the utility now becomes an enabler for the optimum use of these resources by facilitating generation responsive feeders The concept of individual objectives of the customers is critical in describing the support of a global objective of the interconnection of each of the microgrids in support of the CDMG.*

This definition encompasses the function of each of the individual microgrids and the ability to interconnect and provide support of a global objective while still allowing for time-varying individual objectives. DER-CAM provides the opportunity to examine a potential financial value stream of microgrid interconnecting (the Customer Driven Microgrid) and acting in support of a global cost minimization. There is ample room to discuss other issues related to interconnection of microgrids such as outage reduction, resiliency, emissions, and efficiency; however this first analysis is financially based. To establish this type of extensive analysis, hundreds of variables are considered. These include inputs from the load data, technology characteristics, financial options, weather and locational data, utility tariff, fuel pricing, capital and operational/maintenance costs and many others. The configuration models are built and run in DER-CAM and finally evaluated against each other to identify potential value.

C.2 Introduction

The Distributed Energy Resource Customer Adoption Model (DER-CAM) is an economic and environmental model of customer distributed energy resource adoption. The objective of DER-CAM is to minimize total energy cost by operating energy assets of a microgrid. DER-CAM does not currently examine multiple customers acting together, however it is assumed in this first step of analysis that each customer acts to support the global objective of reducing costs energy costs on the distribution feeder based upon the total aggregate demand. Hence the final analysis with DER-CAM examines the customers as an aggregate. DER-CAM requires significant input data based upon: customer load including electrical and thermal loads, utility data including available tariff data, fuel cost, marginal emissions, characterization of different distributed energy resources such as photovoltaics, energy storage, and electrical generators such as internal combustion engines, micro-turbines, gas turbines, and combined heat and power generators, and financial data such as capital cost, O&M fixed and variable costs, interests rates, and payback periods.

This analysis establishes the four individual customers and an aggregate of the four customers as a fifth different case for DER-CAM. Then an analysis is presented on the DER-CAM optimization for each case.

C.2.1 Analysis

The customers on the distribution feeder were identified as particular customer type, annual energy usage (electrical and electrical/thermal), and maximum demand. The initial step was to establish robust assumptions and input data for DER-CAM. From the customer information load profiles were characterized to approximate hourly load data which was facilitated through the OpenEI commercial hourly load profiles. The profiles were then scaled and shifted to match energy usage and maximum demand [97]. TOU electrical tariffs were analyzed for both time of use energy and demand against both individual and aggregate cases. The location (Northern CA) was established for weather and solar irradiance as well as marginal emission data, although emissions were not part of the optimization. Note, this analysis can be applied to any location with these assumptions. Each of the DER-CAM inputs are discussed in C.3 below.

The analysis examines the individual microgrid via DER-CAM in two cases, a base case ("Do Nothing Case") without energy assets and a second case where DER-CAM optimizes energy assets based upon DOE 2020 energy asset costs targets against a generic TOU tariff. The second step of the analysis was to interconnect the four individual microgrids and have allow them to operate as a single system for overall cost optimization. It is recognized that the "regulatory" question must be addressed for microgrid interconnection, in fact most likely poses the largest hurdle in utilizing the distribution feeder as a CDMG. However, as we shift into paradigms of the Smart Grid, it is anticipated that public regulatory bodies and utilities adapt both policy and business models as the current model does not naturally

support features of the Smart Grid.

Stepping aside of the regulator questions, DER-CAM is an effective tool to optimize cost and utilization of energy assets of a microgrid against a load profile and utility tariffs allowing one to pose many "what if" questions to evaluate different financial and technical perspectives.

C.2.2 Scope of Work - Relationship to other DOE Microgrid Program Effects

This work provides a partial extension to the Microgrid Business Case analysis conducted by the DOE and funding opportunities announcement DE-FOA-0000997 [98]. In addition this work relates to the Microgrid Design Toolset being advanced by SNL which leverages and integrates software capabilities developed by SNL, LBNL, and PNNL for the optimization of microgrid designs.

C.3 Cases Analyzed

C.3.1 Distribution Feeder Customers

The four sample customers identified on the distribution feeder are below:

Table 12: Customer Data

	Electrical			Natural Gas	
Customer Type	**Peak Monthly** (kWh)	**Annual Usage** (kWh)	**Max Demand** (kW)	**Monthly Average** (kWh)	**Annual Usage** (kWh)
Campus	93,095	699,956	343	54,420	653,043
Airport	54,862	461,872	145	0	0
Industrial	34,431	338,149	224	35,119	421,431
Retail	8,803	89,939	55	0	0

It should be noted that the Campus and Industrial sites have thermal loads serviced by natural gas boilers and under this circumstance DER-CAM establishes a general use of natural gas to support the thermal load in the "Do Nothing" case. However under the optimization case, DER-CAM can off-set the thermal load with the use of combined heat and power, CHP, enabling a higher efficiency of fuel. Application of CHP enables greater efficiency of the system as a whole should provide improved results for both the Campus and Industrial.

C.3.2 Individual Customer Model

The individual customer load data, annual average, is presented below (Figures 17 - 20 and represented by the annual average weekday, annual average weekend, and annual average peak day load profiles associated for each of the 4 customers identified. These profiles are scaled based upon customer data collected and load profiles from the OpenEI commercial load database which was developed at the National Renewable Energy Laboratory and made available under the ODC-BY 1.0 d.

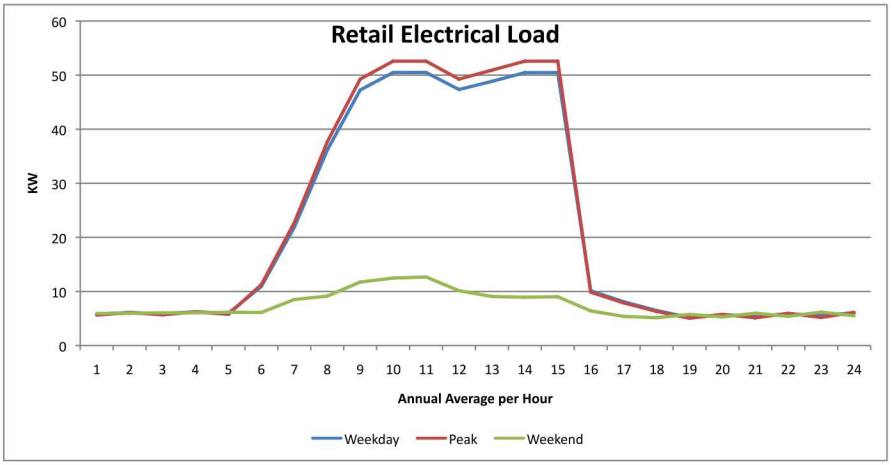

Figure 17: Annual Average Retail Electric Load

C.3.3 Aggregate Customer Model

The aggregate model is the additive sum of each of the individual load profiles hour by hour and is shown in Figure 21.

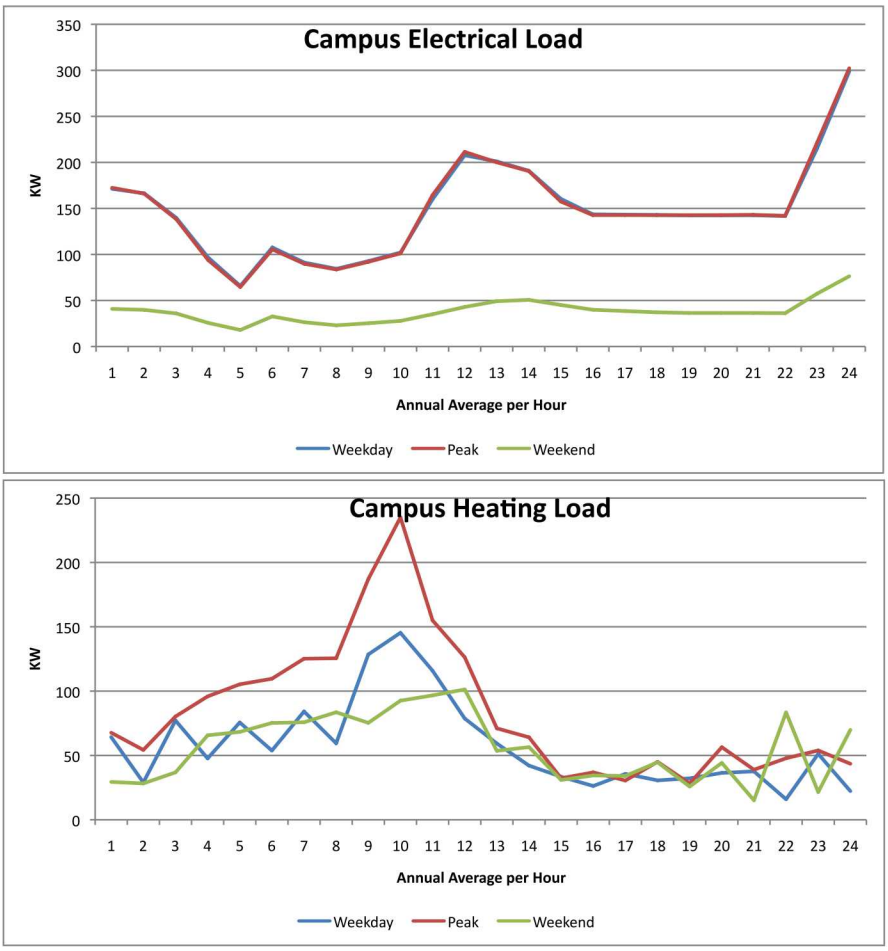

Figure 18: Annual Average Campus Electric and Thermal Load

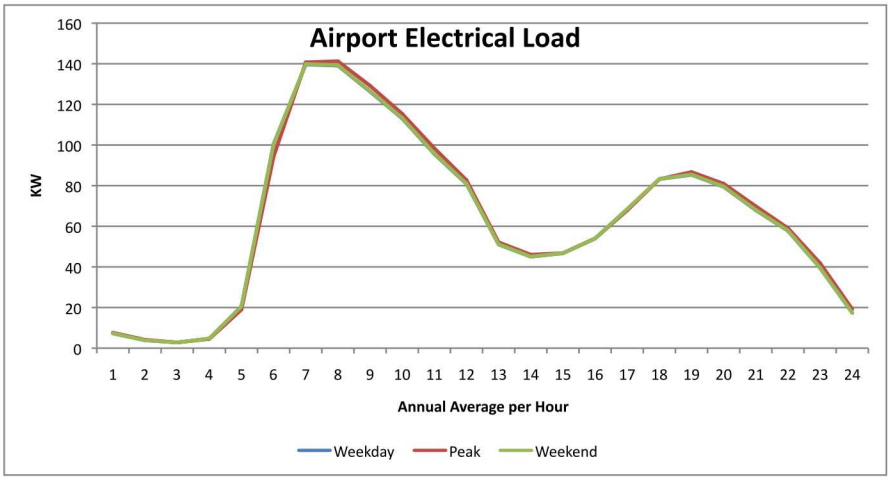

Figure 19: Annual Average Airport Electric Load

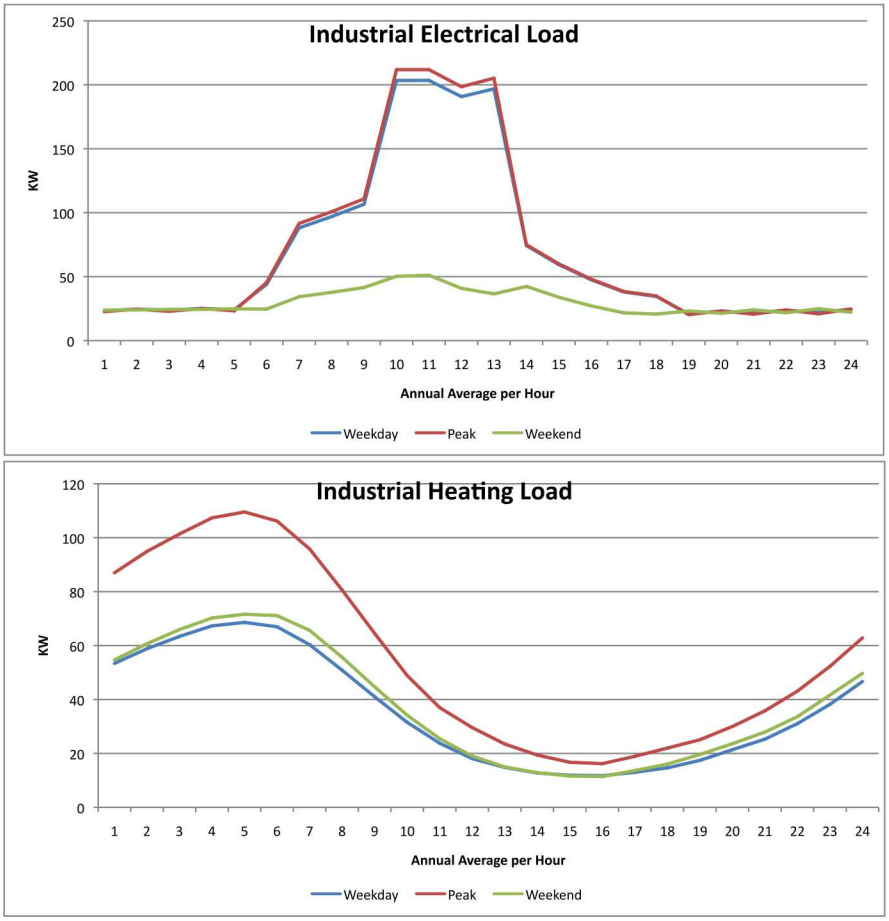

Figure 20: Annual Average Industrial Electric and Thermal Load

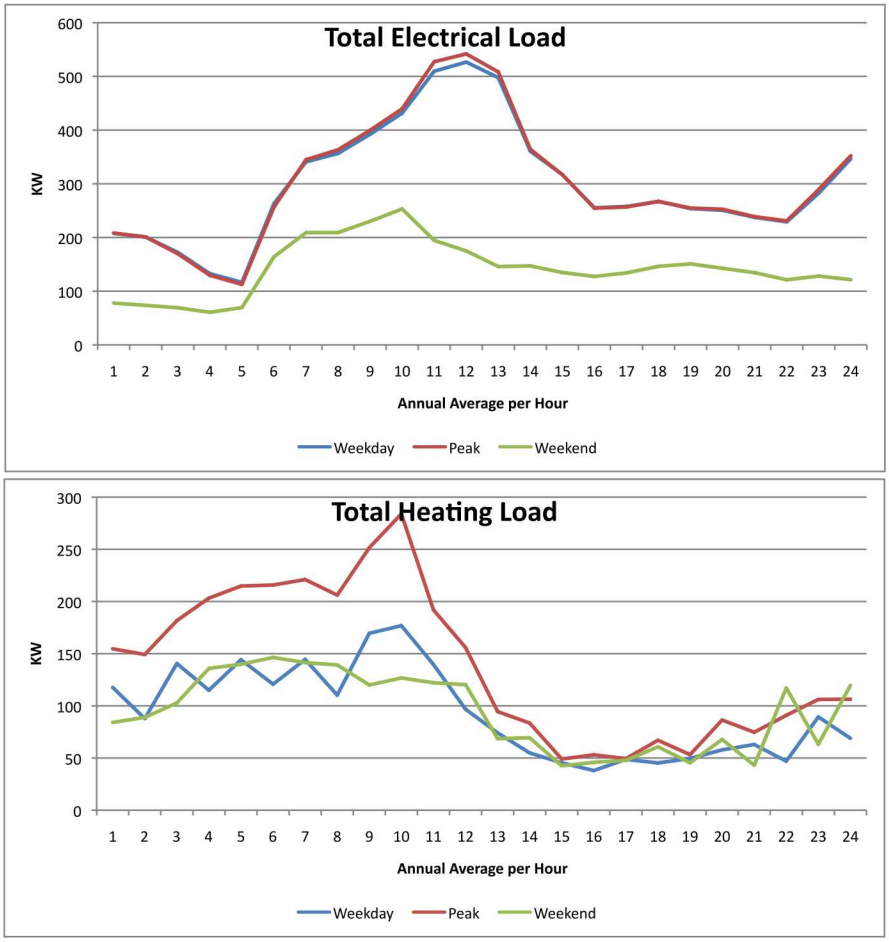

Figure 21: Annual Average Aggregate Electric and Thermal Load

C.4 Analysis Inputs

C.4.1 Assumption Perspective

The four individual customers and one aggregate provided for five total test cases. These are:

1. Campus
2. Airport
3. Industrial
4. Retail
5. Aggregate

Monthly energy usage and maximum demand were provided for each of these customers. Load profiles were characterized from the OpenEI commercial building database and sized and scaled to the appropriate energy usage and peak demand.

One of the difficult tasks in this type of analysis is generalizing the assumptions so that the results can associate with a larger set of examples. This is opposed to providing a narrow set of specific criteria which does not associate with a larger set of examples. Hence all effort was applied to generalizing and documenting to establish a robust set of assumptions for input data to DER-CAM. These assumptions are described below.

C.4.2 Electrical and Thermal Loads

A particular load profile can provide unique properties for any microgrid. In fact, the load profile can be considered an effective energy asset. In this analysis the load profiles were taken from the OpenEI database and sized to the original customer data.

C.4.3 Locational Parameters

This analysis was developed so that different locations can be a variable in the analysis problem. In DER-CAM many of the inputs are locational dependent. Location was not a focus of this analysis, but can be adapted by altering assumptions such as solar irradiance, temperature, wind speed, or other factors deemed necessary. This analysis was based upon northern California data.

C.4.4 Electrical Tariff

Time of use rates (TOU) are becoming more prevalent in many service areas throughout the US. Each of the 12 largest gross metropolitan product areas have TOU energy, TOU demand,

or TOU energy and demand rates and approximately 50% of these are non-voluntary. Hence a set of TOU tariffs were chose for this analysis based upon test case peak demand and usage. The first tariff was simply a time of use energy tariff, the second included a time of use energy with a seasonal demand, the final tariff was a TOU energy and demand tariff. PG&E provides TOU tariff information for small, medium, and large commercial customer. Specifically tariffs A-6, A-10, and E-19 were selected based upon each test case. Similarly natural gas tariffs were chosen for usage based upon the thermal loads, these were PG&E tariffs NG-1 and NG-2. Below is a list test cases and associated tariffs used in DER-CAM.

1. Campus: A-10, NG-1
2. Airport: A-6
3. Industrial: A-10, NG-1
4. Retail: A-6
5. Aggregate: E-19, NG-2

Each electric TOU tariff has two seasonal periods. Winter is November through April and summer is May through September. Winter has both partial peak and off peak time periods and summer has the same off peak as winter, however the partial peak is split to include a peak 6 hours of the 12. A-6 does not include separate demand charges, however A-10 has a standard winter and summer demand charge and E-19 has a full TOU demand charge. It is important to note that the each of the test cases have different tariffs based upon qualifications for the tariff, typically driven by max demand. For example, to remain on tariff A-6 the customer must have a maximum demand below 199kW. Thus the airport and retail customer fall under this tariff.

C.4.5 Natural Gas Tariff

The natural gas tariffs are similar to each other however differ based upon the customer usage. Both NG-1 and NG-2 provide winter and summer rate as well as a lower usage after the first 4k therms.

C.4.6 Marginal CO_2

The marginal CO_2 is data is used in DER-CAM calculation, but not focused on in this analysis. However the correct marginal data, WECC (Western Electricity Coordinating Council) data, was put into the configuration file of DER-CAM so the results could be examined. It is important to note that marginal data can be determined explicitly for the local utility.

C.4.7 Weather

Solar irradiance data was take from 2013 TMY3 data from San Francisco International Airport (SFO), as well as hourly average temperature and wind speed data.

C.4.8 DOE 2020 Cost targets

Beyond locational and load data, financial parameters are a large set of variables for input to DER-CAM. A main section of these focus on the capital, variable, and fix O&M cost with a technology. To align this analysis with the DOE goals, the DOE 2020 cost targets were used for photovoltaic and battery storage. Additionally technology costs of different natural gas engines and CHP systems based upon AEO 2009, AEO 2010, AEO 2011, and CPUC 2011 [84]. These references provided a large section of the financial metrics for DER-CAM

C.4.9 Other Financial Parameters

Additional financial parameters needed for the cost optimization include discount rate and payback period. Both a 10 year and 20 year payback period was examine in this analysis given the absent of any specific target.

C.4.10 Energy Asset Performance Estimates

Characterization of each of the technologies with respect to performance and lifetime was critical in the analysis. This included the utility overall efficiency as well as performance characteristic of potential technology energy assets such as generator efficiency, PV and battery efficiency, battery discharge and charge rates, or alpha of CHP enabled equipment. Additionally equipment expected lifetime and other technology specific parameters are included in each configuration.

C.5 Analysis Method with DER-CAM

Each of the test cases identified and input parameters were built into 5 different configuration files for DER-CAM to optimize. As discussed previously the first case was designed to determine the "Do Nothing" case where annual energy usage and costs are verified against an outside calculation to determine proper set up against original customer data and tariff application without any DER installation.

C.5.1 Base Case / Do-nothing and Verification of Usage and Costs

Each of the base cases was examined via an outside calculation to establish a "sanity" check against implementation of the TOU tariffs. Table 13 provides each test case validation of usage and costs.

Table 13: Base Case Verification

Test Case		Total Electricity usage kWh	Outside Calculation	Outside Calculation	Estimated Electrical Costs $
1	Campus	1,020,151.40	1,020,153.26	$217,017.81	$225,226.66
2	Airport	559,073.80	559,042.85	$120,189.22	$121,245.14
3	Industrial	504,701.60	504,701.60	$97,747.40	$100,189.98
4	Retail	150,441.00	150,380.98	$40,324.06	$38,537.75
5	Aggregate	2,234,280.90	2,234,278.69	$488,135.31	$480,676.79

Additionally provided by DER-CAM is the expected annual energy cost for each test case, Table 14. This information is directly related to the optimized outcomes for each DER-CAM run.

Table 14: Base Case Annual Energy Cost

Test Case		Estimated Total Energy
1	Campus	$229,963.17
2	Airport	$122,327.90
3	Industrial	$104,217.15
4	Retail	$39,620.51
5	Aggregate	$516,822.94

C.5.2 Continuous and Discrete Technology

DER-CAM divides energy generation assets into two groups, discrete and continuous. DER-CAM considers continuous technologies as photovoltaic systems, energy storage (batteries, thermal), solar thermal, EV's, refrigeration, AbsChiller, etc. Discrete technologies are considered internal combustion engines, CHP systems, micro-turbines, gas-turbines, and fuel cells.

The second case after the base case analysis is the optimization of discrete and continuous energy assets by DER-CAM. In this analysis DER-CAM optimizes continuous and discrete technologies based upon costs and technology performance against load and tariff information.

C.6 Unified Analysis

Table 15 represents the DER-CAM analysis for the four individual test cases.

Table 15: Individual DER-CAM Results

Test Case		Energy Costs	Electrical Cost Difference	DG & DG_HX (kW)	PV (kW)	Battery (kWh)	Utility Energy Base (kWh)	Utility Energy MG (kWh)
1	Campus	$157,325.59	$156,475.07	250	295	415	1,020,151	378
2	Airport	$71,706.19	$86,174.45	150	125	40	559,074	80,949
3	Industrial	$83,408.03	$55,271.19	60	146	358	504,701	73,316
4	Retail	$21,115.00	$27,912.34	40	37	26	150,441	24,385
Total		$333,554.81	$325,833.05	500	603	839	2,234,367	179,028

The annual energy costs for each individual test case are reduced significantly in each case, which is supported by the installation of PV and offset by natural gas purchase for on-site electricity generation. Additionally, this is supported by the reduction of purchased electrical energy from the utility. Comparing the results to the aggregate case and associated tariff were given above in Table 2.

The aggregate test case demonstrates a further reduction in total energy costs (approx. 15%) while supporting the same electrical and thermal loads. This is a reflection of installed renewables, storage, self-generation of electricity at higher costs, higher CHP utilization, and efficiency gains of CHP systems.

The following are a few observations of the aggregate system.

1. DER-CAM optimizes the discrete technology (ICE_HX) of the aggregate system to a 300kW system versus the total of individual optimized of 500kW, which most likely supports a higher utilization of the 300kW system over the year for the aggregated load which has a larger base load.
2. The photovoltaic capacity demonstrates simple avoided costs for utility energy; hence the aggregated case is in line with the sum of all the individual cases.
3. The reduction of battery capacity is most likely related to the smoothing of the demand profile from the sum of the individual of each load and the addition of a higher utilization of the discrete technology.
4. The reduction in energy consumption from the utility from the individual microgrids is approximately 92% while the aggregated microgrid demonstrates approximately 98% in energy reduction from the utility supporting the higher utilization of the discrete

technology. This loss of electrical energy sales from the aggregate microgrid has a tremendous impact on the business model of the utility, which is to sell electrical energy. Hence supporting the statement that the regulatory and business implications to the existing business model must be addressed.

Taking a step further, the results from DER-CAM in the aggregate test case demonstrates decreased capacity for DG and storage and increased capacity in PV over the sum of individual cases, however if DER-CAM is forced to choose the same values of capacity for the total of the individual cases improved results are still demonstrated, given in Table 16. An energy cost reduction is observed between the individual total and the aggregated of 14.0%. When the capacity is fixed, as in cases where microgrid assets have been previously chosen and installed, a benefit is still observed between the individual and fixed capacity of 9.5% cost savings.

Observations from Forced Capacity Case to the individual totals:

1. Improved savings in energy cost is realized. This savings could be attributed to the improved demand curve, resulting in improved efficiency of operation of the CHP systems with thermal loads.
2. Overall the installed capacity costs are within 2% of each other (Individual total vs. Aggregated), as the reduction in CHP and battery costs are almost offset by the increase cost of solar capacity.
3. The unconstrained solar area of the optimization plays a role in the analysis. If the area for installation is constrained, this value results in the maximum solar capacity. Hence the solar are for installation was left unconstrained.

Table 16: Forced Capacity Results

Test Case	Energy Costs	DG/CHP	PV	Battery	Tariff
Base total	$516,822.94	0	0	0	A-10 or A-6, NG-1
Individual total	$333,554.81	500	603	839	A-10 or A-6, NG-1
Aggregate	$287,023.42	300	697	545	E-19, NG-2
Aggregate Fixed Capacity	$301,792.56	500	603	839	E-19, NG-2

C.7 Conclusions

Overall this analysis demonstrates that there is a potential financial benefit to interconnect microgrids with some broad assumptions. It does however raise many more questions and

also demonstrates a need to further investigate the issues and potential of interconnection of microgrids. Many of the type of questions being asked about individual microgrid today such as reliability, protection, efficiency, emissions, and other value streams need to be asked about interconnected microgrids. Additional questions might include:

1. Identification of the regulatory hurdles and potential impacts to the utility for microgrid interconnection.
2. Understanding the further aspect of islanding when there is a utility interruption.
3. Cost and usage allocation.
4. Interactions of individual microgrids with alternate objectives and support of a global objective.

Appendix D Defense Strategies for Advanced Metering Infrastructure Against Distributed Denial of Service

Defense Strategies for Advanced Metering Infrastructure Against Distributed Denial of Service

Yonghe Guo, *Student Member, IEEE,* Chee-Wooi Ten, *Senior Member, IEEE,* Shiyan Hu, *Senior Member, IEEE,* and Wayne W. Weaver, *Senior Member, IEEE*

***Abstract*—Imminent attacks on critical infrastructure can disrupt operations and interrupt information availability. One way through cyberspace is to harness the distributed computing power and flood on targeted systems with massive information as a consequence of denial in service. This paper discusses the distributed denial of service (DDoS) attack, a potential cyberthreat in AMI communication network. A typical DDoS includes two stages: (1) *agents recruitment stage* and (2) *actual attack stage*. In this paper, various models of malware installation and flooding attack on AMI devices are introduced and potential impacts are studied. We propose a decision-making model for early detection and prevention of DDoS attack in the network using partially observable Markov decision process (POMDP). Simulation results show that the proposed model can optimally determine defensive strategies.**

***Index Terms*—Advanced metering infrastructure, cybersecurity, distributed denial of service attack, decision making.**

I. Recent AMI Development

INTERNET protocol (IP)-based advanced metering infrastructure (AMI) has been widely implemented in the recent years. This is an extension of existing automatic metering reading (AMR) systems with additional control capabilities. In general, the IP-based devices have been promoted for most home energy management applications [1]. The difference between the AMR and AMI is that the AMI enables bidirectional communication between AMI head-end and smart meters such that the customers can manage their load consumption according to the real-time pricing information. The AMI system consists of microprocessor-based energy meters, communication network, and AMI head-end [2]. The head-end is where the meter data management system (MDMS) is deployed that integrates AMI networks with utility applications.

An AMI network features a hierarchical communication relations including home area network (HAN), neighbor area network (NAN), and wide area network (WAN). The communication technologies can be adopted in AMI network which include wireless communication (Zigbee, WLAN, LTE, etc.), power line carrier (PLC), and optical fiber [3], [4]. A variety of protocols are developed to meet the communication requirements for AMI, including ANSI C12.18/19/21, IEC 61107/62056 and open smart grid protocol (OSGP). The internet protocol suite (IPS) provides rich options for building the scalable communication infrastructure of AMI [5]. A number of existing smart metering protocols can be configured to work over the IPS [6]–[8].

The drawbacks of implementing AMI system are vulnerabilities to potential cyberthreats [3], [9], [10]. The cybersecurity standards of AMI system include confidentiality, integrity, availability, and accountability [11]. The cyberthreats can be divided into two categories: (1) connection-based and (2) device-based vulnerabilities [3]. The connection-based attacks exploit the vulnerabilities existing in communication media and protocols, e.g., RF jamming, wireless scrambling, eavesdropping, message modification and injection, whereas the device-based attacks are being manipulated through security flaws of the device terminal to perform malicious activities, such as metering storage tampering, man-in-the-middle attacks, denial-of-service attacks, or unauthorized use of services. The digital technologies enhance the extensibility and scalability of metering functions. However, it also introduces new attack vectors to AMI system. An attacker can insert malicious code in memory of a smart meter to tamper data in a storage [12]. Penetration testing identifies a number of possible attacks against smart meters including meter spoofing, denial of service, and power disconnection [13]. Cyberattack targeting on AMI could disable real-time metering functionalities and cannot report updated energy usage [14], [15].

A broader effort from government, academia, and industry has been made to address the cybersecurity issues in smart grid. A cybersecurity Risk Management Process (RMP) for smart grids is proposed by the U.S. Department of Energy in cooperation with the National Institute of Standards and Technology (NIST) and the North American Electric Reliability Corporation (NERC) [16]. A wide range of cyberthreats have been explored. [11]–[14]. The intrusion detection system (IDS) has been intensively studied as an effective measure for cyberattack detection. The IDS can deduce potential tampering activities through the observation of related physical or cyber events, *e.g.*, irregular log information, suspicious outage notifications from a particular customer, abnormal communication traffic and communication losses. A typical IDS consist of following components: sensors or agents, management server, database server and user interface [17]. [10] discusses the requirements and architectural directions for AMI intrusion detection. The attack model is studied from different angles including type of attacker, motivation and attack technique. Three possible detection mechanisms are explored, including stateful specification-based monitoring, stateless specification-based monitoring and anomaly-based monitoring. A multi-level distributed intrusion detection system (IDS) for smart grids is proposed in [9]. The proposed model deploys multiple analyzing modules at each level of the smart grid-the home area networks (HANs), neighborhood area networks (NANs) and wide area networks (WANs). Both support vector machine (SVM) and artificial immune system (AIS) are evaluated for the purpose of detecting possible cyberattacks. The specification-based IDS techniques for AMI has been studied in [18], [19]. A energy theft detection oriented IDS named AMIDS is presented by [20]. The AMIDS features an attack graph based information fusion model that utilizes multiple information sources to improve the detection accuracy. These sources include network and host-based intrusion detection systems, on-meter anti-tampering sensors and nonintrusive load monitoring (NILM) based anomalous power consumption detectors which collect and analyze cyber events, physical events and energy consumption data, respectively. This framework is a combination of both with the electricity

This work was partially supported by the United States Department of Energy under the award DE-AC02-06CH11357.

Y. Guo, C.-W. Ten, S. Hu, and W. Weaver are with the Electrical and Computer Engineering Department, Michigan Technological University, Houghton, MI, 49931 USA (e-mails: yongheg@mtu.edu, ten@mtu.edu, shiyan@mtu.edu, and wwweaver@mtu.edu).

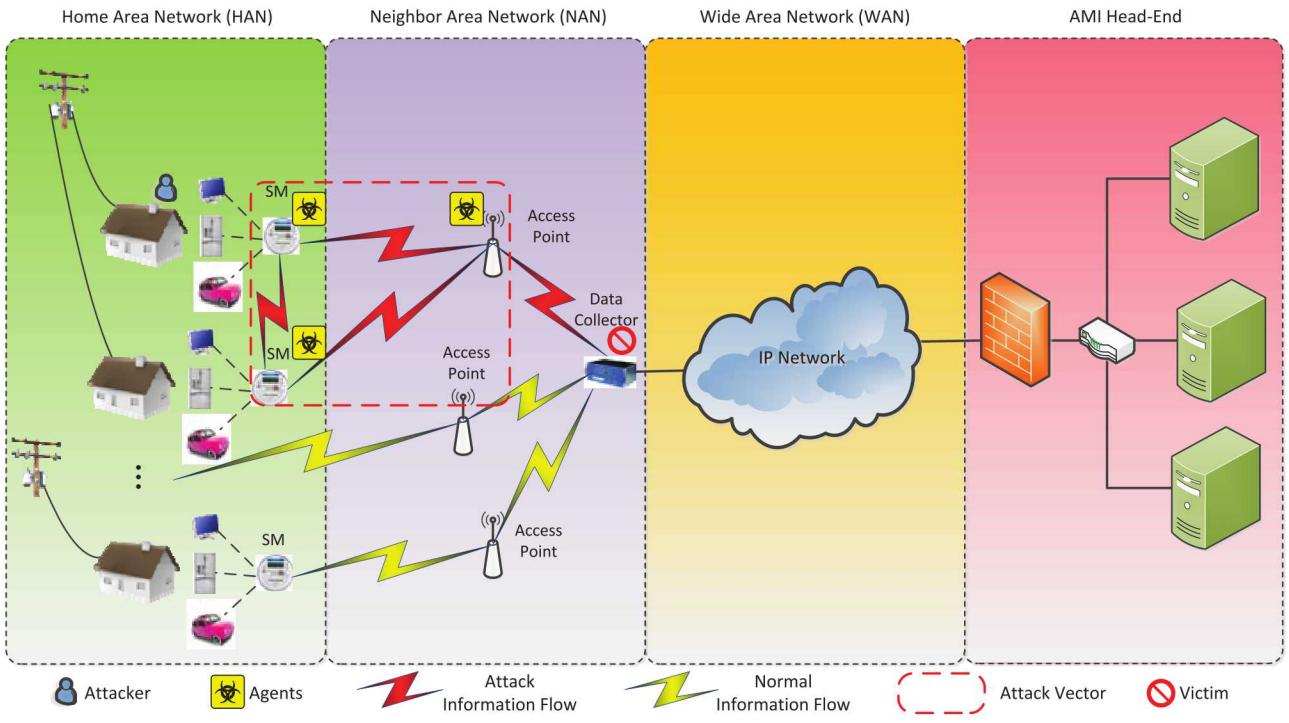

Fig. 1. DDoS attack in AMI communication network

usage analysis and information security techniques. A decision making framework for implementing IDS system in AMI is proposed in [21].

In this work, we focus on the distributed denial of service (DDoS) attack in AMI network. The DDoS attack is initiated by attack agents to exploit system vulnerabilities that affects the availability of network service/devices. The DDoS attack is one of the device-based attacks that targets at interrupting the service availability of AMI. Once initiated, a DDoS attack could cause a significant financial losses to the utility. Discovering the potential attack attempt is vital and is also crucial to strategically respond to the security signals in order to avoid unnecessary detection cost. In this work, we explore the problem with the following steps:

1) Conceptual model of DDoS attack in AMI network has been investigated with the methods adopted by the attackers to manipulate multiple "smart" meters (agents). Various mechanisms of the DDoS attack are also explored.
2) We simulate DDoS mechanism scenarios using NS3 to study the potential impact on AMI communication.
3) Finally, we adopt partially observable Markov decision process (POMDP) model to optimally strategize the decision making when the alarms of potential DDoS attack are observed.

The paper is structured as follows. Section II introduces the DDoS attack model for AMI network. A decision-making framework based on POMDP is proposed in section III. The simulation results are demonstrated in section IV. Finally, section V concludes this paper and discusses the future work.

II. DDoS Attack Modeling in AMI Network

The DDoS attack is initiated by attack agents to exploit system vulnerabilities that affects the availability of network service/devices. A conceptual model of the direct DDoS attack is depicted in Fig.1. This model consists of attacker, victims, and agents [22]. The main objective of attacker is to exhaust the processing power and data bandwidth of the victims, jamming its communication channel [22], [23]. Generally, the DDoS attack can be divided into two stages: (1) *recruitment of attack agents* and (2) *attack phase*.

A. Recruitment of Attack Agents

To be cost-effective in device design, the AMI metering devices are generally built based on the off-the-shelf solutions utilizing the commodity technologies. The key part of the metering device is a system-on-chip (SoC) integrating reduced instruction set computing (RISC)-based microprocessor, memory controller, SRAM, analog/digital converter (ADC), LCD display controller, USB controller, DSP, and communication modules. Some advanced digital meters may have an embedded operating system running on the hardware, *e.g.* Linux [24]. The ADC converts the analog quantities from voltage and current sensors to digital signals which can be processed by DSP and CPU. The communication modules are compatible with a variety of communication mechanisms to provide flexible data exchange configurations.

To launch a DDoS in AMI network, an attacker first needs to identify the vulnerable digital meters as the agents. Since the AMI system features a network with large number of homogeneous device, it is very possible that a security flaw discovered in a single meter could exist in many other ones. Then the attacker requires to communicate with significant number of IP-based smart meters that have already been infected with malicious code. It is impractical for an attacker to physically break into a large number of agents (compromised digital meters). Instead, the attacker can exploit the hardware or software security weakness on the meter to implant malicious program or adversely modify the firmware through the communication module [25]. The attack must select a proper propagation model to spread his malware. There exists 3 popular approaches, i.e. central repository, back-chaining and

autonomous, which are depicted in Fig. 2 [26]. When adopting the central repository approach, the attacker places the malicious program in a file repository, and each agent copies the code from this repository. In the back-chaining model, the attacker can make the compromised agent download the malware from the attacking host. The autonomous approach is similar to the back-chaining one, but differs from the latter one in that the infection process is combined with the exploit thus the agents do not have to download the malware from a dedicated source.

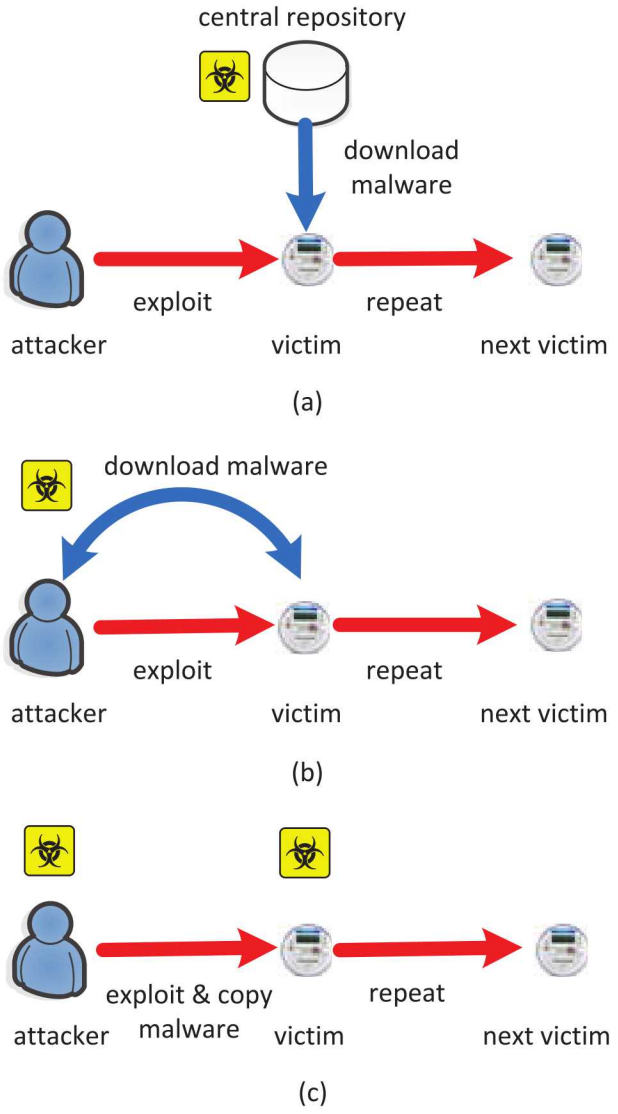

Fig. 2. Propagation methods: (a) central repository, (b) back-chaining, (c) autonomous [26]

B. Mechanisms of DDoS Attacks

There are many methods to initiate a DDoS attack [27]. We enumerate 3 categories of possible attack mechanisms in the AMI network environment.

1) **Attacks on protocol:** The attacker can take advantage of the security risks lying in the protocol to deplete the resources of the victim. For example, some IP-based AMI networks may employ the transportation control protocol (TCP) as the transportation layer protocol. The attacker can launch a TCP SYN flooding attack to disable the service on the AMI head-end or data collecting unit [28].
2) **Attacks on infrastructure:** The AMI system built on the IPS is a packet-exchange network where the routers play an important role. The attacker may intentionally disrupt the routing tables to deteriorate the performance of packet delivery [29], [30].
3) **Attacks on bandwidth:** The attacker can manipulate a large number of agents to send excessive communication packets to the victim. The overwhelming traffic will force the victim to drop an amount of the legitimate packets. A significant packets drop ratio may be observed [31].

The attacker may use IP spoofing to hid his attack agents. This strategy will increase the difficulty for the defender to trace back the source of the attack, especially when there are a huge number smart meters in a network.

C. Case Study of DDoS in AMI

To illustrate the potential impact of the DDoS attack to the AMI communication, we simulate the bandwidth consumption attack using NS3. The case is depicted in Fig. 3. The exemplary IP-based AMI network employs IEEE 802.11 protocols as NAN communication mechanism. The network is a two-level hierarchical wireless LAN communication structure. The first level consists of multiple smart meters and a single access point (AP). These communication entities form a infrastructure basic service set (BSS) in wireless LAN. Within the same infrastructure BSS, one station (smart meter) can communicate with another one via the AP. There is no direct communication between two stations belonging to two different BSSes even though they are within the communication ranges of each other's. The APs are also equipped with the IEEE 802.11s media access control (MAC) protocols to provide mesh station functionalities. In the second level communications, all APs are organized in meshed topology to provide multi-hop packets delivery paths to data collector. In 802.11s amendment, such network is referred as a mesh basic service set (MBSS) [32]. The mesh network is an ideal solution for urban smart metering service since it features the following benefits:

1) **Increased flexibility**. With a wireless link, any AP may be in range of one or several APs. In the MBSS, backhaul refers to a set of consecutive multiple inter-mesh AP links Multiple users data can be backhauled through the mesh cloud to data collector.
2) **Self-forming**. The MBSS can be sexpanded by adding new APs since the MBSS does not require particular infrastructures.
3) **Self-healing**. For any AP in the MBSS, there could exist multiple redundant paths to the data collector. If the AP is able to automatically choose the best path, removing one access point in the mesh cloud simply forces the other access points to find the new best path to the data collector. One malfunctioning AP will not affect the functionality of the whole system.

Fig. 4 depicts the protocol stacks and information flow of the communication system. The smart meter application run over the IPv4 protocol stacks. Depending on the service type, *e.g.* metering data, management information, the application uses either TCP or UDP protocol to send the packet. Then each packet is encapsulated with IPv4 and IEEE 802.11 headers and transmitted to the AP via the wireless medium. The AP serves as a wireless router and mesh gate. it translates between the MBSS and its associated smart meters. The AP is equipped with dynamic (olsr, aodv) or static routing protocols to backhaul the data to data collector. If the AP is in the

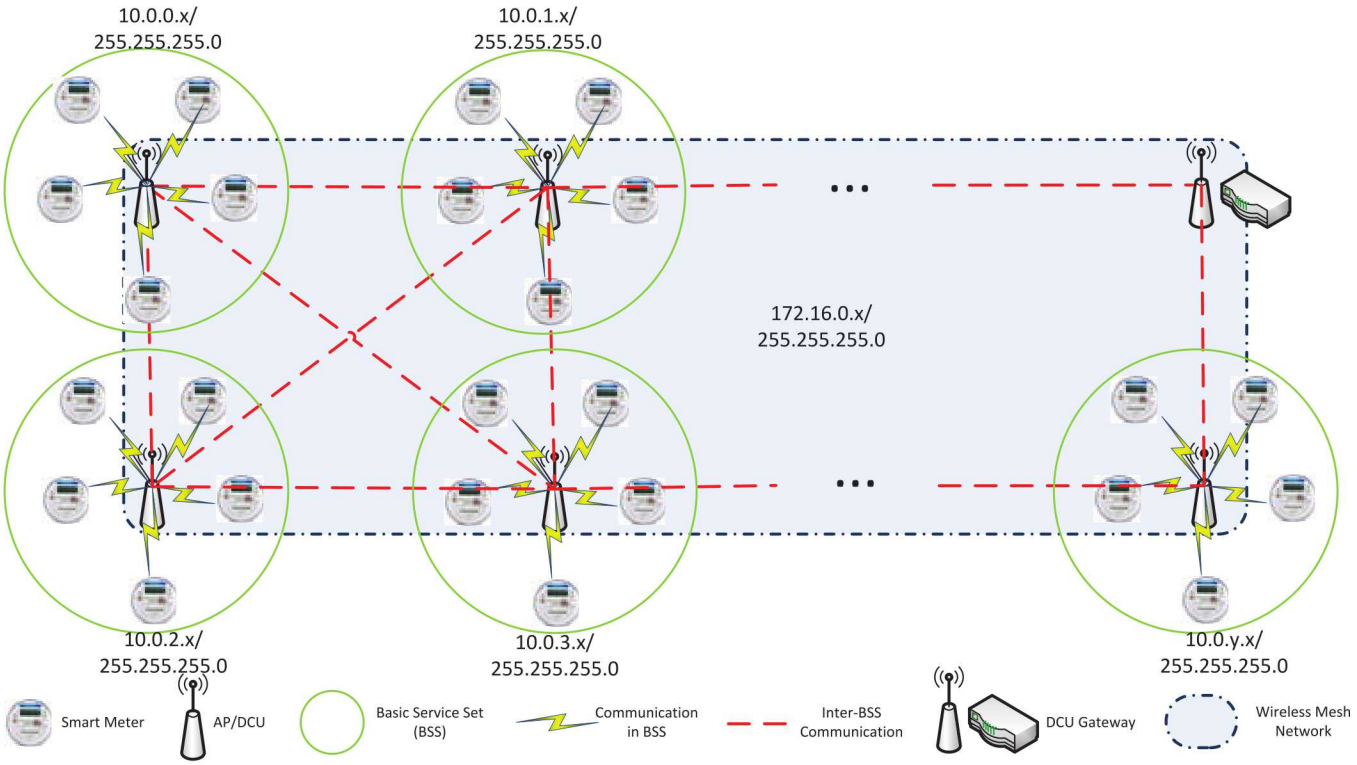

Fig. 3. IP-based wireless mesh NAN of AMI

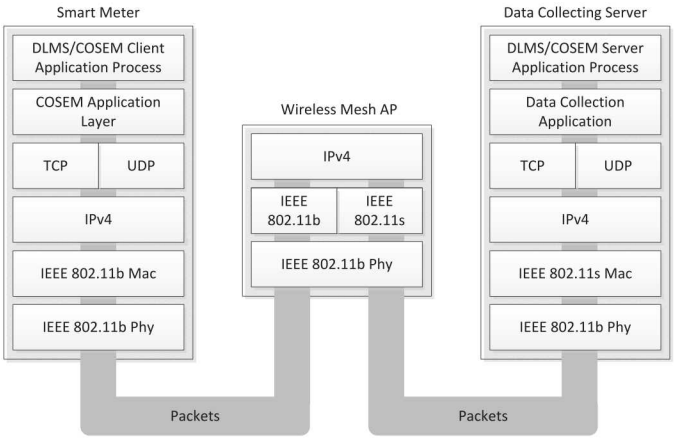

Fig. 4. NAN based on wireless mesh communication system

TABLE I
PARAMETERS SETUP

Parameter	Smart Meter	DCU
Phy	IEEE 802.11b DSSS11Mbps	
Mac	802.11b	802.11s
Trans. layer	TCP	
IP address range	10.0.{0~8}.0/ 255.255.255.0	172.16.0.0/ 255.255.255.0
Service port no.	4059	
Max. comm. hops	2	

range of the data collector, it will directly deliver the packet. Otherwise, it will send the packet to next AP. This process will repeat until the packet reaches the data collector. The example AMI NAN for case study consists of 1 DCU gateway, 10 DCUs and 50 smart meters. Each DCU is associated with 5 smart meters. The parameters setup for the communication entities are shown in table I. The communication entities are distributed in a 150m×150m area.

The smart applications are modeled according to the Device Language Message Specification and Companion Specification for Energy Metering (DLMS/COSEM) defined by IEC 62056 standards [7], [8]. The DLMS/COSEM can be configured with various communication profiles, e.g. HDLC protocol or IPv4 stack [6]. When DLMS/COSEM works with the IPv4 protocol stacks, it can uses either TCP or UDP protocol for communication. The port 4059 is specified for DLMS/COSEM applications.

Under normal conditions, the smart meters are scheduled to report energy usage data every 2 minutes. We assume that each compromised agent can generate 2Mbps UDP flooding attack flow to the DCU gateway. The simulation result is shown in Fig. 5. It can be observed that in a NAN the network performance is seriously deteriorating with the growing number of attack agents. When 60% of the total meters are compromised and used as agents, near 50% packets are dropped, and the average and maximum end-to-end delays are 13.5 and 5.48 times higher than that when the system is in normal condition. As we discussed in previous sections, the bandwidth consumption attack can seriously affect the data availability of AMI system.

III. DDoS Prevention in AMI Network

DDoS attacks over the Internet have been studied [27]. Similarly, the effects of DDoS on AMI network are critical issues to utilities. To defend this, it is important to detect and prevent potentially malicious attempts before the attack is launched. One practical option for defender to protect their critical cyber assets is to deploy the intrusion detection system

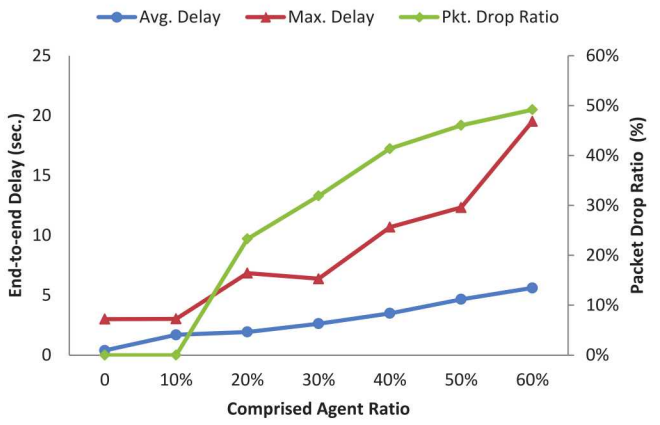

Fig. 5. Impact of DDoS on end-to-end delay

(IDS). The IDS deployment schemes can be divided into 3 categories: centralized, embedded and dedicated [21].

Due to the false positive errors and labor-intensive cost, inspecting every meter after seeing an alarm may not be the best decision. We utilize the Partially Observable Markov Game (POMG) model to determine the optimal responses from the defender's perspective based on the feedback from IDS system. Since our main focus is the defender's policies, we assume that the attacker adopts a static, time-invariant stochastic policy independent from defender's action for each discrete time state. Therefore, the POMG problem can be reduced to a Partially Observable Markov Decision Process (POMDP) problem with the defender as the only decision maker [33]. A POMDP is an extension of a Hidden Markov Model (HMM) by introducing a decision maker. At each state, the decision maker has multiple choices, described by an action space, and corresponding incentives for choices, described by the reward function. The state transitions of a POMDP possess the Markov property. The goal of solving a POMDP is to find a policy for the decision maker.

A. Partially Observable Markov Decision Process

The general POMDP problem can be described by a tuple $\langle \mathcal{S}, \mathcal{A}, T, \mathcal{O}, \Omega, R \rangle$ [34]. A given system is described by a finite states set $\mathcal{S}$. The decision maker (defender) has a finite set of actions to handle current state, which comprises the action space A. The exact current system state is unknown to the decision maker. Instead it is given a finite set of observations $\mathcal{O}$ which provide implicit information of system states. The transition function between states $T : \mathcal{S} \times \mathcal{A} \times \mathcal{O} \to [0, 1]$ gives a probability distribution for a system state, decision maker's action.

We define $T(s', a, s) = P(s'|a, s)$. The mapping between the state space, defender's action space and the observation space is described by the observation function $\Omega : \mathcal{S} \times \mathcal{A} \times \mathcal{S} \to [0, 1]$ which provides a probability distribution over the observation. We define $\Omega(o, a, s') = P(o|a, s')$. Finally, after taking a particular action at a specific state, the defender will receive some immediate expected reward, which can be described by the reward function $R : \mathcal{S} \times \mathcal{A} \times \mathcal{S} \to \mathbb{R}$. We define $R(s', a, s)$ as the reward received when the play takes action a at state s, and the next state is s'. In the security context, the reward can be viewed as the cost paid by the defender to prevent an attack attempt or the losses due to such attack.

In the POMDP model, the decision maker (defender) does not have the explicit knowledge of current state. Instead it generates actions according to a state estimator, which is defined as the belief state b. A belief state is a probability distribution over the state space. At each time step t, the decision maker (defender) needs to update the its current belief state based upon the previous belief state, last action and current observation. Let $b(s)$ denote the probability associated with state s, and the updated belief state can be calculate using the Bayesian rule

$$b(s') = P(s'|o, a, s) = \frac{\Omega(o, a, s') \sum_{s \in \mathcal{S}} T(s', a, s) b(s)}{P(o|a, b)} \quad (1)$$

where

$$P(o|a, b) = \sum_{s' \in \mathcal{S}} \Omega(o, a, s') \sum_{s \in \mathcal{S}} T(s', a, s) b(s) \quad (2)$$

is the normalizing value. The belief state implies all the previous information. The POMDP is also a belief MDP that can be represented by a tuple $\langle \mathcal{B}, \mathcal{A}, \rho, \tau \rangle$, where $\mathcal{B}$ is the belief space with infinite belief states, $\mathcal{A}$ is action space with finite actions, $\rho : \mathcal{B} \times \mathcal{A} \to \mathbb{R}$ is the intermediate reward

$$\rho(a, b) = \sum_{s \in \mathcal{S}} \sum_{s' \in \mathcal{S}} b(s) R(s', a, s) T(s', a, s), \quad (3)$$

and $\tau : \mathcal{B} \times \mathcal{A} \times \mathcal{B} \to \mathbb{R}$ is the belief state transition function

$$\tau(b', a, b) = P(b'|a, b) = \sum_{o \in \mathcal{O}} P(b'|b, a, o) P(o|a, b). \quad (4)$$

A policy $\pi : \mathcal{B} \to \mathcal{A}$ is a mapping from the belief space to action space. In the infinite-horizon model, the POMDP focuses on finding the best policy that can generate the optimal the long term expected discounted reward of the decision maker (defender):

$$E\Big[\sum_{t=0}^{\infty} \gamma^t \cdot r_t\Big], \quad (5)$$

where r_t is the reward for step t and γ is the discount factor. At each step, the decision maker (defender) needs to act to optimize its future reward. The Bellman equation of the belief MDP for the infinite-horizon model can be given

$$V^*(b) = \max_{a \in \mathcal{A}} \left\{ \rho(a, b) + \sum_{b' \in \mathcal{B}} \tau(b', a, b) V^*(b') \right\}, \quad (6)$$

where $V^*(b)$ denotes the optimal value function maximizing eq. (5) for belief state b. Let $\varphi : \mathcal{B} \times \mathcal{A} \times \mathcal{O} \to \mathcal{B}$ denote the deterministic transition function between the input of previous belief state b, action a and the observation o and the output of current belief state b'. The eq. (6) can be written as

$$V^*(b) = \max_{a \in \mathcal{A}} \left\{ \rho(a, b) + \sum_{o \in \mathcal{O}} P(o|b, a) V^*(\varphi(b, a, o)) \right\}. \quad (7)$$

The optimal policy can be determined as

$$\pi^*(b) = \arg\max_{a \in \mathcal{A}} \left\{ \rho(a, b) + \sum_{o \in \mathcal{O}} P(o|b, a) V^*(\varphi(b, a, o)) \right\}. \quad (8)$$

B. Application of MDP in Decision Making

All parameters need to be determined or approximated when adopting the POMDP model to specific security problem. In this preliminary work, we consider a special case: the AMI network can be divided into several subnetwork (NAN), and for each subnetwork there is a dedicated IDS monitoring the network communication flow. Based on the abnormality evaluation, the IDS gives a set of observations as the indication of the system status. Given a NAN with n smart meters, We consider that the system state space is represented by $\mathcal{S} = \mathcal{S}_1 \bigcup \mathcal{S}_2 = \{s_0, s_1, s_2, \cdots, s_n\} \bigcup \{s_l^*, s_{l+1}^*, s_n^*\}$ where the subscript of each entry denotes the number of compromised meters. The $\mathcal{S}_1$ represents the system states at the agent recruitment state, while $\mathcal{S}_2$ is a set of system states at which the attacker has already launched a DDoS attack. The subscript of the first element in $\mathcal{S}_2$ represents the least required number of compromised meters in order to launch an effective attack. The observation space is $\mathcal{O} = \{o_0, o_1, s_o, \cdots, o_n\}$, where the subscript of each entry denotes the number of compromised meters inferred from the IDS detection result. We assume that the defender has two possible actions:

1) a_1: Monitor the NAN through the IDS sensor, and
2) a_2: Conduct on-site inspection on each meters and recover the compromised ones.

Let C_I be the labor cost for on-site inspection on each smart meter, C_R be the cost for recovering the compromised smart meters and L_D be the losses due to the successfully launched DDoS attack. The reward function can be calculated as

$$\begin{cases} R(s_j, a1, s_i) = -(j-i) \cdot C_R \\ R(s_j, a2, s_i) = -nC_I \\ R(s_j^*, a1, s) = -L_D \qquad \forall s \in \mathcal{S} \end{cases} \tag{9}$$

The attacker also has a finite action space $\mathcal{A}^a = \{a_0^a, a_1^a, \cdots, a_m^a, \hat{a}\}$. Here, for a_k^a the subscription represents the number of hijacked smart meters at current step. The $\hat{a}$ represents the successfully DDoS attack. The attacker is assumed to adopt a fixed stochastic policy for each state. That is, $P(a^a|s)$ is time-invariant for $\forall a^a \in \mathcal{A}^a$ and $\forall s \in \mathcal{S}$. The state transition function when the defender generates action a_1 can be given

$$T(s_j, a_1, s_i) = \begin{cases} P(a_{j-i}^a|s_i) & \text{if } j \geqslant i \\ 0 & \text{else} \end{cases} \tag{10}$$

and

$$T(s_j^*, a_1, s_i) = \begin{cases} P(\hat{a}^a|s_i) & \text{if } j = i \\ 0 & \text{else} \end{cases} . \tag{11}$$

When the defender adopts action a_2, we assume that the next system state will be always s_0. Then the state transition function is

$$T(s', a_2, s) = \begin{cases} 1 & \text{if } s' = s_0 \\ 0 & \text{otherwise} \end{cases} . \tag{12}$$

Let p and q be the probability of false negative and positive errors when detecting a single compromised meter by IDS, that is, the detection probability and accuracy are $1-p$ and $1-q$, respectively. We hypothesize that both p and q for individual smart meters are independent from and equal to each other. The observation function for action a_1 can be given

$$\begin{aligned} \Omega(o_j, a_1, s_i^*) &= \Omega(o_j, a_1, s_i) \\ &= \sum_{k=\underline{k}}^{\overline{k}} \binom{i}{i-k} p^{i-k}(1-p)^k \\ &\cdot \binom{n-i}{j-k} q^{j-k}(1-q)^{n-i-(j-k)} \end{aligned} \tag{13}$$

where

$$(\underline{k}, \overline{k}) = \begin{cases} (0, j) & \text{for } 0 < j \leqslant i, j \leqslant n-i \\ (j-n+i, j) & \text{for } 0 < j \leqslant i, j > n-i \\ (0, i) & \text{for } j > i, j \leqslant n-i \\ (j-n+i, i) & \text{for } j > i, j > n-i \end{cases} . \tag{14}$$

The observation function for action a_2 is

$$\Omega(o, a_2, s') = \begin{cases} 1 & \text{if } o = o_0 \\ 0 & \text{otherwise} \end{cases} . \tag{15}$$

IV. Simulation Results

A. Simulation Setup

We use the POMDP model to evaluate a NAN case for demonstration that consists of 10 smart meters and is monitored by a single dedicated IDS. The attacker may use faked IP addresses to avoid being traced back. We assume the attacker have to control at least half of total smart meters to launch a DDoS attack. Thus, there are 11 entries in $\mathcal{S}_1$ and 6 entries in $\mathcal{S}_2$. The cardinality of system state space is 17. The state transition function $T(s', a_1, s)$ is heavily dependent on the attacker's intentions, techniques and objective. In this preliminary, we tentatively setup the state transition probability. We assume the priori probability of the presence of attacker in the system to be 0.1, that is, $T(s_0, a_1, s_0) = 0.9$. At the agents recruitment stage, we hypothesize that number of compromised meters by the attacker at each state follows some particular "bell shape" discrete probability distribution. Once the attacker enters the DDoS attack stage, i.e., any state in $\mathcal{S}_2$, the next state will always stay at current one if the defender takes action a_1. The setup of $T(s', a_1, s)$ is depicted in Fig. 6, where entries in $\mathcal{S}_1$ are indexed by numbers from 1 to 11, and that in $\mathcal{S}_2$ are indexed by numbers from 12 to 17.

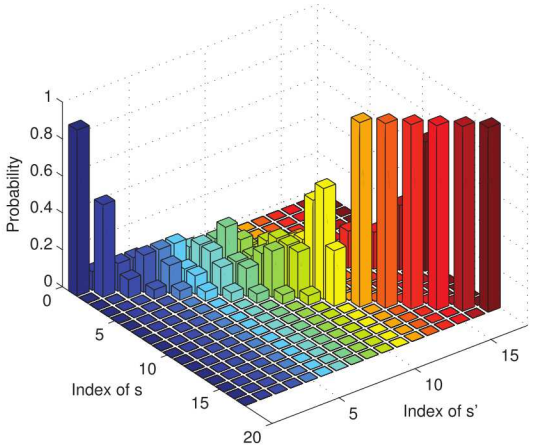

Fig. 6. Setup of transition function $T(s', a_1, s)$

The remaining parameters is listed in table II. We set C_R and C_I for each individual smart meters to be 150$ and 30$, respectively. The values for p and q are assumed to be 0.1 and 0.05, respectively. The observation function $\Omega(o, a_1, s')$ can be calculated by Eq. (13). The result is shown in Fig.7, where the indexing scheme for s' in state space is the same as that in Fig.6. The discount factor γ is set to be 0.9.

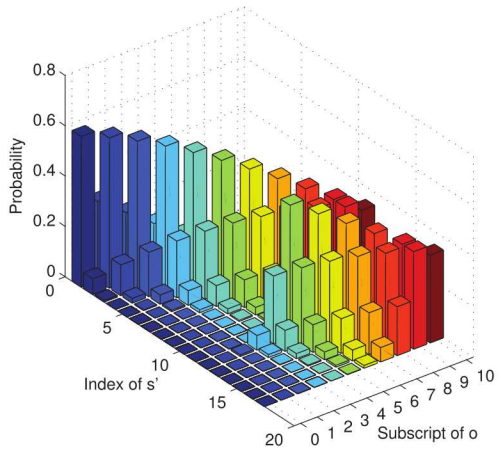

Fig. 7. Setup of observation function $\Omega(o, a_1, s')$

TABLE II
TEST CASE PARAMETERS SETUP

Parameter	Value	Unit
C_R	\$150	dollars
C_I	\$30	dollars
L_D	\$60,000	dollars
p	0.1	
q	0.05	
γ	0.9	

B. Simulation Results

The formulated POMDP model for DDoS detection decision making is solved based on value function and the policy graph [35]. The value function $V^*(b)$ is a piecewise-linear hyperplane over the belief space which can be represented by a set of coefficient vectors. Fig. 8 depicts negative value of the coefficient vector set for the formulated POMDP model. The piecewise-linear hyperplane consists of 23 components. The length of each vector is equal to the cardinality of the state space. Let $\mathcal{C}$ denote the coefficient vector set. Given $\forall b \in \mathcal{B}$, the value for $V^*(b)$ can be obtained as $V^*(b) = \max_{c \in \mathcal{C}} c \cdot b, \forall c \in \mathcal{C}$.

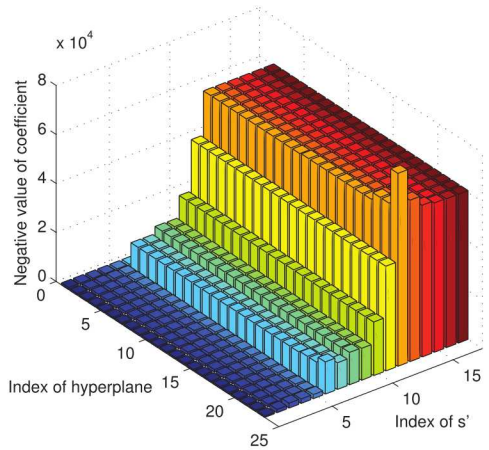

Fig. 8. Coefficient vector of the piecewise-linear hyperplane

The strategy of acting in the POMDP can be described by a directed graph, which is referred as policy graph. The policy graph for the formulated POMDP model is depicted in Fig. 9. Each node in the graph corresponds to a component of the piecewise-linear hyperplane and is associated with an action. Each transition arc going out a node represents a possible observation for that node. Given a start node, acting according to a policy graph is straightforward. First, the decision maker executes the action associated with current node. Based the observation resulted from the action, the policy graph transits to the next node. Then the decision maker repeats the aforementioned process.

For example, if the defender finds that the current node in Fig. 9 is node 3, he will need to execute action a_1, since this action can give him the best long-term reward. Assuming that he receives the observation o_1 after the action, the next node will be 2 and the associated action is still a_1. The policy graph serves as a state controller. The state transition is determined by the observation after each action execution.

V. Conclusion and Future Work

Cybersecurity is a challenging issue in smart grid implementation. The model of DDoS attack is discussed in AMI system. The difference between the DDoS attack in AMI system compared with the Internet version is that the defender in AMI system not only needs to protect the information infrastructures such as AMI head-end or DCU, but also has to secure the "smart" meters. Based on that, we proposed a model of decision making for the DDoS attack prevention. The model adopts POMDP. Preliminary simulation result shows promising potential of the proposed model. The future work will focus on improving the proposed model including state transition function that may not accessible to the defender in practice. Multiple attackers may also implement adaptive attack techniques as a countermeasure to the defender's actions.

References

[1] Y. Yan, Y. Qian, H. Sharif, and D. Tipper, "A survey on smart grid communication infrastructures: Motivations, requirements and challenges," *IEEE Commun. Surveys Tuts.*, vol. 15, no. 1, pp. 5–20, 2013.

[2] M. A. Faisal, Z. Aung, J. R. Williams, and A. Sanchez, "Securing advanced metering infrastructure using intrusion detection system with data stream mining," in *Pacific Asia Workshop, PAISI 2012*, Kuala Lumpur, Malaysia, May 29, 2012, pp. 96–111.

[3] E. Bou-Harb, C. Fachkha, M. Pourzandi, M. Debbabi, and C. Assi, "Communication security for smart grid distribution networks," *IEEE Commun. Mag.*, vol. 51, no. 1, pp. 42–49, 2013.

[4] Y. Yan, Y. Qian, H. Sharif, and D. Tipper, "A survey on cyber security for smart grid," *IEEE Commun. Surveys Tuts.*, vol. 14, no. 4, pp. 998–1010, 2012.

[5] F. Baker and D. Meyer. Internet protocols for the smart grid. IETF RFC6272, June. 2011. [Online]. Available: http://tools.ietf.org/html/rfc6272#section-3.2

[6] DLMS/COSEM Architecture and Protocols. Dec. 2009. [Online]. Available: http://dlms.com/documents/Excerpt_GB7.pdf

[7] *International Standard IEC 62056-61.*, International Electrotechnical Commission, Geneve, 2006.

[8] *International Standard IEC 62056-62.*, International Electrotechnical Commission, Geneve, 2006.

[9] Y. Zhang, L. Wang, W. Sun, R. C. Green, and M. Alam, "Distributed intrusion detection system in a multi-layer network architecture of smart grids," *IEEE Trans. Smart Grid*, vol. 2, no. 99, pp. 796–808, July 2011.

[10] R. Berthier, W. H. Sanders, and H. Khurana, "Intrusion detection for advanced metering infrastructures: Requirements and architectural directions," in *in Proceedings of the 1st IEEE International Conference on Smart Grid Communications (SmartGridComm)*, Gaithersburg, Maryland, Oct. 4-6, 2010, pp. 350–355.

[11] F. M. Cleveland, "Cybersecurity issues for advanced metering infrastructure (AMI)," in *Proc. IEEE Power and Energy Society General Meeting - Conversion and Delivery of Electrical Energy in the 21st Century*, Jul. 20–24, 2008, pp. 1–5.

[12] S. McLaughlin, D. Podkuiko, and P. McDaniel, "Energy theft in the advanced metering infrastructure," in *Proc. 4th Int. Workshop Crit. Inf. Infrastruct. Security (CRITIS 2009)*, Bonn, Germany, Sep. 2009, pp. 176–187.

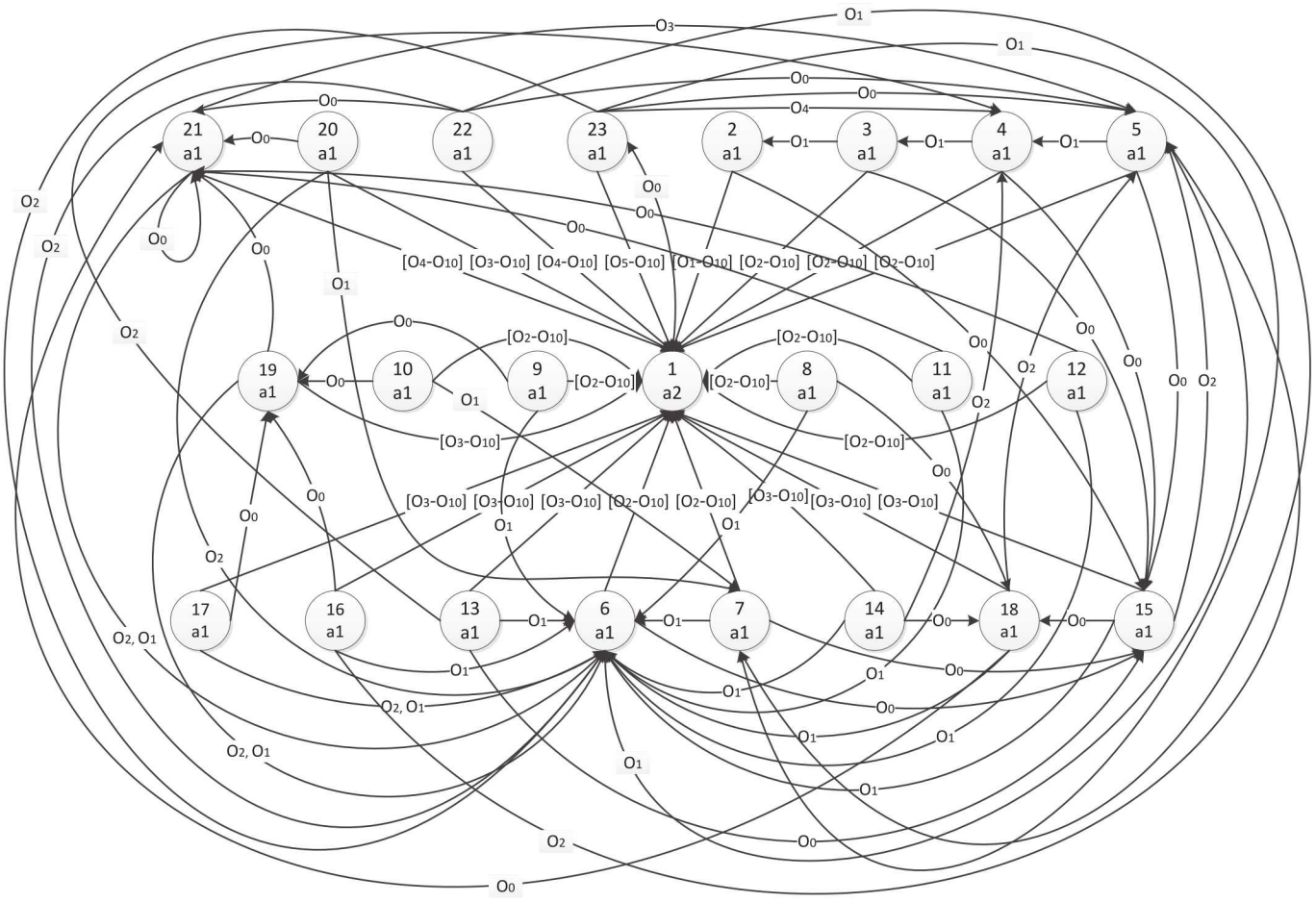

Fig. 9. Policy graph of the formulated model

[13] S. McLaughlin, D. Podkuiko, S. Miadzvezhanka, A. Delozier, and P. McDaniel, "Multi-vendor penetration testing in the advanced metering infrastructure," in *Proc. Annual Computer Security Applications Conference*, ACM, 2010, pp. 107–116.

[14] P. McDaniel and S. McLaughlin, "Security and privacy challenges in the smart grid," *IEEE Security Privacy*, vol. 7, pp. 75–77, 2009.

[15] FBI Warns Smart Meter Hacking May Cost Utility Companies $400 Million A Year. [Online]. Available: http://www.networkworld.com/community/blog/fbi-warns-smart-meter-hacking-may-cost-utilities-400-million-year

[16] (2012) Cybersecurity risk management process. [Online]. Available: ttp://energy.gov/oe/downloads/cybersecurity-risk-management-process-rmp-guideline-final-may-2012

[17] K. Scarfone and P. Mell. Guide to Intrusion Detection and Prevention Systems (IDPS). NIST (National Institute of Standards and Technology) special publication 800-94, 2007. [Online]. Available: http://csrc.nist.gov/publications/nistpubs/800-94/SP800-94.pdf

[18] P. Jokar, H. Nicanfar, and V. Leung, "Specification-based intrusion detection for home area networks in smart grids," in *IEEE International Conference on Smart Grid Communications (SmartGridComm)*, Oct. 2011, pp. 208–213.

[19] R. Berthier and W. Sanders, "Specification-based intrusion detection for advanced metering infrastructures," in *IEEE Pacific Rim International Symposium on Dependable Computing*, 2011, pp. 184–193.

[20] S. McLaughlin, B. Holbert, A. Fawaz, R. Berthier, and S. Zonouz, "A multi-sensor energy theft detection framework for advanced metering infrastructures," *IEEE J. Sel. Areas Commun.*, vol. 31, no. 7, pp. 1319–1330, July 2013.

[21] A. A. Crdenas, R. Berthier, R. B. Bobba, J. H. Huh, D. G. Jorjeta G. Jetcheva, and W. H. Sanders, "A framework for evaluating intrusion detection architectures in advanced metering infrastructures," *IEEE Trans. Smart Grid*, vol. 5, no. 2, pp. 906 – 915, March 2014.

[22] R. K. C. Chang, "Defending against flooding-based distributed denial-of-service attacks: A tutorial," *IEEE Commun. Mag.*, vol. 40, no. 10, pp. 42–51, 2002.

[23] D. S. Yeung, S. Jin, and X. Wang, "Covariance-matrix modeling and detecting various flooding attacks," *IEEE Trans. Syst., Man, Cybern. A*, vol. 30, no. 2, pp. 157–169, 2007.

[24] Smart E-Meter: AMR/AMI. Smart Electricity Meter: AMR/AMI Solutions from Texas Instruments. [Online]. Available: http://www.ti.com/solution/docs/appsolution.tsp?appId=407

[25] J. Larsen. CyberSecurity of Field Equipment of SCADA. TCIPG Seminar. [Online]. Available: http://tcipg.org/sites/tcipg.org/files/slides/2012_11-02_Larsen.pdf

[26] K. J. Houle, G. M. Weaver, N. Long, and R. Thomas. Trends in Denial of Service Attack Technology. Technical Report, CERT Coordination Center, October 2001. [Online]. Available: http://www.cert.org/archive/pdf/DoS_trends.pdf

[27] S. T. Zargar, J. Joshi, and D. Tipper, "A survey of defense mechanisms against distributed denial of service (ddos) flooding attacks," *IEEE Commun. Surveys Tuts.*, vol. 15, no. 4, pp. 2046–2069, 2013.

[28] CERT Coordination Center. CERT Advisory CA 1996-21, TCP SYN Flooding and IP Spoofing Attacks. September 1996; revised November 2000. [Online]. Available: http://www.cert.org/historical/advisories/CA-1996-21.cfm

[29] B. Greene. BGPv4 Security Risk Assessment. Cisco white paper, June 2002. [Online]. Available: http://www.cymru.com/Documents/barry2.pdf

[30] X. Zhao, D. Pei, L. Wang, D. Massey, A. Mankin, S. F. Wu, and L. Zhang, "Detection of invalid routing announcement in the internet," in *Proceedings of the International Conference on Dependable Systems and Networks (DSN02)*, 2002, pp. 59–68.

[31] K. Mirkovic, S. Dietrich, D. Dittrich, and P. Reiher, *Internet Denial of Service: Attack and Defense Mechanisms*, 1st ed. Prentice Hall, 2005.

[32] K. Andreev and P. Boyko. Ieee 802.11s mesh networking ns-3 model. [Online]. Available: http://www.nsnam.org/workshops/wns3-2010/dot11s.pdf

[33] T. Alpcan and T. Basar, *Network Security: A Decision and Game-Theoretic Approach*, 1st ed. Cambridge University Press, 2011.

[34] L. P. Kaelbling, M. L. Littman, and A. R. Cassandra, "Planning and acting in partially observable stochastic domains," *Artificial intelligence*, vol. 101, no. 1, pp. 99–134, 1998.

[35] A. R. Cassandra. POMDP solver software, version 5.3. [Online]. Available: http://www.pomdp.org/code/index.shtml

Appendix E Image-Extracted Energy Information Based on Existing Electromechanical Analog Meters

Image-Extracted Energy Information Based on Existing Electromechanical Analog Meters

Yachen Tang, *Student Member, IEEE,* Chee-Wooi Ten, *Senior Member, IEEE,*
Chaoli Wang, *Member, IEEE,* and Gordon Parker, *Member, IEEE*

***Abstract*—There has been an ongoing effort to increase the number of advanced metering infrastructure (AMI) devices to improve system observability. Deployed AMI, across distribution secondary networks, provides load and consumption information for individual households which can improve grid management. A barrier to implementation is the significant upgrade costs associated with retrofitting existing meters with network-capable sensing. One economic way is to utilize mobile devices to transfer pictorial information and extract those images in digital form. This paper presents a solution using real-time transmission of power consumption information to a cloud server without modifying the existing electromechanical analog meters. In this framework, a systematic approach to extract energy data from images is applied to replace manual reading process. A case study is presented where the digital imaging approach is compared to the averages determined by visual readings over a one month epoch.**

***Index Terms*—Advanced metering infrastructure, electromechanical analog meters, image data extraction, time-activity curves.**

I. Introduction

AVERAGE coverage of advanced metering infrastructure (AMI) in US power utilities has risen to 15.3 percent as of 2014 [1]. Although the increase of metering points improves system observability and consumer load models, the rate of deploying AMI devices remains at a slow pace. The IP-based electricity meter is the typical device use to collect real-time consumption data in secondary distribution systems [2]. Real-time data acquisition is one of the primary tasks where usage information is periodically polled and transmitted to a central database using an IP-based communication network [3], [4]. As the first major milestone and the fundamental structure of the overall smart grid, an AMI is a system that measures, collects, and analyzes data about energy usage and power quality from the terminal smart meters, and achieves valid data exchange between the distribution dispatching center and customer billing network [5], [6]. Due to the pivotal role of information exchange between metering devices and the power distribution station, data observation and management of IP-based AMI are considered important roles in modernizing the distribution grid [7].

Pervasive computing on mobile devices has revolutionized consumer electronic products and provided diverse applications in social networking. These devices are often embedded with powerful processors that can be utilized to perform relatively demanding tasks [8], [9]. The rapid pace of mobile device technology development results in a large secondary market of inexpensive devices with computing and imaging capability suitable for capturing and transmitting power consumption information from existing analog meters.

With accurate and timely information, the monitoring element has the capacity to detect energy quality and the state of the distribution system while the management console is able to realize troubleshooting and electricity control strategies [10]–[12]. Distribution substations can guarantee high-efficiency electric energy and control the power transmission capacity according to the real-time load feedback facilitating energy conservation [13]. The contribution of this work is to establish a framework to perform real-time energy information extraction from images of the existing electromechanical analog meters. Section II describes the metering infrastructure of a campus distribution system to motivate this solution and as background for the case studies considered later. Section III details the algorithm of image data extraction. Section IV provides case study results with conclusions provided in Section V.

II. Campus Metering Infrastructure

An AMI deployment was commissioned on 11 buildings out of a 38 building campus in January 2012. This provides approximately half of the total campus power consumption and load information in real-time at an installation cost of $60,000. A low cost solution was desired to capture the total campus load with similar bandwidth. Although the upgraded infrastructure provides high percentage coverage of system observability at this time it is known that load consumption characteristics change as the campus grows. The current subset of instrumented buildings is not guaranteed to be dominant in the future. Within the campus Intranet, subnets of different

This work was partially supported by the United States Department of Energy under the award DE-AC02-06CH11357.

Y. Tang and C.-W. Ten are with the Department of Electrical and Computer Engineering, Michigan Technological University, Houghton, MI, 49931 USA (e-mails: yachent@mtu.edu and ten@mtu.edu).

C. Wang is with the Department of Computer Science, Michigan Technological University, Houghton, MI, 49931 USA (e-mail: chaoliw@mtu.edu).

G. Parker is with the Department of Mechanical Engineering-Engineering Mechanics, Michigan Technological University, Houghton, MI, 49931 USA (e-mail: ggparker@mtu.edu).

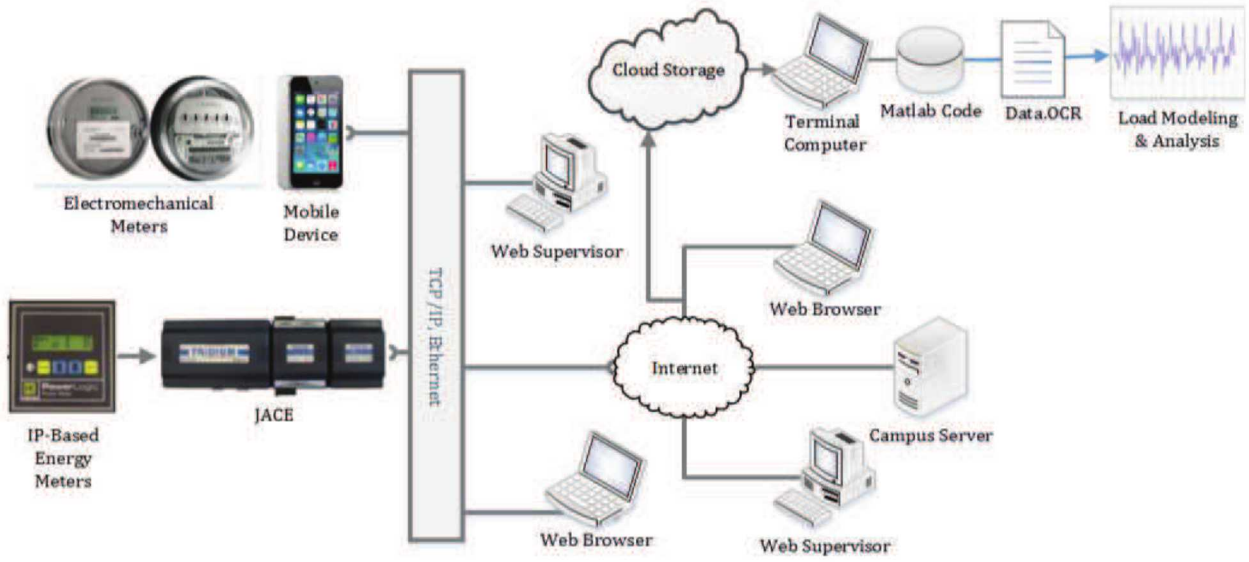

Fig. 1. Metering infrastructure for campus distribution system

buildings are connected and are routed through the campus-wide communication backbone network to other internal networks for real-time information sharing. This demonstration project is to increase a greater number of metering points for the lower priority buildings by deploying mobile devices that pictorially acquire energy information from existing electromechanical analog meters instead of dedicated IP-based energy meters.

Fig. 1 depicts the mobile devices for transferring pictorial data between campus networks. The mobile devices are implemented to capture images from the analog meters and the image data are transferred to a centralized database. The IP-based energy meters accurately transmit the consumption data with other communication means. The figure also illustrates the basic architecture of AX Supervisor.

A. Data Acquisition from IP-Based Energy Meters

The IP-based energy meters of the campus-wide distribution grid are monitored by the AX Supervisor. It is a flexible network server applied in operations where multiple Java application control engine (JACE) controllers can be networked together [14]. Real-time energy consumption information is displayed on the energy meter as well as uploaded to the Internet through the IP-based Internet link module (ILM) [15].

For security reasons, ingress restriction and identification in communication protocols is configured for Internet connection and access [16]. The users and supervisors are capable of executing operations with virtual private network (VPN) verification together with a firewall [17], [18].

B. Pictorial Data from Electromechanical Meters

Unlike IP-based "smart" meters, the electromechanical analog meters do not establish network connection and require periodic manual reading. The typical analog meter has four pointers with different order of magnitudes to show scaled energy consumption.

The overall approach for real-time data extraction from the traditional mechanical meters is to apply live image transmission technology with information upload to private cloud storage through the campus Intranet with synchronization achieved at the download side [19]. The operational approach is to have a mobile device with a timer camera application acquiring images every c minutes. [20]. The device is installed and placed in front of the dial plate with a stand support. The automatic upload function in the mobile device uploads the photo stream to the private cloud through the Internet and then the photo appears at the monitoring terminal computer immediately for image processing and consumption data extraction. [21].

Data samples of the IP-instrumented buildings were used to find a suitable value of c; trading off frequency resolution and phase lag with data set size. Fig. 2 shows the effect of different image capture times, c. The estimated power in kW is determined based on a first order finite difference of the two snapshots of images

$$P_{est} = \frac{E_{mec}(t) - E_{mec}(t-1)}{c} \quad (1)$$

where $E_{mec}(t)$ and $E_{mec}(t-1)$ are the latest image snapshots from an electromechanical analog meter defined by the time

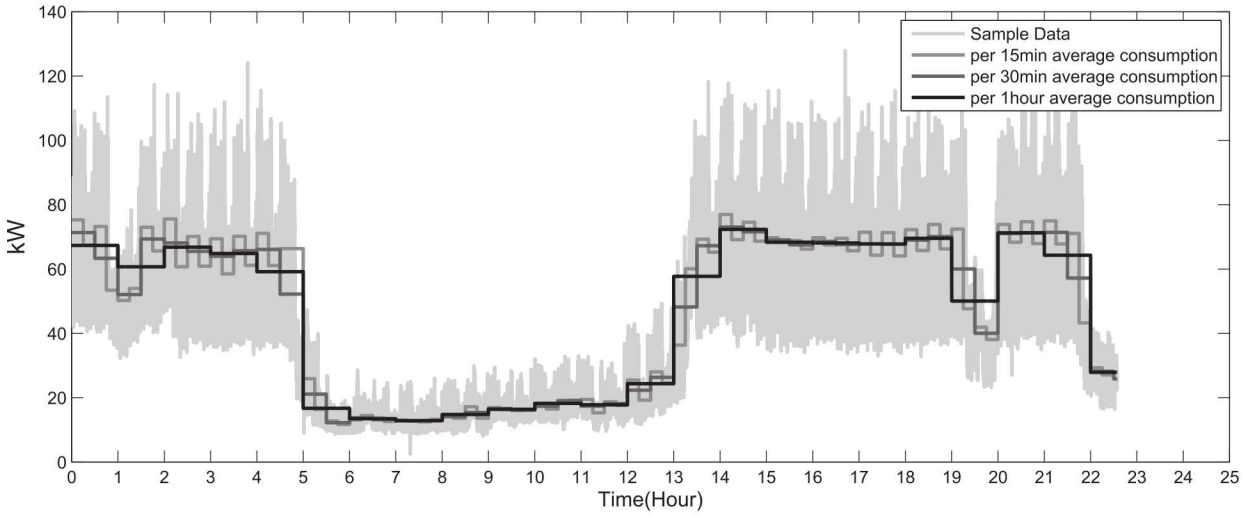

Fig. 2. Proposed simulation of energy consumption for sample data

interval c. If restricting the interval to be every 10 minutes, then $c = \frac{1}{6}$ in hourly base.

III. Image Data Extraction

Image segmentation is presented in Section III-A and the digital image preprocessing approach in Section III-B. The algorithm for identifying indicator readings algorithm is detailed in Section III-C.

A. Image Segmentation

Fig. 3a shows an image of a four-dial plate electromechanical meter. The processing area is formed using a rectangular crop shown in Fig. 3b. To deploy a modular pointer extraction algorithm, a strategy was developed to extract each of the circular dials, Fig 3c, with elimination of the background shown in Fig. 3d.

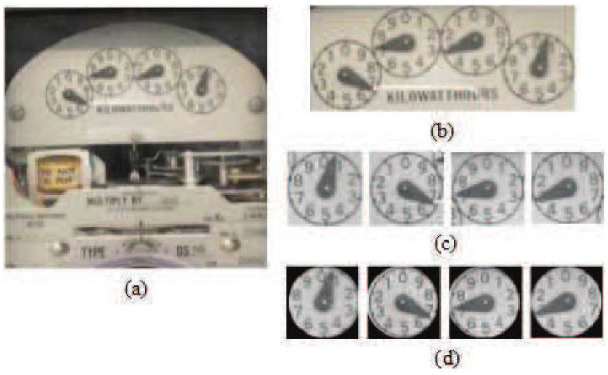

Fig. 3. Image segmentation

B. Digital Image Perprocessing

The change in lighting conditions can lead to color and contrast variance. In order to avoid the identification error generated from this situation, the first step is to produce parallel grayscale images from segmented areas. Discerning grayscale images directly is often accompanied by random noise as well as diverse shade degree in reorganization zone of images. Here, we utilize grayscale image binarization to acquire analyzable outcomes with little identification error. It is noted that the threshold value of binarization of 0.6 was used to magnify the contrast ratio of white objects.

To further improve the resolution of the binary image, we applied morphological operations, dilating and corroding, to simplify the image data structure. The dilating operation expands and enhances the edge of the object to dislodge or cover blank spots around object edges while the corroding operation eliminates external pixels to reduce "burrs" in edges.

The preprocessed, inverted image is shown in Fig. 4 and is ready for pointer extraction.

Fig. 4. Exported images after segmentation and preprocessing

C. Matrix Border Grayscale Detection Algorithm

The pointer extraction algorithm in this section is based on the characteristics in binary image matrix. This is designed to intercept a square matrix border within the exported images from previous processing that is illustrated in Fig. 5. We detect that the first and the last coincident points of the matrix border and pointer pixels matrix in the image identification area to confirm the matrix coordinate of midpoint between these two conjunctions. The deviation angle of pointer can be determined by the line segment of center of the circle and the midpoint.

Angular deviation of each pointer is determined corresponding to the values shown in Table I. The scale of each digit is identified and saved in the data sheet.

Fig. 5. Intercept a square matrix border within the export image

TABLE I
ANGLE AND NUMBER MAPPING TABLE

Angle(Degree)	Clockwise	Anticlockwise
0-36	0	9
36-72	1	8
72-108	2	7
108-144	3	6
144-180	4	5
180-216	5	4
216-252	6	3
252-288	7	2
288-324	8	1
324-360	9	0

Interception of matrix border with a square shape ensures the center of the circular target acquired from image segmentation as the matrix's center and two-third radius as the length of square edge. Gray values of pixels in the matrix border is compared with the given threshold value, recording the coordinates of coincident points between square edge and the pointer.

There are scenarios on the images taken by the camera that are not considered successful. Sometimes, there is one or two splashes that meet the threshold value at the position before or after the authentic coincident point. Setting a criteria of minimizing the number of gray points in dissected matrix edge can eliminate the confusion caused by remaining defects. Inspection of such scenarios is well handled in the code to ensure if exiting pixels within the marginal matrix intercept between the two initial points. If the ungratified point lies in the half portion close to the first gratified point, the satisfied point next to it is selected as the initiative point. If the error point exists in the other side, the last gratified point is chosen before the splash as the destination. This process repeats until there are no dissatisfactory points between intercepted points in the border matrix. The algorithm slightly adjusts the degree of accuracy for those images.

Then, the midpoint position of authentic coincident points is determined. Depending on the midpoint and the center of a circle, corresponding deviation angle trigonometric function formula is applied to calculate the angle value. For example, pointer direction is clockwise and the line segment is in quadrant four, the result should be the deviation angle in this quadrant plus 90 degree. The required deviation angles in different quadrants are illustrate in Fig. 6.

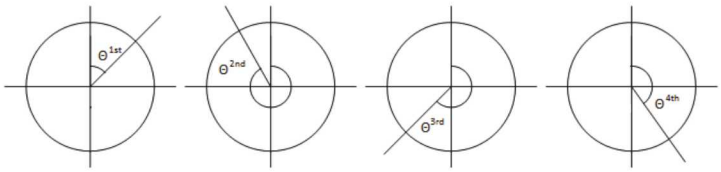

Fig. 6. Deviation angles in different quadrants

The offset angle is calculated based on the pointer position in each quadrant. If pointer is in quadrant one or three, offset angle is calculated by Eq. (2) where the sequence of P constant indicates the first and third quadrant. If pointer locates in quadrant two or four, we apply Eq. (3) where the sequence of Q constant indicates the second and forth quadrant. The Θ is offset angle with corresponding quadrant, and X_{mid}, Y_{mid} and X_{center}, Y_{center} present the coordinate of midpoint and center of circle, respectively.

Under certain circumstance, the adjacent pointers in traditional electromechanical analog meters may have an inverse numerical plate. This is why there are two columns of numbers in Table I. In order to improve the accuracy of final result, we divide each digit span in the last digital dial plate into 10 sections and divide the corresponding value in Table I as well. For example, if the deviation degree is 0 to 3.6, the reading result of clockwise should be 0.1 rather than 0. Fig.7 demonstrates the flow chart of overview process of image data extracting.

IV. CASE STUDY

The proposed method is simulated and validated on a test case using the existing electromechanical analog meters in a building connected to part of the Michigan Tech distribution system. The simulation of time-activity curves is discussed in this section.

$$\Theta = \arctan\left(\frac{|X_{mid} - X_{center}|}{|Y_{mid} - Y_{center}|}\right) + P, \text{ where } P = 0^\circ \text{ or } 180^\circ \tag{2}$$

$$\Theta = \arctan\left(\frac{|Y_{mid} - Y_{center}|}{|X_{mid} - X_{center}|}\right) + Q, \text{ where } Q = 270^\circ \text{ or } 90^\circ \tag{3}$$

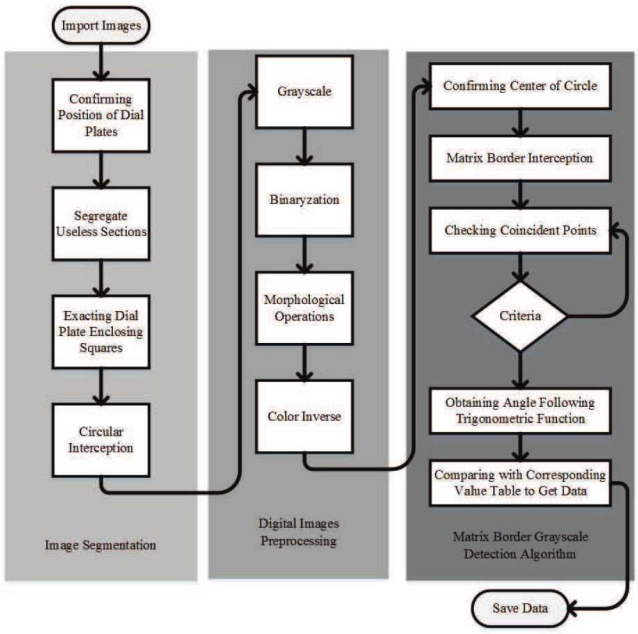

Fig. 7. Intercept a square matrix border within the exported image

A. Test Case Setup

Fig. 8 is the geographical map of the campus distribution network with numbered buildings. In the existing grid infrastructure, there is one substation and four generating units in building 41 which is also the facilities management site. There are three existing distribution feeders and each building is connected to a primary feeder and a backup feeder. The dark gray circles are the 11 buildings deployed with IP-based electricity meters. In this study, an unmetered building (Building 20 highlighted with light gray) was chosen for the study. This building was selected because it has a relatively high consumption percentage relative to the other unmetered buildings and it has the required Wi-Fi and available power.

Two different types of electromechanical analog meters were present in Building 20's electrical room - 208V and 480V. The 208-V meter monitors low power-driven equipment such as lighting and electronic locks while the 480-V meter detects high-power machinery loads. The case study was based on both meters and the datasets obtained from meter readings were recorded for nine days.

Two mobile devices were deployed with the timer camera application and placed in front of the dial plates with the car stand support as illustred in Fig. 9. The charge line ensures continuous power supply to the mobile devices. The captured pictures were automatically uploaded to the photo stream and were shown in the shared computer directory every 15 minutes via the cloud.

B. Study Results

Converted meter readings were saved in an OCR file for future analysis. Finite difference, time-activity curves for both

Fig. 9. Timer camera in operational mode

meters are illustrated in Fig. 10 and Fig. 11. The curve of actual image extracted data from 208-V circuit is similar to a bar chart rather than the typical line chart because the energy consumption of low power devices is limited during 15-minute cycle, the image data extraction program has constrained capacity to detect the slight angular deflection in dial plate. The short period of cyclic snapshots shows obvious bump-up or zero values.

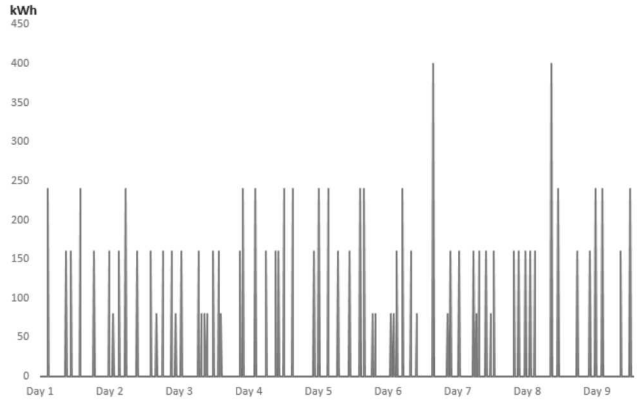

Fig. 10. Energy consumption of building-20 208-V circuit between 3/22/2014 and 3/30/2014

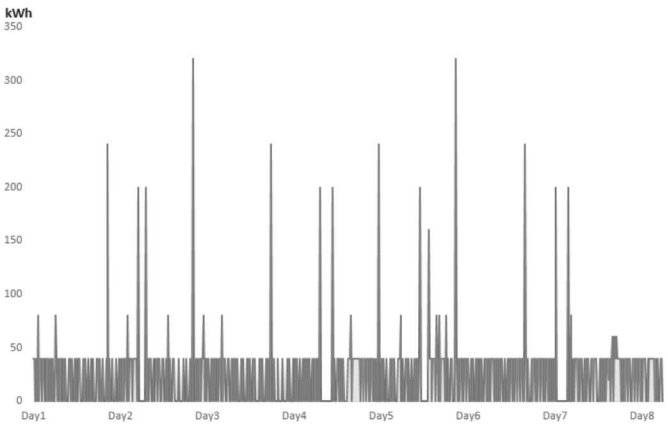

Fig. 11. Energy consumption of building-20 480-V circuit between 3/22/2014 and 3/29/2014

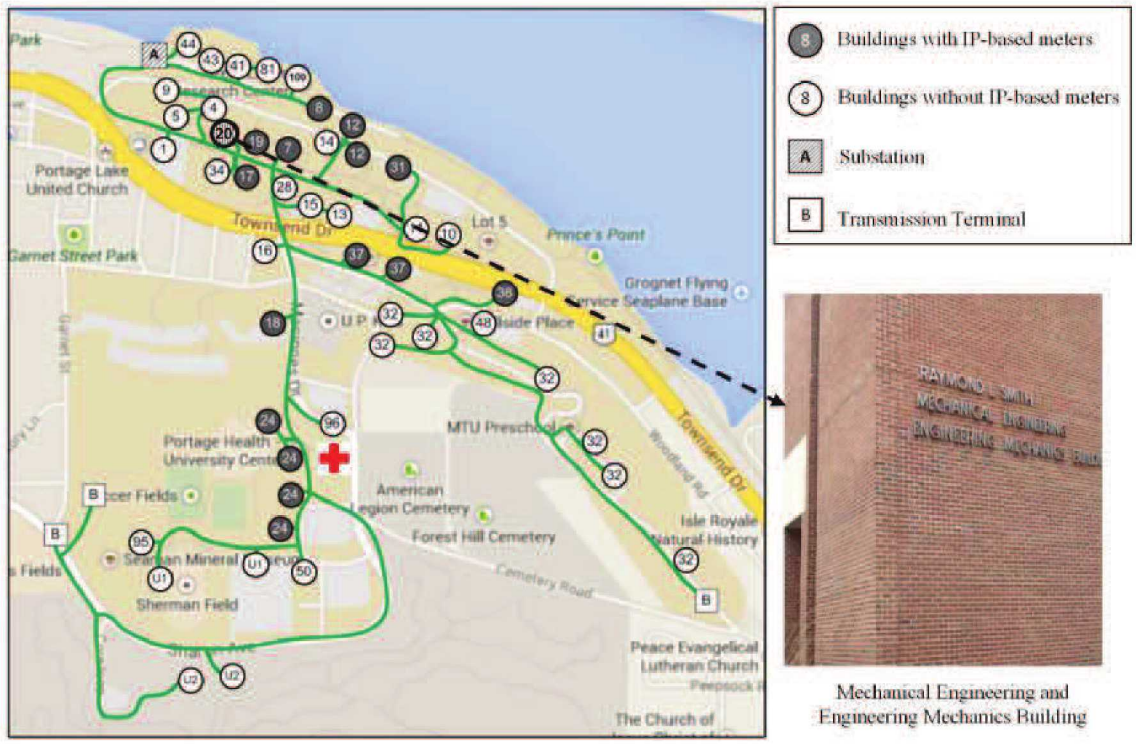

Fig. 8. Campus-wide distribution system with 38 buildings

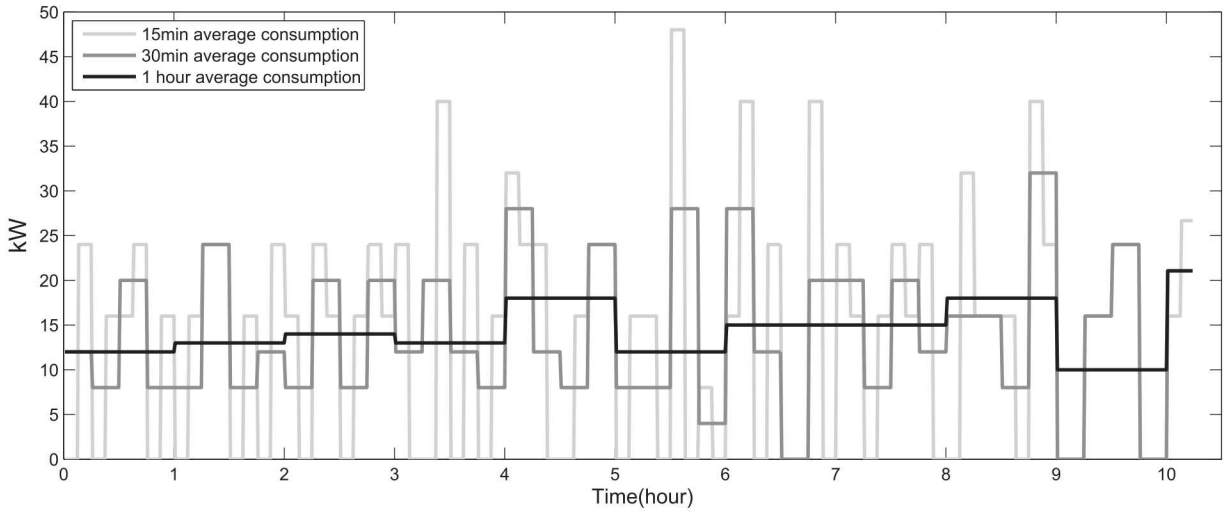

Fig. 12. Average consumption for building-20 208-V circuit

As the rotation of the electromechanical blade can be slow (scale of 800), considering average consumption time-activity curves with 15-minute, 30-minute, and an-hour timescale can help to estimate and predict energy consumption over a longer period of time. The initial experimental outcome of the datasets is shown in Figs. 12 and 13 corresponding to 208-V and 480-V circuits, respectively.

Considering pictorial data acquisition from building 20 and metering information to the entire distribution system, comparison between the building and campus-wide distribution system is made. The combined circuits of 208V and 480V provides a total sum of the building between March 22 and March 29. Not all numerical values are reflected from the extraction due to slow angular movement of point as a result of the zero values. The mean value shown in Fig.14 could be much smaller than the actusal average of power usage. Fig. 15 shows the piecharts in percentage for the lump sum of metered and unmetered buildings as well as building-20 total consumption. The statistics are obtained from the building management system of AX Supervisor database under the

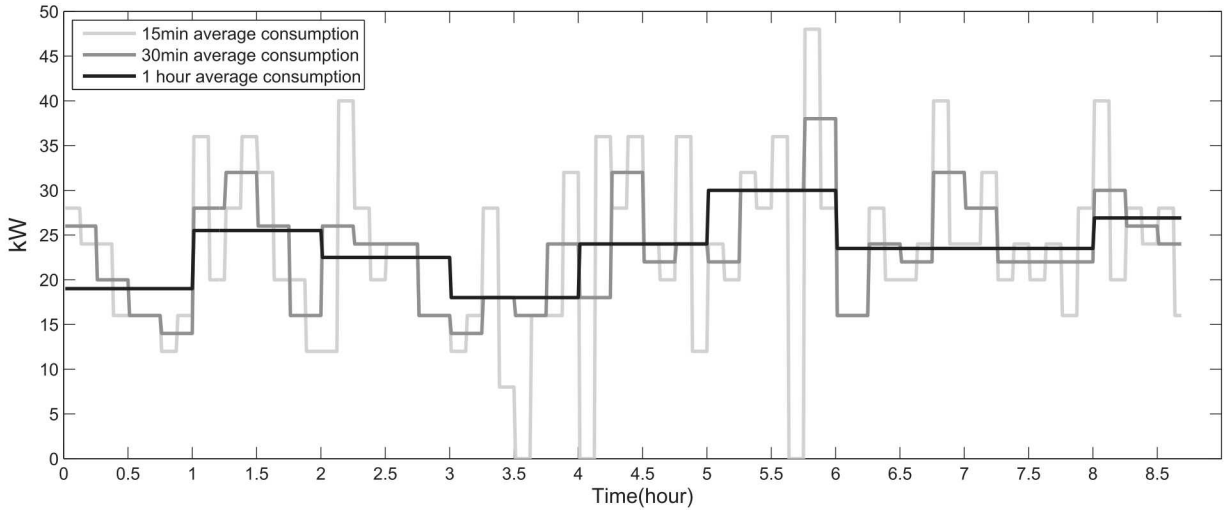

Fig. 13. Average consumption for building-20 480-V circuit

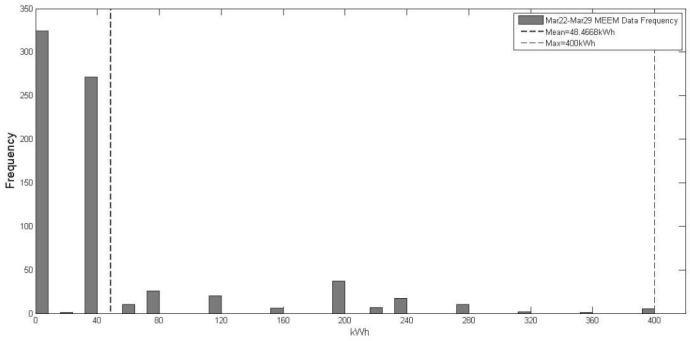

Fig. 14. Data histogram between 3/22/2014 and 3/29/2014

same time period. These piecharts show different duration with accumulative energy values for 6 hours, 12 hours, 1 day, 2 days, 5 days, and 10 days.

This simulation consists of 6 different time durations. The metering infrastructure deployment represents the completed IP-based AMI system while the remaining deployment represents buildings with electromechanical analog meters or other types meters that could not execute intelligent reading through IP-based network.

In most cases on those 6 durations, the proportion of energy usage of IP-based metering buildings is estimated to be about 70 percentage. As one of unmetered buildings, the energy consumption of building 20 is apparently higher than the other 25 buildings. By observation, the energy consumption of building 20 consistently shows between 3.3 and 3.5 percent relatively to the system load. The monthly consumption percentage in March 2014 is close to the average values with 3.51 percent. This indicates the pictorial extraction algorithm indicates reasonable outcome of the energy consumption for that building.

V. Conclusion and Future Work

The proposed method is designed to automatically extract data from images of electromechanical analog meters without "smart" IP-based energy meter. The proposed framework requires wireless network environment and continuous power supply in existing electromechanical analog meters' location as well as Internet availability for real-time transmission to the cloud. The algorithm includes image segmentation, digital image processing, and matrix border grayscale detection analysis. It is noted that there are a few error points during the process of matrix boarder grayscale detection. Setting a criterion of restricting the region of getting correct points will decrease the number of significant errors whereas the accuracy rating of these arranged images will be influenced slightly. Simulation results show that the proposed method provides periodically extracted data to generate time-activity curves with other IP-based metering devices. The proposed application has been tested to one of the unmetered buildings which has reasonably large consumptions among those. It is important to implement Wi-Fi reception for meter locations or replace the mobile device to ensure images can be transferred as well as with outlets in order to provide continuous power supply. Future work would append additional circle recognition algorithm, which could apply specific radius detection method in the existing algorithm.

Acknowledgments

The authors would like thank Mr. G. Kaurala for providing the building load profiles and assistance throughout this study.

References

[1] (2014, Feb.) Advanced metering infrastructure and customer systems. SmartGrid.gov. [Online]. Available: http://www.smartgrid.gov/recovery_act/deployment_status/ami_and_customer_systems.

Appendix F Cybersecurity of Distribution Devices and Systems

1

Cybersecurity of Distribution Devices and Systems

Yonghe Guo and Chee-Wooi Ten

1.1 Metering Infrastructure in Power Distribution Networks

Over the past decade, advanced metering infrastructure (AMI) devices have been deployed to improve the infrastructure of electrical distribution grids. These devices not only include the highly publicized "smart" meters replacing the older mechanical meters for consumers, but also additional remote metering and instrumentation across electrical distribution grids. The key feature of deploying this technology is to increase the number of additional IP-based data collection points across the electrical grid so that a closer to real-time measurement status of the electrical distribution grid can be available to utilities. These data points are networked over an existing communication infrastructure connecting to a distribution dispatching center (DDC) with distribution management system (DMS) with supervisory control and data acquisition (SCADA) functionalities. The functionalities include accumulating the data, performing network analysis and outage management, and then recommending engineering solutions to improve system reliability.

Cyberinfrastructure of distribution control networks has been the central hub of system operations where DMS is the key component of the SCADA system. Typically, it is a multi-computer system networked with redundant servers and workstations with online software packages. The basic applications provided by DMS generally include network outage management, unbalanced power flow, short circuit analysis, fault location, isolation and service restoration, load modeling and forecast. The system enables operators to reconfigure the system under emergency conditions for improving overall system reliability.

This chapter introduces statistical methods to discover meaningful system normal/abnormal patterns as well as to assimilate insightful information for decision-making. This includes data validation framework between (1) substation remote terminal units (RTU), (2) pole-mounted advanced communication unit, such as feeder remote terminal units (FRTU/FTU), (3) distribution transformer monitoring units, as well as (4) advanced metering infrastructure (AMI) against malicious manipulation of real-time data. This cross-domain physical network application provides an assisted fraud analytics by inferring anomalies within distribution network subsystems.

Handbook of Smart Grid Development C.-C. Liu, S. McArthur, and S.-J. Lee

1.1.1 Non-Technical Losses of Utilities

Non-technical losses are referred to intentional reduction of utility revenue by potentially malicious consumers either by physical or electronic means. One of them is the electricity theft that has been the longstanding issues to utilities as it can cause billions of financial losses (Nagi *et al.* 2010; Smith 2004; Winther 2012). Traditionally, the methods of stealing electricity include directly connecting unregistered electrical appliances to power grid (Nizar *et al.* 2008; Suriyamongkol 2002), using alternative neutral lines, tampering meters / terminals, sabotaging control wires, using magnets to decelerate the spinning discs for recording the energy consumption, and tapping off a neighbor legal consumer (McLaughlin *et al.* 2009). Efforts on electricity theft issues are related to variate of techniques and setbacks for controlling electricity theft (Depuru *et al.* 2010a). The strategies proposed can fall into three major categories: (1) historical electricity usage analysis, (2) information security approaches, and (3) metering data mutual validation. Pattern recognition and data mining approaches have been widely applied in historical electricity usage analysis. A genetic algorithm - support vector machines (GA-SVM) based framework is proposed to detect the electricity theft in (Nagi *et al.* 2009) and SVM is also used in (Nagi *et al.* 2010; Depuru *et al.* 2011). Extreme learning machine method is applied to identify energy consumption by evaluating irregular load behavior in (Nizar *et al.* 2008). Due to lack of real-time data, the methods used in off-line analysis use monthly meter reading data collection. The detection accuracy may be impacted by the emerging implementation of demand response (DR) and time of use (TOU). Another concern of the pattern recognition approaches is that the detection results can hardly be used as evidence of electricity theft. Energy theft detection has been proposed utilizing attack graph features based information fusion model to improve the detection accuracy (McLaughlin *et al.* 2013). The harmonic generator is introduced in (Depuru *et al.* 2010b) to penalize the malicious customers if an anomaly has been detected that is deviated from the norm profile. The method first disconnects all genuine customers who are with smart meters from the distribution system. Upon the completion of disconnection of those customers, a harmonic generator is operated for a few seconds to destroy the appliances of malicious consumers. Then, power supply are restored by reconnecting them back to the grid.

1.1.2 Emerging Security Threats and Cyberdefense Framework

The possibilities of non-technical losses have gradually extended to the cyberspace due to the broader deployment of cyberinfrastructure. Despite an enormous investment in ubiquitous sensors monitoring in different parts of distribution network, online system-wide coordination of technical auditing and the establishment of fraud analytics have been nonexistent, leaving the new metering and instrumentation data susceptible to cybertampering. Although countermeasures have been established to strengthen AMI security, inclusion of additional metering points with an existing control center would overwhelm already overstressed operators at distribution control center.

Studies have been focused on security requirements, threats, and efficient security enhancement for AMI multi-path routing protocol (Cleveland 2008; Vaidya *et al.* 2012). These requirements, not only do not address any potential consequence of cyberattack, but it does not help to improve the investment planning for utility to enhance the cyberinfrastructure

with security protection. There have been studies on methods of physical attack and cyberattack against smart meters with a distributed agent-based protection system to protect the infrastructure (McLaughlin *et al.* 2009; Ross *et al.* 2013). Research focusing on AMI protocol security between smart meters and access points with two-phase authentication scheme has been identified in order to reject the connections from unauthorized nodes (Yan *et al.* 2013b; Mehra *et al.* 2013).

Security vulnerabilities and attacks in wireless mesh network (WMN) based smart distribution grid include denial of service, eavesdropping by nodes outside network, eavesdropping by malicious nodes and launching security attacks by nodes within the network (Wang and Yi 2011). Typical means of denial of service (DoS) in smart grid wireless communication network is traffic jamming (Pelechrinis *et al.* 2011). (Pelechrinis *et al.* 2011) reviews the attack means and defense technologies of traffic jamming DoS attack in wireless network. The main limitation of mutual validation method is that it may fail to detect the collusive attack. The collusive attack refers a collaboration among different meters. An attacker attempts to lower the electricity reading of his or her own meter while fraudulently increasing others. The attacker would need to compromise neighborhood meters.

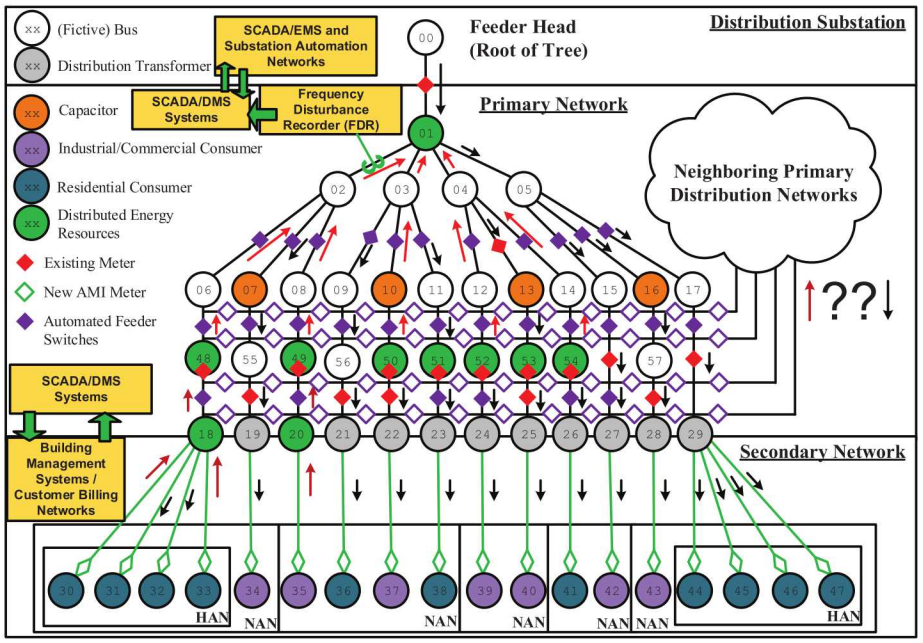

Figure 1.1 Metering infrastructure within primary and secondary distribution networks

1.2 Centralized Control Networks

Centralized control framework empowered by computer systems and applications has advanced system observability and controllability. The control center sends commands either to open or closed on the pole-mounted and substation devices for reconfiguration during fault occurrence. The operations have undergone major improvements with state-of-the-art technologies. The communication technologies include the pole-mounted devices that are located around the distribution network, transmitting the analog and digital measurements to the distribution dispatching center (DDC). The pathways are between communication devices and DDC. As these metering devices are also connected with the switching devices, the dispatchers at DDC would be able to send the control commands to the devices either in open or closed state through SCADA functions. Remote control capability includes the switching devices in distribution substation or the any part of the distribution network with FRTU/FTU. This is recommended by DMS applications to identify the most economic paths during emergency conditions that helps restoring power from other feeders with sequential switching procedures. As shown in Fig. 1.1, major categories of IP-based metering infrastructure in both primary and secondary distribution networks are summarized as follows:

1. Remote terminal units (RTU) instrumenting circuit breakers at the feeder head of distribution substations in primary network.
2. Feeder remote terminal units (FRTU/FTU) connecting to load break switches or reclosers in primary network. The combined elements of switches and sensors are referred as "feeder automated switches."
3. Distribution transformer monitoring (DTM) units in secondary network.
4. "Smart" meters at the customer level of secondary network. This is referred to AMR or AMI. Energy meters (EM) is used throughout the chapter.
5. Frequency disturbance recorder (FDR) in secondary network. This is sometimes named as "single-phase phasor measurement units (PMU)."

There has been cybersecurity research discusses a multi-level information and communication model for smart grid, and then studies the communication and cybersecurity standards for smart grid from three dimensions: smart grid dominies, layers of the proposed information and communication model and stages of the information system life cycle (Wang *et al.* 2011). Surveys indicates that there has been vulnerability on existing smart grid communication system and motivations, requirements, and challenges have been discussed (Yan *et al.* 2012, 2013a). Public key infrastructures of SCADA system and trusted computing is addressed based on the application for SCADA systems for distribution network and potential impact of cyberinfrastructure on utility (Coates *et al.* 2010; Kim *et al.* 2010; Metke and Ekl 2010). Determination of honeypot and its feasibility to protect SCADA system has been identifiy (Disso *et al.* 2013). Security assessment of communication network has been studied using attack graph with multiple criteria decision making strategies (Liu *et al.* 2010). Threats and countermeasures for protecting the communication security with hierarchical conceptual framework has been proposed to protect physical system against cyberattacks (Wei *et al.* 2011).

The cyberthreats to the DMS includes software vulnerability or hardware malfunction. Software vulnerability issues may lead a backdoor for unauthorized access (Bou-Harb

et al. 2013). Cyberintruders who successfully gain administrative privilege of a control network would enable them to execute disruptive control commands resulting in unexpected consequence. DMS and its applications can be compromised and the disruptive execution of DMS functionalities can result in catastrophic consequences. One way to prevent cyberattack on DMS system is to deploy intrusion detection system (IDS) in multi-level distributed fashion (Zhang *et al.* 2011). In some cases, analyzing potential threats using wireless mesh network communication system would be effective in term of detecting intrusion with possible countermeasures (Wang and Yi 2011). Feasibility study on security issues with possible technological countermeasures has been discussed (Bou-Harb *et al.* 2013).

1.2.1 Substation Remote Terminal Units

The communication of distribution substations has a similar communication infrastructure compared to the larger transmission substation. Fundamentally, the instrumentation of substation automation system includes remote terminal units (RTU), circuit breaker, human machine interfaces (HMI), communication devices such as switches, hubs, and routers, log servers, data concentrators, and a protocol gateway (Yan *et al.* 2012). The basic requirements of substation communication security are related to network availability, data integrity, and privacy-related issues (Lu *et al.* 2010). IEC61850 standard has represented the IP-based communication architecture in substation level network for data collection with real-time security analysis tools (Song *et al.* 2013).

1.2.2 Feeder Remote Terminal Units

Feeder remote terminal unit (FRTU/FTU) is the pole-mounted communication device connected to a switching device, e.g., load break switches or reclosers, for remote-controlled and sensing purposes. These are the units deployed in primary distribution network for reconfiguration. Due to the cost constraints, not every switching device is installed with an FRTU. There has been research in system planning to optimally deploy FRTU considering cybersecurity of the secondary network for cross validation between two domain networks (Liao *et al.* 2013). The measurements of FRTU can also be utilized for load estimation that can be useful for advanced DMS applications (Meliopoulos *et al.* 2013). A preliminary investigation of data validation framework on both domain networks has been reported (Guo *et al.* 2014).

1.2.3 Distribution Transformer Monitoring Units

Distribution transformer monitoring device has been installed to observe the health of the physical system for the purpose of preventive maintenance. The benefits to prevent periodic inspection would effectively monitor the transformer and facilitate on-site diagnostics that can avoid forced outages. This will save costs and prolong the expected service time of existing electrical equipment (Bengtsson 1996). These devices consist of on-line diagnostic software, field devices, and communication system that is based on a embedded system with multiple sensors, A/D converters, microcontroller and communication module (Leibfried 1998). The field devices gather parameters related to operating status of the transformers, *i.e.*, voltages, currents, tap changer position, gas-in-oil, and temperatures. The diagnostic

software is installed on a central server at DDC for analyzing data collection and inferring accurate operating status of the transformers. Artificial neural network (ANN) is applied in this process (Ding and Cai 2001). The data flow between field devices and diagnostic server is achieved through the communication system. The typical communication mechanisms include ZigBee and global system for mobile (GSM) communications (Pandey 2013; Al-Ali *et al.* 2004).

The metering data mutual validation adopts multi-level metering data sources, e.g., home energy meter, field remote terminal unit (FRTU) and distribution transformer monitoring device (DTM), to cross check the data authenticity and integrity. A classical application of this principle is the power system state estimation. The method is rather straightforward to implement in practice. Some utility *e.g.*, LADWP, has already installed the distribution transformer sensor to detect potential electricity theft, monitor the status of DT and report power outage. Some related works are briefly introduced following. In (Bandim *et al.* 2003), a central observer meter is installed on the distribution transformer to identify energy theft and tampered meter by comparing overall energy usage with individual customer meters. The proposed model solves an N linearly independent equations system by statistical analysis methods. The coefficient associated with each customer indicates the presence of the energy theft or electricity fraud. (Xiao *et al.* 2013) proposes a cross inspection strategy by deploying two smart meters on both the provider's end and the customer's end of the power line. The peer-to-peer comparison between two smart meters aims to ensure non-repudiation.

1.2.4 Advanced Metering Infrastructure

Automatic metering reading (AMR) is introduced to address the issues of improving load observation. These are IP-based electricity meters (EM) installed at each household premise to transmit energy usage information in real time to customers billing center from each consumer with meters. The technological advance improves utility business model to provide additional choices to consumers. Meanwhile, the electricity theft means have evolved into the electronic fashion (McDaniel and McLaughlin 2009). The technology has further enhanced with control capability in advanced metering infrastructure (AMI). The AMI consists of the following components: "smart" meter, customer gateway, AMI communications network, and AMI headend. (Cleveland 2008). The deployment of AMI supported by communication technologies provides unprecedented observability of distribution system to utilities. It is envisioned that such effort will improve the efficiency of power delivery (Gellings 2009).

The information security methods have been focused on the security oriented design of energy metering devices and intrusion detection system (IDS). The security oriented design aims to increase the difficulty of tampering and probability of energy theft detection. Some smart meters are designed to send alerts when the tampering attempts are detected. The IDS can deduce potential tampering activities through the observation of related physical or cyber events, *e.g.*, irregular log information, suspicious outage notifications from a particular customer, abnormal communication traffic and communication losses. A typical IDS consist of following components: sensors or agents, management server, database server and user interface (Scarfone and Mell 2007). (Berthier *et al.* 2010) discusses the requirements and architectural directions for AMI intrusion detection. The attack model is studied from different angles including type of attacker, motivation and attack technique. Three possible detection mechanisms are explored, including stateful specification-based

monitoring, stateless specification-based monitoring and anomaly-based monitoring. A multi-level distributed intrusion detection system (IDS) for smart grids is proposed in (Zhang *et al.* 2011). The proposed model deploys multiple analyzing modules at each level of the smart grid-the home area networks (HANs), neighborhood area networks (NANs) and wide area networks (WANs). Both support vector machine (SVM) and artificial immune system (AIS) are evaluated for the purpose of detecting possible cyberattacks. The specification-based IDS techniques for AMI has been studied in (Jokar *et al.* 2011; Berthier and Sanders 2011). An intrusion detection system (IDS) for energy theft has been presented featuring an attack graph based information fusion model for improving detection accuracy (McLaughlin *et al.* 2013). These sources include network and host-based intrusion detection systems, on-meter anti-tampering sensors and nonintrusive load monitoring (NILM) based anomalous power consumption detectors which collect and analyze cyber events, physical events and energy consumption data, respectively. This framework is a combination of both electricity usage analysis and information security techniques. Specific requirement studies of IDS techinques for AMI has been investigated (Jokar *et al.* 2011; Berthier and Sanders 2011).

Cybertampering refers to a way to manipulates the energy usage data collected from AMI by the utility. This activity is related to energy theft. When the consumers participate in distributed energy resources, attackers can not only tamper with the energy consumption data, but also falsify the reading of energy production to power grid for financial gain. ybertampering scenarios include malicious modification of meter firmware, meter storage tampering and meter spoofing (McLaughlin *et al.* 2009). Studies show that encryption and authentication alone does not sufficiently protect the AMI from being cyberattacks (Cleveland 2008; McLaughlin *et al.* 2010).

Electrical Vehicle Charging

Plug-in hybrid electric vehicle (PHEV) has contributed to load consumptions of individual household and the charging schedule can be programmed based on the time of use (TOU) pricing. A PHEV is a hybrid vehicle powered by rechargeable batteries or alternative energy storage device which can be restored to full charge by connecting a plug to an external electric power source, *e.g.*, electric wall socket. Vehicle-to-grid (V2G) enables bi-directional charge/discharge capabilities of electrical vechicles to provide ancillary services and peak shaving for the power grid. The loading caused by PHEV charging is dependent on the charging rate, which has multiple levels (Morrow *et al.* 2008). Weaknesses of the NISTIR 7628 framework have been identified in designing the electrical vehicles charging infrastructure that include device authentication and privacy of EV owner protection (Chan and Zhou 2013).

Home Energy Management Systems

Demand response (DR) is adopted by utilities to manage the loading condition by offering the incentives to customers. Baltimore Gas and Electric Company (BGE) and Arizona Public Service Company (APS) are the uilities that implement this by installing intelligent thermostats on customer's central air conditioner, through which the AC can be circled off or controlled to reduce the energy consumption during summer days (APS; BGE). Pacific Gas and Electric Company (PG&E) provides a Base Interruptible Program (BIP) to achieve the

DR (PG&E 2014). The BIP pays the customers an incentive to reduce their facility's load to or below a pre-selected level. Instead of direct control of customer's load, the program encourages customers to manage the load by themselves. Home appliance loads can be predicted by building the load profiles. It all depends on appliance vendors, range of power in Watts, and the average annual electricity usage in kilo-Watt hours (kWh) for the appliances. Existing appliances are divided into 3 major categories: (1) air conditioners, (2) general appliances, and (3) kitchen appliances. Major appliance loads including air conditioners, freezers, refrigerator, swimming pool pump motor, and water heater, contributing to the base loads of household.

Residential Distributed Energy Resources

Photovoltaic (PV) system is one of the distributed energy resources that has been widely deployed in residential areas. PV system can directly convert solar radiation into electric power. A typical PV system consists of following major components: solar panel array, tracking system, charge controller, battery, and inverter. Solar panel array is a linked assembly of solar cell modules. In order to get the appropriate voltage, the modules are firstly wired in series to form individual strings. Then the strings are connected in parallel to generate more current. The charge controller can prevent from being damaged by excessive charging and discharging and enable optimal output of modules by maximum power point tracking (MPPT). The inverter converts the DC output from solar modules into utility frequency AC so that the electricity produced by PV system can be fed back to power grid. The energy production of a PV system is determined by a number of factors, including total incident radiation, module area, module efficiency at a given incident global radiation level and overall DC to AC derate factor (Soto *et al.* 2006).

1.2.5 Frequency Disturbance Recorder

Frequency disturbance recorder (FDR) is a digital sensor unit that is connected to low voltage power outlet for acquiring real-time voltage, frequency, and angle information that are in synchronism with GPS time clock. There have been applications of using such datasets for wide area control and monitoring in transmission network during system disturbance. The information security of the FDR units connecting to FNET has been addressed (Zhang *et al.* 2010; Power IT Lab 2007). As the FDR units are the ubiquitous devices in secondary distribution network, there are applications that would utilize these devices for distribution monitoring and load modeling.

1.3 Identification of Subsystem within Primary Metering Infrastructure

The previous sections provide an overview of metering infrastructure for distribution system and escalating cyber-related issues. This section provides the methodology to systematically identify a subsystem within primary network for data validation.

Data validation is to verify the metering information across the two network domains ensuring that the datasets are consistent. Due to the tree structure of the distribution feeder, these metering data can be cross validated. The most common devices in primary networks

are the substation RTUs at the feeder head and the feeder automated switches introduced previously with FRTU/FTU. The motivation here is to cluster a set of subsystem by determining the credible metering points can be used for validation. This subsystem will then be compared with the secondary network metering devices which are DTM and EM units. In general, the topology of the distribution feeder and FRTU/FTU are the subsystem that can be modeled using connection matrix as follows: (Guo *et al.* 2014):

$$\mathbf{\Delta} = \begin{pmatrix} \delta_{1,1} & \cdots & \delta_{1,j} & \cdots & \delta_{1,n} \\ \vdots & \ddots & \vdots & \ddots & \vdots \\ \delta_{i,1} & \cdots & \delta_{i,j} & \cdots & \delta_{i,n} \\ \vdots & \ddots & \vdots & \ddots & \vdots \\ \delta_{n,1} & \cdots & \delta_{n,j} & \cdots & \delta_{n,n} \end{pmatrix} \tag{1.1}$$

where i and j are the numbering index of FRTU, and

$$\delta_{i,1} = \begin{cases} -1 & \text{if } j \text{ is the upstream} \\ & \text{neighboring FRTU of } i, \\ 1 & \text{if } j \text{ is the downstream} \\ & \text{neighboring FRTU of } i, \\ 0 & \text{if } i = j \text{ or i and j are} \\ & \text{not neighboring FRTU.} \end{cases} \tag{1.2}$$

Each row of the connection matrix indicates the neighboring FRTUs of the corresponding FRTU. In a radial system, each FRTU can only have 1 upstream FRTU, thus each row can only have one element equal to -1. The number of a row and the column indices of the elements equal to 1 represent an FRTU and its downstream neighboring downstream FRTUs that determine the boundary FRTU set of a subsystem. The connection matrix is a sparse matrix and can be expressed as

$$\mathbf{\Delta} = \mathbf{U} + \mathbf{D} + \mathbf{L}, \tag{1.3}$$

where $\mathbf{U}$ and $\mathbf{L}$ are the upper and lower triangle matrix of $\mathbf{\Delta}$, respectively, and $\mathbf{D}$ is the diagonal consist of diagonal elements of $\mathbf{\Delta}$. Obviously, the matrices $\mathbf{U}$, $\mathbf{L}$ and $\mathbf{D}$ have the following properties

$$\mathbf{L} = -\mathbf{U}^{\mathrm{T}}, \text{ and } \mathbf{D} = 0. \tag{1.4}$$

However, it is subject to the availability of FRTUs. Generally, factors considered that FRTU might be malfunctional include the loss of power supply that does not function as it should or communication failure. The key attribute to determine what FRTU should be part of the subset of subsystems is the availability and integrity of the measurements. This is crucial as the FRTU measurements would be used as the credible sources for cross-validation with the secondary network. In real-time scenario, if an FRTU is losing communication with DDC, power supply warning, or irregular response, the unit is considered not trustworthy. This process can be summarized by a boolean function:

$$\mathrm{T}_{\mathrm{FRTU}} = \overline{E_1 \cup E_2 \cup \cdots \cup E_N} \tag{1.5}$$

where $\mathrm{T}_{\mathrm{FRTU}}$ is a boolean variable indicating whether the corresponding FRTU is trustworthy ($\mathrm{T}_{\mathrm{FRTU}} = 1$) or otherwise ($\mathrm{T}_{\mathrm{FRTU}} = 0$), $E_1, E_2, \cdots, E_N$ are the indicators

of the corresponding anomaly events that can make the FRTU untrustworthy. An FRTU is deemed trustworthy if none of the aforementioned malfunction events presents. The subsystems are divided based on the trustworthy FRTU set. A diagonal trustworthy matrix is defined to represent the availability status of each FRTU:

$$\mathbf{T} = \mathbf{diag}\left(\mathrm{T}_{\mathrm{FRTU},1}, \mathrm{T}_{\mathrm{FRTU},2}, \cdots, \mathrm{T}_{\mathrm{FRTU},n}\right) \tag{1.6}$$

where T_i is the corresponding boolean variable of FRTU i. Fig. 1.3 shows an example of combinations clustering the subsystems based on credibility of FRTU statuses.

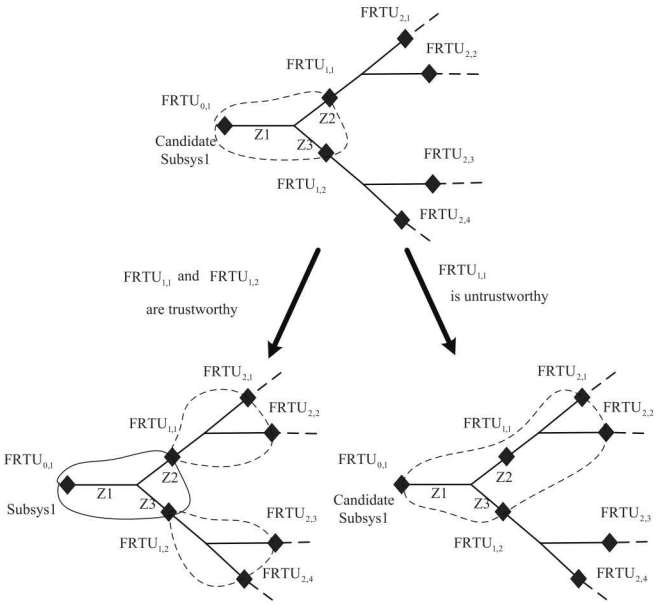

Figure 1.2 Clustering subsystem based on credible metering points in primary network

Subsystem grouping is based on the trustworthy FRTU set. The new FRTU connection matrix can be obtained from the original connection matrix $\mathbf{\Delta}$ and the trustworthy matrix $\mathbf{T}$. The algorithm is summarized in Algorithm 1. The algorithm first calculates a new intermediate matrix $\widehat{\mathbf{\Delta}}$, and then checks whether there are any columns in $\widehat{\mathbf{\Delta}}$ equal to 0. The existence of such zero column vectors indicates the presence of unreliable FRTUs which must be excluded from the trustworthy FRTU set. A new connection matrix of trustworthy FRTU needs to be constructed. The algorithm calls the FINDPARENT procedure to recursively find the new upstream neighboring FRTUs of the trustworthy FRTU set and then calculates the updated the connection matrix.

Algorithm 1 Topological Grouping for a Subsystem (Guo *et al.* 2014)

Require: Determine the $\mathbf{\Delta}$, $\mathbf{T}$ where both from metering data points both from primary and secondary networks. If the FRTU cannot indicate the availability of the accurate switch status and require metering information, then update of connection matrix to determine subsystem will be performed next.

Ensure: To determine the new connection matrix $\mathbf{\Delta}'$

$\widehat{\mathbf{\Delta}} \leftarrow \mathbf{\Delta} \cdot \mathbf{T}$
Let $\widehat{\mathbf{c}}_i$ and $\widehat{\mathbf{r}}_i$ be the i-th column and row of $\widehat{\mathbf{\Delta}}$, respectively
for each column $\widehat{\mathbf{c}}_i$ in $\widehat{\mathbf{\Delta}}$ **do**
    if $\widehat{\mathbf{c}}_i = 0$ **then**
        $j \leftarrow$ FINDPARENT($\widehat{\mathbf{\Delta}}$, i)
        $\widehat{\mathbf{r}}_j \leftarrow \widehat{\mathbf{r}}_j + \widehat{\mathbf{r}}_i$
    end if
end for
for each column $\widehat{\mathbf{c}}_i$ in $\widehat{\mathbf{\Delta}}$ **do**
    if $\widehat{\mathbf{c}}_i = 0$ **then**
        $\widehat{\mathbf{r}}_i \leftarrow 0$
    end if
end for
Decompose $\widehat{\mathbf{\Delta}} = \widehat{\mathbf{L}} + \widehat{\mathbf{D}} + \widehat{\mathbf{U}}$
$\mathbf{\Delta}' = \widehat{\mathbf{U}} - \widehat{\mathbf{U}}^{\mathrm{T}}$

procedure FINDPARENT($\mathbf{\Delta}$, $\widehat{\mathbf{\Delta}}$, i)
    Find $\mathbf{\Delta}[i, j] = -1$
    if $\widehat{\mathbf{\Delta}}[i, j] = -1$ **then**
        return j
    else
        return FINDPARENT($\mathbf{\Delta}$, $\widehat{\mathbf{\Delta}}$, j)
    end if
end procedure

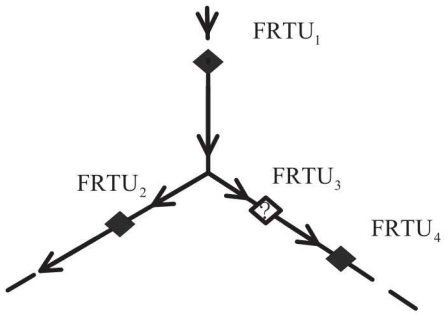

Figure 1.3 Example of four-FRTU connection matrix update

An example is shown in Fig. 1.3, which shows that the FRTU_3 is not available, *i.e.*, $\mathbf{T}(3,3)$ is set to be 0. The original connection matrix and trustworthy matrix are

$$\mathbf{\Delta} = \begin{array}{c} \\ 1 \\ 2 \\ 3 \\ 4 \end{array} \begin{array}{c} \begin{array}{cccc} 1 & 2 & 3 & 4 \end{array} \\ \begin{pmatrix} 0 & 1 & 1 & 0 \\ -1 & 0 & 0 & 0 \\ -1 & 0 & 0 & 1 \\ 0 & 0 & -1 & 0 \end{pmatrix} \end{array}, \tag{1.7}$$

and

$$\mathbf{T} = \begin{array}{c} \\ 1 \\ 2 \\ 3 \\ 4 \end{array} \begin{array}{c} \begin{array}{cccc} 1 & 2 & 3 & 4 \end{array} \\ \begin{pmatrix} 1 & 0 & 0 & 0 \\ 0 & 1 & 0 & 0 \\ 0 & 0 & 0 & 0 \\ 0 & 0 & 0 & 1 \end{pmatrix} \end{array} \tag{1.8}$$

The intermediate matrix can be calculated as

$$\widehat{\mathbf{\Delta}} = \mathbf{\Delta} \cdot \mathbf{T} = \begin{array}{c} \\ 1 \\ 2 \\ 3 \\ 4 \end{array} \begin{array}{c} \begin{array}{cccc} 1 & 2 & 3 & 4 \end{array} \\ \begin{pmatrix} 0 & 1 & 0 & 0 \\ -1 & 0 & 0 & 0 \\ -1 & 0 & 0 & 1 \\ 0 & 0 & 0 & 0 \end{pmatrix} \end{array}. \tag{1.9}$$

Note that the third column vector of the intermediate matrix $\widehat{\mathbf{\Delta}}$ equals 0. Then call the procedure FINDPARENT to find its parent FRTU and update the intermediate matrix:

$$\widehat{\mathbf{\Delta}} = \begin{array}{c} \\ 1 \\ 2 \\ 3 \\ 4 \end{array} \begin{array}{c} \begin{array}{cccc} 1 & 2 & 3 & 4 \end{array} \\ \begin{pmatrix} -1 & 1 & 0 & 1 \\ -1 & 0 & 0 & 0 \\ 0 & 0 & 0 & 0 \\ 0 & 0 & 0 & 0 \end{pmatrix} \end{array}. \tag{1.10}$$

Decompose the intermediate matrix to obtain the upper diagonal matrix $\widehat{\mathbf{U}}$

$$\widehat{\mathbf{U}} = \begin{array}{c} \\ 1 \\ 2 \\ 3 \\ 4 \end{array} \begin{array}{c} \begin{array}{cccc} 1 & 2 & 3 & 4 \end{array} \\ \begin{pmatrix} 0 & 1 & 0 & 1 \\ 0 & 0 & 0 & 0 \\ 0 & 0 & 0 & 0 \\ 0 & 0 & 0 & 0 \end{pmatrix} \end{array}. \tag{1.11}$$

The updated connection matrix can be calculated as

$$\boldsymbol{\Delta}' = \widehat{\mathbf{U}} - \widehat{\mathbf{U}}^{\mathrm{T}} = \begin{array}{c} \\ 1 \\ 2 \\ 3 \\ 4 \end{array} \begin{array}{c} \begin{array}{cccc} 1 & 2 & 3 & 4 \end{array} \\ \begin{pmatrix} 0 & 1 & 0 & 1 \\ -1 & 0 & 0 & 0 \\ 0 & 0 & 0 & 0 \\ -1 & 0 & 0 & 0 \end{pmatrix} \end{array}. \tag{1.12}$$

1.4 Estimating Subsystem Thresholds

This section expands step-two approach of the proposed framework in (Guo *et al.* 2014) with extended statistical analysis for threshold estimation including subsystem load(s) using kernel density estimation (KDE) technique. The KDE method is a non-parametric density estimation method. The parametric methods typically assume that the underlying probability distribution function (PDF) belongs to a certain family of PDF, *e.g.*, normal distribution, and estimate the parameters based on observations.

The root FRTU serves as a power injection point of the subsystem. The leaf FRTUs located at the points downstream subtrees are treated as the border switches, which are the leaf nodes of a spanning tree. Real-time power flow measurements of these FRTUs represent lumped loads of the other subsystems connected to them. This subsystem is then validated by distribution power flow module to estimate its power losses.

The frequency of data from FRTU and customer meters are not identical. The sampling rate for SCADA network is significantly higher than consumer electronic meters and is typically polls the real-time measurements between $3-10$ seconds. The data transfer between distribution operations and customer billing center is assumed to be 15-minute time interval, which follows the cycle of consumer electronic meters. The time intervals between FRTUs and consumer energy meters is defined by $K = \frac{\Delta t_{\mathrm{EM}}}{\Delta t_{\mathrm{FRTU}}}$. FRTUs in primary distribution network are assumed to provide a 3-second measurement data. Thus, measurement data from FRTUs in a 15-minute time interval is normalized with the IP-based energy meters as $\overline{\mathbf{P}}_{\mathrm{FRTU},i} = \frac{\sum_{n=1}^{K} \mathbf{P}_{\mathrm{FRTU},i}(n)}{K}$ and $\overline{\mathbf{Q}}_{\mathrm{FRTU},i} = \frac{\sum_{n=1}^{K} \mathbf{Q}_{\mathrm{FRTU},i}(n)}{K}$ where $\overline{\mathbf{P}}_{\mathrm{FRTU},i}$ and $\overline{\mathbf{Q}}_{\mathrm{FRTU},i}$ are the average three-phase active and reactive power from the i FRTU at time slot n.

The Eq. (4) of (Guo *et al.* 2014) defines the mismatch ratio (MR) between datasets from primary and secondary measurement sources. The MR is modeled as a random variable with a probability density function (PDF). Due to the intrinsic measurement errors, the accuracy losses of data sampling and the limitation of computational precision, the MR may not be perfectly zero under normal conditions. Accurate MR approximation of its PDF is critical

in step-two validation. Let's denote a set of the MR observations $\mathbf{X} = \{x_1, x_2, \cdots, x_n\}$ as random variables. A kernel density estimation (KDE) of the PDF $f(x)$ is

$$f(x) \approx \widehat{f}(x) = \frac{1}{m}\sum_{k=1}^{m} \omega_h(x - x_k) \tag{1.13}$$

where the $\omega_B(x - x_k)$ is the weighting functions. The weighting functions are all of the following form

$$\omega_B(x - x_k) = \frac{1}{B} K\left(\frac{x - x_k}{B}\right) \tag{1.14}$$

where h is the bandwidth and $K(\cdot)$ denotes the kernel function, which consists of the following properties: $\int_{-\infty}^{+\infty} K(x)dx = 1$, $\int_{-\infty}^{+\infty} x \cdot K(x)dx = 0$ and $0 < \int_{-\infty}^{+\infty} x^2 \cdot K(x)dx < \infty$. For the convenience of computation, Gaussian kernel is utilized for the density estimator in this work.

The bandwidth B is the key parameter that can affect the accuracy of $\widehat{f}(x)$. The accuracy of the estimator is the mean integrated squared error (MISE), which is defined by:

$$\begin{aligned}
\text{MISE} &= E\int_{-\infty}^{+\infty} \left(\widehat{f}(x) - f(x)\right)^2 dx \\
&= \int_{-\infty}^{+\infty} \underbrace{\left(E\widehat{f}(x) - f(x)\right)^2}_{\text{pointwise bias of } f} dx \\
&\quad + \int_{-\infty}^{+\infty} \underbrace{\left(E\widehat{f}(x) - \widehat{f}(x)\right)^2}_{\text{pointwise variance of } f} dx
\end{aligned} \tag{1.15}$$

For simplicity, the first-order asymptotic approximation of MISE (AMISE) is used to determine optimal bandwidth, which is given by:

$$\text{AMISE} = \frac{r(K)}{m \cdot B} + \frac{1}{4} k_2(K)^2 B^4 \beta(f) \tag{1.16}$$

where $R_1(K) = \int K(x)^2 dx$, $R_2(K) = \int x^2 K(x)dx$ and $R_3(f) = \int (f''(x))^2 dx$. The optimal bandwidth can be obtained by minimizing Eq. (1.16)

$$B_{\text{AMISE}} = \left(\frac{r(K)}{k_2(K)^2 \beta(f) m}\right)^{1/5} \tag{1.17}$$

However, the Eq. (1.17) cannot be directly used to calculate the optimal bandwidth in practice since it depends on the parameters of PDF $f(x)$. Possible methods of selecting bandwidth include Gaussian distribution reference, cross-validation, and plug-in approaches, depending on the estimator accuracy and computational efficiency.

A numerical result is depicted in Fig.1.4 that estimates the distribution of mismatch ratio of subsystem 70 from (Guo *et al.* 2014). The probability density of MR_i is estimated by Gaussian kernels with 300 historical samples. The histogram shows the shape of PDF is close to a Gaussian distribution. The bandwidth h can be calculated as 0.0558% using the

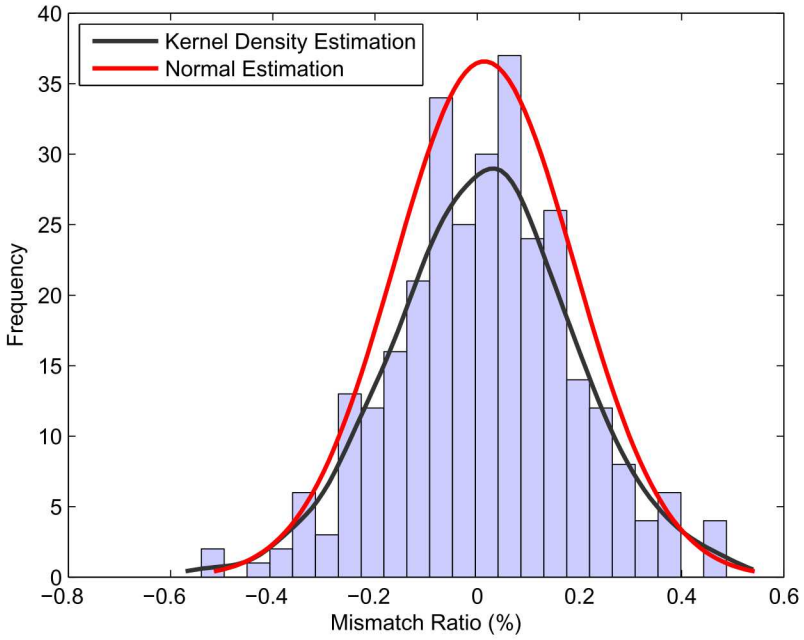

Figure 1.4 Mismatch ratio distribution under normal condition for subsystem 70

Gaussian distribution approach. The simulation shows that the KDE method fits the given samples better than the parametric normal PDF estimation. Similar results are observed in other subsystems.

With the PDF of MR_i estimated, the threshold γ can now be set based on the principle of balancing the possibilities of false positive and negative errors. Let T be the boolean variable indicating the occurrence of tampering events. The probability of false positive errors can be obtained by

$$\begin{aligned} Pr\{|\mathrm{MR}_i| \geq \gamma \mid \overline{T}\} &\approx 1 - \int_{-\gamma}^{\gamma} \widehat{f}(x)dx \\ &= 1 - F(\gamma) + F(-\gamma) \\ &= G(\gamma) \end{aligned} \tag{1.18}$$

where $F(\cdot)$ is the cumulative distribution function (CDF) of MR_i. Intuitively, a smaller threshold value would increase the detection probability of tampering events, *i.e.*, it might decrease the probability of undetected events. Thus, the probability of false negative errors is a non-decreasing function of γ. Given a maximal acceptable probability p_{max} of false

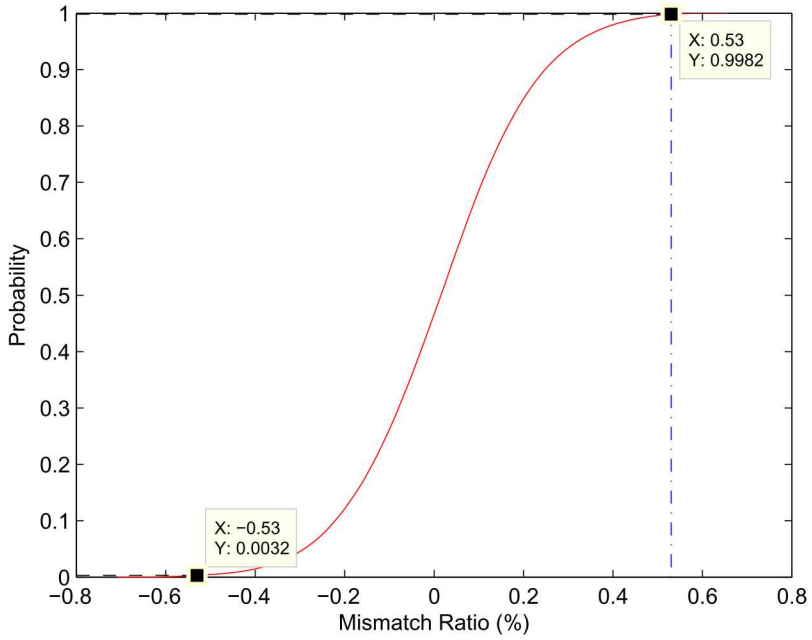

Figure 1.5 Cumulative distribution function of the KDE for subsystem 70

positive errors, the threshold can be set by calculating the corresponding γ

$$\gamma = G^{-1}(p_{max}). \tag{1.19}$$

Fig. 1.5 depicts the estimated CDF of MR for subsystem 70. In the selected simulation case, the p_{max} is set to be 0.5%. It can be observed that $F(0.0053) \approx 0.9982$ and $F(-0.0053) \approx 0.0032$. Then the $G(0.0053)$ can be calculated to be 0.5%. Thus, the value of γ is 0.53%.

Determining an accurate value of the threshold for subsystem is an important step. The threshold settings are recommended statistically under the following assumptions: (1) Only measurement errors of EMs and FRTUs are considered in the analysis. Network topology and parameters are assumed to be accurate. (2) The MR_i has a continuous PDF which is close to the PDF of normal distribution. Through the KDE approach, the PDF of MR can be estimated using the historical samples. Simulation results show that the KDE method can better fit the historical data. Then the estimator $\widehat{f}(x)$ can be used to conduct the hypothesis testing to determine the statistical significance of tampering occurrence.

1.5 Conclusion

This chapter enumerates current metering technologies in distribution system. Although observability has gradually improved over time, it also introduces cyber-related challenges.

Cyberattacks can be launched through any IP-based metering devices both from primary and secondary networks. Depending on the motive of attackers, likelihood of attack occurrence would be that malicious consumers are incentivized by tampering IP-based devices, resulting in erroneous electricity bill. The proposed three-step data validation approach is a means to cross-check consistency of metering datasets across two domains. This chapter focuses on step-two with extended statistical improvement. Future research includes studies on the strategic locations of metering placement while optimizing infrastructure investment.

References

Nagi J, Yap KS, Tiong SK, Ahmed SK, and Mohamad M 2010 Nontechnical loss detection for metered customers in power utility using support vector machines. *IEEE Trans. Power Del* **25**, 1162–1171.

Smith TB 2004 Electricity theft: A comparative analysis. *Energy Policy* **32**, 2067–2076.

Winther T 2004 Electricity theft as a relational issue: A comparative look at Zanzibar, Tanzania, and the Sunderban Islands, India. *Energy for Sustainable Development* **16**, 111–119.

Nizar AH, Dong ZY, and Wang Y 2008 Power utility non-technical loss analysis with extreme learning machine method. *IEEE Trans. Power Syst.* **23**, 946–955.

Suriyamongkol D 2002 Non-technical losses in electrical power systems. Masters thesis, Ohio University, Electrical Engineering and Computer Science, Ohio.

McLaughlin S, Podkuiko D, and McDaniel P 2009 Energy theft in the advanced metering infrastructure. In *Proc. 4th Int. Workshop Crit. Inf. Infrastruct. Security (CRITIS 2009)*, 176–187.

Gellings CW 2009 *The Smart Grid: Enabling Energy Efficiency and Demand Response*, 1st edn. CRC Press.

McDaniel P and McLaughlin S 2009 Security and privacy challenges in the smart grid. *IEEE Security Privacy* **7**, 75–77.

Cleveland F 2008 Cybersecurity issues for Advanced Metering Infrastructure (AMI) In*Proc. IEEE Power and Energy Society General Meeting - Conversion and Delivery of Electrical Energy in the 21st Century*, 1–5.

McLaughlin S, Podkuiko D, Miadzvezhanka S, Delozier A, and McDaniel P 2010 Multi-vendor penetration testing in the advanced metering infrastructure. In *Proc. Annual Computer Security Applications Conference*, 107–116.

Depuru SSSR, Devabhaktuni V, Wang L, and Gudi N 2010 Measures and setbacks for controlling electricity theft. In *North American Power Symposium (NAPS), 2010*, 26–28.

Nagi J, Yap KS, Tiong SK, Ahmed SK, and Mohamad M 2009 Detection of abnormalities and electricity theft using genetic support vector machines. In *Proc. IEEE Region 10 Conference TENCON* 1–6.

Depuru SSSR, Wang L, and Devabhaktuni V 2011 Support vector machine based data classification for detection of electricity theft. In *Power Systems Conference and Exposition (PSCE), 2011 IEEE/PES*, 1–8.

Scarfone K and Mell P 2007 Guide to Intrusion Detection and Prevention Systems (IDPS). NIST (National Institute of Standards and Technology) special publication 800-94. [Online]. Available: http://csrc.nist.gov/publications/nistpubs/800-94/SP800-94.pdf.

Berthier R, Sanders WH, and Khurana H 2010 Intrusion detection for advanced metering infrastructures: Requirements and architectural directions. In *Proceedings of the 1st IEEE International Conference on Smart Grid Communications (SmartGridComm)*, 350–355.

Zhang Y, Wang L, Sun W, Green RC, and Alam M 2011 Distributed intrusion detection system in a multi-layer network architecture of smart grids. *IEEE Trans. Smart Grid* **2**, 796–808.

Jokar P, Nicanfar H, and Leung V, 2011 Specification-based intrusion detection for home area networks in smart grids. In *Smart Grid Communications (SmartGridComm), 2011 IEEE International Conference on*, 208–213.

Berthier R and Sanders WH 2011 Specification-based intrusion detection for advanced metering infrastructures. In *IEEE Pacific Rim International Symposium on Dependable Computing*, 184–193.

McLaughlin S, Holbert B, Fawaz A, Berthier R, and Zonouz S 2013 A multi-sensor energy theft detection framework for advanced metering infrastructures. *IEEE J. Sel. Areas Commun.* **31**, 1319–1330.

Bandim CJ, Alves JER Jr, Pinto AV Jr, Souza FC, Loureiro MRB, Magalhaes CA, and Galvez-Durand F 2003 SIdentification of energy theft and tampered meters using a central observer meter: a mathematical approach. In *IEEE/PES Transmission and Distribution Conference and Exposition*, vol 1, 163–168.

Xiao Z, Xiao Y, and Du DCH 2013 Non-repudiation in neighborhood area networks for smart grid. *IEEE Commun. Mag.* **51**, 18–26.

Depuru SSSR, Wang L, and Devabhaktuni V 2010 A conceptual design using harmonics to reduce pilfering of electricity. In *IEEE Power and Energy Society General Meeting*, 1–7.

Soto WD, Klein SA, and Beckman WA 2006 Improvement and validation of a model for photovoltaic array performance. *IEEE Commun. Mag.* **80**, 78–88.

Morrow K, Karner D, and Francfort J 2008 Plug-in hybrid electric vehicle charging infrastructure review. [Online]. Available: http://www1.eere.energy.gov/vehiclesandfuels/avta/pdfs/phev/phev_infrastructure_report_08.pdf.

Pelechrinis K, Iliofotou M, and Krishnamurthy SV 2011 Denial of Service Attacks in Wireless Networks: The Case of Jammers. *IEEE Communications Surveys & Tutorials* **13**, 245–257.

Lu Z, Lu X, Wang W, and Wang C 2010 Review and evaluation of security threats on the communication networks in the smart grid. In *Military Communications Conference, 2010 - MILCOM 2010* , 1830–1835.

Wang X and Yi P 2011 Security Framework for Wireless Communications in Smart Distribution Grid. *IEEE Trans. Smart Grid* **2**, 809–818.

Yan Y, Qian Y, Sharif H, and Tipper D 2012 A Survey on Cyber Security for Smart Grid Communications. *IEEE Communications Surveys & Tutorials* **14**, 998–1010.

Coates GM, Hopkinson KM, Graham SR, and Kurkowski SH 2010 A Trust System Architecture for SCADA Network Security. *IEEE Trans. Power Del* **25**, 158–169.

Kim J, Ahn S, Kim Y, Lee K, and Kim S 2010 Sensor network-based AMI network security. In *Transmission and Distribution Conference and Exposition, 2010 IEEE PES*, 1–5.

Liu N, Zhang J, Zhang H, and Liu W 2010 Security Assessment for Communication Networks of Power Control Systems Using Attack Graph and MCDM. *IEEE Trans. Power Del* **25**, 1492–1500.

Wei D,, Lu Y, Jafari M, Skare PM, and Rohde K 2011 Protecting Smart Grid Automation Systems Against Cyberattacks. *IEEE Trans. Smart Grid* **2**, 782–795.

Yan Y, Qian Y, Sharif H, and Tipper D 2013 A Survey on Smart Grid Communication Infrastructures: Motivations, Requirements and Challenges. *IEEE Communications Surveys & Tutorials* **15**, 5–20.

Wang Y, Zhang B, Lin W, and Zhang T 2011 Smart grid information security - a research on standards. In *Advanced Power System Automation and Protection (APAP), 2011 International Conference on*, vol 2, 1188–1194.

Song IK, Yun SY, Kwon SC, and Kwak NH 2013 Design of Smart Distribution Management System for Obtaining Real-Time Security Analysis and Predictive Operation in Korea. *IEEE Trans. Smart Grid* **4**, 375–382.

Bou-Harb E, Fachkha C, Pourzandi M, Debbabi M, and Assi C 2013 Communication security for smart grid distribution networks. *IEEE Commun. Mag.* **51**, 42–49.

Chan A and Zhou J 2013 On smart grid cybersecurity standardization: Issues of designing with NISTIR 7628. *IEEE Commun. Mag.* **51**, 58–65.

Vaidya B, Makrakis D, and Mouftah H 2012 Secure multipath routing for AMI network in Smart Grid. in *Performance Computing and Communications Conference (IPCCC), 2012 IEEE 31st International* 408–415.

Ross KJ, Hopkinson KM, and Pachter M 2013 Using a Distributed Agent-Based Communication Enabled Special Protection System to Enhance Smart Grid Security. *IEEE Trans. Smart Grid* **4**, 1216–1224.

Liao C, Ten CW, and Hu S 2013 Strategic FRTU Deployment Considering Cybersecurity in Secondary Distribution Network. *IEEE Trans. Smart Grid* **4**, 1264–1274.

Yan Y, Hu RQ, Das SK, Sharif H, and Qian Y 2013 An efficient security protocol for advanced metering infrastructure in smart grid. *IEEE Network* **27** 64–71.

Mehra T Dehalwar V and Kolhe M 2013 Data Communication Security of Advanced Metering Infrastructure in Smart Grid. in *Computational Intelligence and Communication Networks (CICN), 2013 5th International Conference on* 394–399.

Meliopoulos APS, Polymeneas E, Tan Z, Huang R and Zhao D 2013 Advanced Distribution Management System. *IEEE Trans. Smart Grid* **4**, 2109–2117.

Metke AR and Ekl RL 2010 Security Technology for Smart Grid Networks. *IEEE Trans. Smart Grid* **1**, 99–107.

Disso JP, Jones K, and Bailey S 2013 A Plausible Solution to SCADA Security Honeypot Systems. in *Broadband and Wireless Computing, Communication and Applications (BWCCA), 2013 Eighth International Conference on* 443–448.

Guo Y, Ten CW, and Jirutitijaroen P 2014 Online Data Validation for Distribution Operations Against Cybertampering. *IEEE Trans. Power Syst.* **2**, 550–560.

Zhang Y, Markham P, Xia T, Chen L, Wu Z, Yuan Z, Wang L, Bank J, Burgett J, Conners R, and Liu Y 2010 Online Data Validation for Distribution Operations Against Cybertampering. *IEEE Trans. Smart Grid* **1**, 159–167.

Liu Y 2005 Frequency Monitoring Network (FNET) Web Display. Power Information Technology Laboratory at the University of Tennessee-Knoxville. [Online]. Available: http://fnetpublic.utk.edu/index.html.

Bengtsson C 1996 Status and trends in transformer monitoring. *IEEE Trans. Power Del* **11**, 1379–1384.

Leibfried T 1998 Online monitors keep transformers in service. *IEEE Computer Applications in Power* **11**, 36–42.

Ding X and Cai H 2001 On-line transformer winding's fault monitoring and condition assessment. In *Proceedings of 2001 International Symposium on Electrical Insulating Materials, 2001. (ISEIM 2001)*, 801–804.

Pandey RK and Kumar D 2013 Distributed transformer monitoring system based on zigbee technology. *International Journal of Engineering Trends and Technology* **4**, 1981–1983.

Al-Ali AR, Khaliq A and Arshad M Cai H 2004 GSM-based distribution transformer monitoring system. In *Proceedings of the 12th IEEE Mediterranean Electrotechnical Conference, 2004. MELECON 2004.*, vol 3, 999–1002.

Thermostats and load control. Arizona Public Service (APS) Company, Arizona. [Online]. Available: http://www.aps.com/en/business/savemoney/solutionsbyequipmenttype/Pages/thermostats-and-energy-controls.aspx.

Demand Response Service. Baltimore Gas and Electric (BGE) Company, Maryland. [Online]. Available: http://www.bge.com/myaccount/billsrates/ratestariffs/electricservice/electric services rates and tariffs/rdr_15.pdf.
Base Interruptible Program (BIP). Pacific Gas and Electric (PGE) Company, California. [Online]. Available: http://www.pge.com/mybusiness/energysavingsrebates/demandresponse/baseinterruptible/.

Acknowledgments The authors would like to thank the many experts that contributed to the development of this document. This project was funded by the US Department of Energy Office of Electricity Delivery and Energy Reliability Smart Grid R&D. This work was supported by United States Department of Energy award DE-AC02-06CH11357.

DER-CAM has been funded partly by the Office of Electricity Delivery and Energy Reliability, Distributed Energy Program of the U.S. Department of Energy under Contract No. DE-AC02-05CH11231. The Distributed Energy Resources Customer Adoption Model (DER-CAM) has been designed at Lawrence Berkeley National Laboratory (LBNL). I also want to thank Michael Stadler and Goncalo Cardoso from LBNL for their valuable support and help during the DER-CAM runs.

References

[1] D. E. King, "The regulatory environment for interconnected electric power microgrids: insights from state regulatory officials," *Carnegie Mellon Electricity Industry Center Working Paper CEIC-05-08*, May 2008. [Online]. Available: https://wpweb2.tepper.cmu.edu/ceic/pdfs/CEIC_05_08.pdf

[2] W. Bower *et al.*, "The advanced microgrid integration and interoperability," *Sandia Report SAND2014-1535*, March 2014.

[3] P. Denholm and R. M. Margolis, "Evaluating the limits of solar photovoltaics (pv) in traditional electric power systems," *Energy Policy*, vol. 35, no. 5, pp. 2852 – 2861, 2007. [Online]. Available: http://www.sciencedirect.com/science/article/pii/S0301421506003740

[4] P. Denholm and M. Hand, "Grid flexibility and storage required to achieve very high penetration of variable renewable electricity," *Energy Policy*, vol. 39, no. 3, pp. 1817 – 1830, 2011. [Online]. Available: http://www.sciencedirect.com/science/article/pii/S0301421511000292

[5] M. A. Hyams, "Microgrids: An assessment of the value, opportunities and barriers to deployment in new york state," *New York State Energy Research and Development Authority (NYSERDA)*, Sep 2010. [Online]. Available: http://nechpi.org/wp-content/uploads/2012/07/NYS-Microgrids-Roadmap.pdf

[6] E. Alliance, "Dc microgrids advanced power distribution platforms for flexibility, savings & sustainability in buildings," last visited on 06/05/2014. [Online]. Available: http://portal.emergealliance.org/DesktopModules/Inventure_Document/FileDownload.aspx\?ContentID=20116

[7] R. Lasseter, "Smart distribution: Coupled microgrids," *Proceedings of the IEEE*, vol. 99, no. 6, pp. 1074–1082, June 2011.

[8] M. Vadari and G. Stokes, "Utility 2.0 and the dynamic microgrid," Nov 2013. [Online]. Available: http://www.fortnightly.com/fortnightly/2013/11/utility-20-and-dynamic-microgrid

[9] F. Shahnia, R. Chandrasena, S. Rajakaruna, and A. Ghosh, "Interconnected autonomous microgrids in smart grids with self-healing capability," in *Renewable Energy Integration*, ser. Green Energy and Technology, J. Hossain and A. Mahmud, Eds. Springer Singapore, 2014, pp. 347–381. [Online]. Available: http://dx.doi.org/10.1007/978-981-4585-27-9_15

[10] G. Kasbekar and S. Sarkar, "Pricing games among interconnected microgrids," in *Power and Energy Society General Meeting, 2012 IEEE*, July 2012, pp. 1–8.

[11] M. Fathi and H. Bevrani, "Statistical cooperative power dispatching in interconnected microgrids," *Sustainable Energy, IEEE Transactions on*, vol. 4, no. 3, pp. 586–593, July 2013.

[12] P. Carson, "Grid-tied microgrids: a utility's best friend? remote microgrids grow for under-served end-users." Jan 2012. [Online]. Available: http://www.intelligentutility.com/article/12/01/grid-tied-microgrids-utilitys-best-friend

[13] J. Berst, "The microgrid primer every power engineer should study," Jul 2013. [Online]. Available: http://www.smartgridnews.com/artman/publish/Delivery_Microgrids/The-microgrid-primer-every-power-engineer-should-study-5860.html#.U5HhIa1dXXo

[14] L. Polycarpou, "The microgrid solution," Jun 2013. [Online]. Available: http://www.resilience.org/stories/2013-06-15/the-microgrid-solution

[15] [Online]. Available: http://www.paretoenergy.com/the-company.html

[16] IEEE Standards Coordinating Committee 21. IEEE Std 1547.4-2011.

[17] Information Technology Industry Council. Iti (cbema) curve. [Online]. Available: http://microblog.routed.net/wp-content/uploads/2007/09/iticurv.pdf

[18] IEEE recommended practices and requirements for harmonic control in electrical power systems. (1993) IEEE Std 519-1992.

[19] K. Nigim and W.-J. Lee, "Micro grid integration opportunities and challenges," in *Power Engineering Society General Meeting, 2007. IEEE*, June 2007, pp. 1–6.

[20] C. Hill, M. Such, D. Chen, J. Gonzalez, and W. Grady, "Battery energy storage for enabling integration of distributed solar power generation," *Smart Grid, IEEE Transactions on*, vol. 3, no. 2, pp. 850–857, June 2012.

[21] Q. Fu, L. Montoya, A. Solanki, A. Nasiri, V. Bhavaraju, T. Abdallah, and D. Yu, "Microgrid generation capacity design with renewables and energy storage addressing power quality and surety," *Smart Grid, IEEE Transactions on*, vol. 3, no. 4, pp. 2019–2027, Dec 2012.

[22] D. Wilson, R. Robinett, and S. Goldsmith, "Renewable energy microgrid control with energy storage integration," in *Power Electronics, Electrical Drives, Automation and Motion (SPEEDAM), 2012 International Symposium on*, June 2012, pp. 158–163.

[23] B. Johnson, R. Lasseter, F. Alvarado, and R. Adapa, "Expandable multiterminal dc systems based on voltage droop," *Power Delivery, IEEE Transactions on*, vol. 8, no. 4, pp. 1926–1932, Oct 1993.

[24] A. Nagliero, R. Mastromauro, D. Ricchiuto, M. Liserre, and M. Nitti, "Gain-scheduling-based droop control for universal operation of small wind turbine systems," in *Industrial Electronics (ISIE), 2011 IEEE International Symposium on*, June 2011, pp. 1459–1464.

[25] W. Weaver and P. Krein, "Game-theoretic control of small-scale power systems," *Power Delivery, IEEE Transactions on*, vol. 24, no. 3, pp. 1560–1567, July 2009.

[26] W. Weaver, "Dynamic energy resource control of power electronics in local area power networks," *Power Electronics, IEEE Transactions on*, vol. 26, no. 3, pp. 852–859, March 2011.

[27] W. Weaver and P. Krein, "Optimal geometric control of power buffers," *Power Electronics, IEEE Transactions on*, vol. 24, no. 5, pp. 1248–1258, May 2009.

[28] A. Dimeas and N. Hatziargyriou, "Operation of a multiagent system for microgrid control," *Power Systems, IEEE Transactions on*, vol. 20, no. 3, pp. 1447–1455, Aug 2005.

[29] J. Guerrero, M. Chandorkar, T. Lee, and P. Loh, "Advanced control architectures for intelligent microgrids-part i: Decentralized and hierarchical control," *Industrial Electronics, IEEE Transactions on*, vol. 60, no. 4, pp. 1254–1262, April 2013.

[30] J. Guerrero, P. C. Loh, T.-L. Lee, and M. Chandorkar, "Advanced control architectures for intelligent microgrids-part ii: Power quality, energy storage, and ac/dc microgrids," *Industrial Electronics, IEEE Transactions on*, vol. 60, no. 4, pp. 1263–1270, April 2013.

[31] A. Kwasinski, "Quantitative evaluation of dc microgrids availability: Effects of system architecture and converter topology design choices," *Power Electronics, IEEE Transactions on*, vol. 26, no. 3, pp. 835–851, March 2011.

[32] Y. Gu, X. Xiang, W. Li, and X. He, "Mode-adaptive decentralized control for renewable dc microgrid with enhanced reliability and flexibility," *Power Electronics, IEEE Transactions on*, vol. 29, no. 9, pp. 5072–5080, Sept 2014.

[33] A. Morelato and A. Monticelli, "Heuristic search approach to distribution system restoration," *Power Delivery, IEEE Transactions on*, vol. 4, no. 4, pp. 2235–2241, Oct 1989.

[34] D. Shirmohammadi, "Service restoration in distribution networks via network reconfiguration," *Power Delivery, IEEE Transactions on*, vol. 7, no. 2, pp. 952–958, Apr 1992.

[35] M. F. AlHajri and M. El-Hawary, "Exploiting the radial distribution structure in developing a fast and flexible radial power flow for unbalanced three-phase networks," *Power Delivery, IEEE Transactions on*, vol. 25, no. 1, pp. 378–389, Jan 2010.

[36] M. Dilek, F. de Leon, R. Broadwater, and S. Lee, "A robust multiphase power flow for general distribution networks," *Power Systems, IEEE Transactions on*, vol. 25, no. 2, pp. 760–768, May 2010.

[37] G. Chang, S. Chu, and H. Wang, "An improved backward/forward sweep load flow algorithm for radial distribution systems," *Power Systems, IEEE Transactions on*, vol. 22, no. 2, pp. 882–884, May 2007.

[38] M.-S. Kang, C.-S. Chen, C.-H. Lin, C.-W. Huang, and M.-F. Kao, "A systematic loss analysis of taipower distribution system," *Power Systems, IEEE Transactions on*, vol. 21, no. 3, pp. 1062–1068, Aug 2006.

[39] Y. Gou *et al.*, "Defense strategies for advanced metering infrastructure against distributed denial of service," in *IEEE Transactions on Smart Grid*, 2014.

[40] Y. Tang *et al.*, "Image-extracted energy information based on existing electromechanical analog meters," in *IEEE Transactions on Smart Grid*, 2014.

[41] R. Robinett and S. Glover, "Enabling secure, scalable microgrids with high penetration renewables: Grand challenge laboratory directed research and development," *Sandia National Laboratoires*, Mar 2011, fact Sheet.

[42] R. Robinett, D. Wilson, and S. Goldsmith, "Collective control of networked microgrids with high penetration of variable resources part i: Theory," in *Cyber Technology in Automation, Control, and Intelligent Systems (CYBER), 2012 IEEE International Conference on*, May 2012, pp. 1–4.

[43] W. D.G. *et al.*, "Hamiltonian control design for dc microgrids with stochastic sources and loads with applications," in *Power Electronics, Electrical Drives, Automation and Motion (SPEEDAM), 2014 International Symposium on*, 2014.

[44] A. Giacomoni, S. Goldsmith, S. Amin, and B. Wollenberg, "Analysis, modeling, and simulation of autonomous microgrids with a high penetration of renewables," in *Power and Energy Society General Meeting, 2012 IEEE*, July 2012, pp. 1–6.

[45] C. Marnay, G. Venkataramanan, M. Stadler, A. S. Siddiqui, R. Firestone, and B. Chandran, "Optimal technology selection and operation of commercial-building microgrids," *Power Systems, IEEE Transactions on*, vol. 23, no. 3, pp. 975–982, 2008.

[46] C. Marnay, N. DeForest, and J. Lai, "A green prison: The santa rita jail campus microgrid," in *Power and Energy Society General Meeting, 2012 IEEE*, July 2012, pp. 1–2.

[47] P. Smith, "Operational realities of a large office/research campus microgrid," Mar 2013. [Online]. Available: http://www.microgridworldforum.com/pdf/phil-smith.pdf

[48] H. Farhangi, "The path of the smart grid," *Power and Energy Magazine, IEEE*, vol. 8, no. 1, pp. 18–28, January 2010.

[49] M. Amin, "Toward self-healing energy infrastructure systems," *Computer Applications in Power, IEEE*, vol. 14, no. 1, pp. 20–28, Jan 2001.

[50] T. Li and B. Xu, "The self-healing technologies of smart distribution grid," in *Electricity Distribution (CICED), 2010 China International Conference on*, Sept 2010, pp. 1–6.

[51] C. Moreira, F. O. Resende, and J. Peas Lopes, "Using low voltage microgrids for service restoration," *Power Systems, IEEE Transactions on*, vol. 22, no. 1, pp. 395–403, Feb 2007.

[52] S. Ghosn, P. Ranganathan, S. Salem, J. Tang, D. Loegering, and K. Nygard, "Agent-oriented designs for a self healing smart grid," in *Smart Grid Communications (SmartGridComm), 2010 First IEEE International Conference on*, Oct 2010, pp. 461–466.

[53] R. Lasseter, "Smart distribution: Coupled microgrids," *Proceedings of the IEEE*, vol. 99, no. 6, pp. 1074–1082, June 2011.

[54] W. Su and J. Wang, "Energy management systems in microgrid operations," *The Electricity Journal*, vol. 25, no. 8, pp. 45 – 60, 2012. [Online]. Available: http://www.sciencedirect.com/science/article/pii/S104061901200214X

[55] Q. Jiang, M. Xue, and G. Geng, "Energy management of microgrid in grid-connected and stand-alone modes," *Power Systems, IEEE Transactions on*, vol. 28, no. 3, pp. 3380–3389, Aug 2013.

[56] R. Firestone and C. Marnay, "Energy manager design for microgrids," March 2005. [Online]. Available: http://www.osti.gov/scitech/servlets/purl/838178

[57] J. D. Kueck, R. Staunton, S. D. Labinov, and B. Kirby, "Microgrid energy management system," Jan 2003. [Online]. Available: http://www.consultkirby.com/files/TM2002-242_Microgrid.pdf

[58] Y. Zhang, N. Gatsis, and G. Giannakis, "Robust energy management for microgrids with high-penetration renewables," *Sustainable Energy, IEEE Transactions on*, vol. 4, no. 4, pp. 944–953, Oct 2013.

[59] H. Kanchev, D. Lu, F. Colas, V. Lazarov, and B. Francois, "Energy management and operational planning of a microgrid with a pv-based active generator for smart grid applications," *Industrial Electronics, IEEE Transactions on*, vol. 58, no. 10, pp. 4583–4592, Oct 2011.

[60] "National Electrical Code, NFPA70," *National Fire Protection Association, Batterymarch, MA.*

[61] "National Electrical Safety Code," *NFPA, Batterymarch, MA.*, 2012.

[62] [Online]. Available: https://www.misoenergy.org

[63] J. M. Beer, "High efficiency electric power generation: The environmental role," *Progress in Energy and Combustion Science*, vol. 33, no. 2, pp. 107 – 134, 2007. [Online]. Available: http://www.sciencedirect.com/science/article/pii/S0360128506000347

[64] G. Pepermans, J. Driesen, D. Haeseldonckx, R. Belmans, and W. Dhaeseleer, "Distributed generation: definition, benefits and issues," *Energy Policy*, vol. 33, no. 6, pp. 787 – 798, 2005. [Online]. Available: http://www.sciencedirect.com/science/article/pii/S0301421503003069

[65] D. Barr *et al.*, "Microgrid effects and opportunities for utilities," *Burns and McDonnell*, Feb 2013. [Online]. Available: http://www.burnsmcd.com/Resource_/PressRelease/2894/FileUpload/White-Paper-Microgrid-Effects-Opportunities-for-Utilities-031113.pdf

[66] D. Todd *et al.*, "Providing reliability services through demand response: A preliminary evaluation of the demand response capabilities of alcoa inc." *Office of Electricity Delivery and Energy Reliability Transmission Reliability Program U.S. Department of Energy*, 2009. [Online]. Available: http://www.ferc.gov/eventcalendar/Files/20100526085850-ALCOA\%20Study.pdf

[67] D. Todd, "Alcoa - dynamic demand response doe workshop - 10/25-10/26," Oct 2011. [Online]. Available: http://www1.eere.energy.gov/analysis/pdfs/alcoa_dewayne_todd.pdf

[68] K. H. LaCommare and J. H. Eto, "Cost of power interruptions to electricity consumers in the united states (us)," *Energy*, vol. 31, no. 12, pp. 1845 – 1855, 2006. [Online]. Available: http://www.sciencedirect.com/science/article/pii/S036054420600051X

[69] A. Makhijani, "After sandy: Mitigation or adaptation?" Nov 2012. [Online]. Available: http://ieer.org/energy-systems/after-sandy-mitigation-or-adaptation/

[70] S.-H. Song, S. il Kang, and N. kun Hahm, "Implementation and control of grid connected ac-dc-ac power converter for variable speed wind energy conversion system," in *Applied Power Electronics Conference and Exposition, 2003. APEC '03. Eighteenth Annual IEEE*, vol. 1, Feb 2003, pp. 154–158 vol.1.

[71] C. Yang, H. Liang, and J. Jiang, "Modeling and simulation of ac-dc-ac converter system for mw-level direct-drive wind turbine grid interface," in *Power Electronics Specialists Conference, 2006. PESC '06. 37th IEEE*, June 2006, pp. 1–4.

[72] B. Novakovic, Y. Duan, M. Solvenson, A. Nasiri, and D. Ionel, "Multi-physics system simulation for wind turbines with permanent magnet generator and full conversion power electronics," in *Electric Machines Drives Conference (IEMDC), 2013 IEEE International*, May 2013, pp. 541–548.

[73] Y. Li, D. Vilathgamuwa, and P. C. Loh, "Microgrid power quality enhancement using a three-phase four-wire grid-interfacing compensator," *Industry Applications, IEEE Transactions on*, vol. 41, no. 6, pp. 1707–1719, Nov 2005.

[74] S. Rahmani, N. Mendalek, and K. Al-Haddad, "Experimental design of a nonlinear control technique for three-phase shunt active power filter," *Industrial Electronics, IEEE Transactions on*, vol. 57, no. 10, pp. 3364–3375, Oct 2010.

[75] I. Vechiu, G. Gurguiatu, and E. Rosu, "Advanced active power conditioner to improve power quality in microgrids," in *IPEC, 2010 Conference Proceedings*, Oct 2010, pp. 728–733.

[76] S. Pourmousavi and M. Nehrir, "Real-time central demand response for primary frequency regulation in microgrids," *Smart Grid, IEEE Transactions on*, vol. 3, no. 4, pp. 1988–1996, Dec 2012.

[77] L. Watson and J. Kimball, "Frequency regulation of a microgrid using solar power," in *Applied Power Electronics Conference and Exposition (APEC), 2011 Twenty-Sixth Annual IEEE*, March 2011, pp. 321–326.

[78] Z. Li and H. Daneshi, "Some observations on market clearing price and locational marginal price," in *Power Engineering Society General Meeting, 2005. IEEE*, June 2005, pp. 2042–2049 Vol. 2.

[79] MISO, "Miso 2013 winter assessment report," May 2013. [Online]. Available: https://www.misoenergy.org/Library/Repository/Report/Seasonal\%20Market\%20Assessments/2013\%20Winter\%20Assessment\%20Report.pdf

[80] C. Yuen, A. Oudalov, and A. Timbus, "The provision of frequency control reserves from multiple microgrids," *Industrial Electronics, IEEE Transactions on*, vol. 58, no. 1, pp. 173–183, Jan 2011.

[81] C. Yuen and A. Oudalov, "The feasibility and profitability of ancillary services provision from multi-microgrids," in *Power Tech, 2007 IEEE Lausanne*, July 2007, pp. 598–603.

[82] B. Kirby, "Ancillary services: Technical and commercial insights," *prepared for Wrtsil*, 2007. [Online]. Available: http://www.science.smith.edu/~jcardell/Courses/EGR325/Readings/Ancillary_Services_Kirby.pdf

[83] T. Mohn, "Growing the microgrid market. will they threaten utilities?" Feb 2013. [Online]. Available: http://www.energybiz.com/magazine/article/296727/growing-microgrid-market

[84] M. Stadler, M. Groissbock, G. Cardoso, A. Muller, and J. Lai, "Encouraging combined heat and power in california buildings," *Lawrence Berkeley National Laboratory*, 2013.

[85] J. St.John, "Microgrids: Utility vs. private ownership," Feb 2010. [Online]. Available: http://gigaom.com/2010/02/24/microgrids-utility-vs-private-ownership/

[86] R. Lasseter, J. Eto, B. Schenkman, J. Stevens, H. Vollkommer, D. Klapp, E. Linton, H. Hurtado, and J. Roy, "Certs microgrid laboratory test bed," *Power Delivery, IEEE Transactions on*, vol. 26, no. 1, pp. 325–332, Jan 2011.

[87] R. Martin, "Worldwide capacity of utility distribution microgrids to nearly triple by 2018," Dec 2012. [Online]. Available: http://www.navigantresearch.com/newsroom/worldwide-capacity-of-utility-distribution-microgrids-to-nearly-triple-by-2018

[88] R. Schleicher-Tappeser, "How renewables will change electricity markets in the next five years," *Energy Policy*, vol. 48, no. 0, pp. 64 – 75, 2012, special Section: Frontiers of Sustainability. [Online]. Available: http://www.sciencedirect.com/science/article/pii/S0301421512003473

[89] D. Erickson, "Microgrids: A regulatory perspective. overview of the regulatory implications of microgrid implementation in california," Feb 2013. [Online]. Available: http://www.districtenergy.org/assets/pdfs/2013CampConference/MicroGrids/Microgrids-and-Reliability/ERICKSONPUCMicrogrids-for-IDEA-v3.pdf

[90] H. Ibrahim, A. Ilinca, and J. Perron, "Energy storage systemscharacteristics and comparisons," *Renewable and Sustainable Energy Reviews*, vol. 12, no. 5, pp. 1221 – 1250, 2008. [Online]. Available: http://www.sciencedirect.com/science/article/pii/S1364032107000238

[91] B. Dunn, H. Kamath, and J.-M. Tarascon, "Electrical energy storage for the grid: A battery of choices," *Science*, vol. 334, no. 6058, pp. 928–935, 2011. [Online]. Available: http://www.sciencemag.org/content/334/6058/928.abstract

[92] R. Martin, "Utility distribution microgrids will reach nearly $3.3 billion in market value by 2018, according to pike research," Dec 2012. [Online]. Available: http://www.navigantresearch.com/newsroom/utility-distribution-microgrids-will-reach-nearly-3-3-billion-in-market-value-by-2018

[93] R. Hales, "Microgrid-as-a-service & other alternatives to conventional macrogrids," Feb 2014. [Online]. Available: http://cleantechnica.com/2014/02/10/microgrid-service-alternatives-conventional-macrogrids/

[94] S. Schneider, "March of the microgrids. technology is changing the game. is your utility ready?" Jan 2013. [Online]. Available: http://www.fortnightly.com/fortnightly/2013/01/march-microgrids

[95] M. Stadler, "DER-CAM," *Lawrence Berkeley National Laboratory*, May 2014. [Online]. Available: http://building-microgrid.lbl.gov/projects/der-cam

[96] J. Mitra and S. J. Ranade, "Power system hardening through autonomous customer-driven microgrids," *Power Engineering Society General Meeting 2007*, 2007.

[97] National Renewable Energy Laboratory, "Open ei commercial and residential hourly load profiles for all tmy3 locations in the united states," May 2014. [Online]. Available: http://en.openei.org/datasets/node/961

[98] U.S. DOE/NETL, "Microgrid research, development, and system design funding opportunity number de-foa-0000997," *National Energy Technology laboratory, Golden, CO*, Jan 2014.

DISTRIBUTION

1	MS1124	David Wilson	6122
1	MS1152	Steven Glover	1353
1	MS1152	Jason Neely	1353
1	MS1188	Steve Bukowski	6114
1	MS1188	Marvin Cook	6114
1	MS0899	Technical Library	9536 (electronic copy)


Sandia National Laboratories